Deutsches Institut für Ernährungsforschung Potsdam-Rehbrücke
Abteilung Gastrointestinale Mikrobiologie

DIfE

Influence of intestinal inflammation on bacterial protein expression in monoassociated mice

DISSERTATION

zur Erlangung des akademischen Grades

doctor rerum naturalium
(Dr. rer. nat.)

in der Wissenschaftsdisziplin
„Gastrointestinale Mikrobiologie"

eingereicht an der Mathematisch-Naturwissenschaftlichen Fakultät
der Universität Potsdam

von

Diplom-Biochemikerin
SARA SCHUMANN

geboren am 29.04.1984 in Halle/Saale

Potsdam, im März 2013

I. TABLE OF CONTENTS

II. LIST OF FIGURES

III. LIST OF TABLES

IV. ABBREVIATIONS

AA	Acrylamide/Bis-Acrylamide
AIEC	Adherent-invasive *Escherichia coli*
APS	Ammonium persulfate
ATG16L1	*Autophagy related 16-like 1*
CARD	Caspase recruitment domain
CD	Crohn's disease
CD3	Cluster of differentiation 3
CDH1	*Cadherin 1*
cDNA	Complementary DNA
CFU	Colony-forming units
CHAPS	3-[(3-Cholamidopropyl)-dimethylammonio]-1-propanesulfonate
CRC	Colorectal cancer
Cxcl10	Chemokine (C-X-C motif) ligand 10
DEPC	Diethylpyrocarbonate
DC	Dentritic cell
2D-DIGE	Two-dimensional fluorescence difference gel electrophoresis
DMEM	Dulbecco's Modified Eagle's Medium
DNA	Deoxyribonucleic acid
DP	2,2'-Dipyridyl
DSS	Dextran sodium sulphate
DTT	Dithiothreitol
ECM1	*Extracellular matrix protein 1*
EcN	*E. coli* Nissle
E. coli	*Escherichia coli*
EDTA	Ethylenediaminetetraacetic acid
hBD-2	Human beta defensin 2
H&E staining	Hematoxylin and eosin staining
HLA-B27 rats	Human leukocyte antigen B27
H_2O_2	Hydrogen peroxide
Hprt1	*Hypoxanthine guanine phosphoribosyl transferase*
IBD	Inflammatory bowel disease
IEC	Intestinal epithelial cell
IEF	Isoelectric focusing
Ifng	*Interferon γ*
IL	Interleukin
IL-10$^{-/-}$ mice	Interleukin 10-deficient mice
IPTG	Isopropyl β-D-1-thiogalactopyranoside
IRGM	*Immunity-related GTPase family, M*
ISC	Iron sulphur cluster
Ivy	Inhibitor of vertebrate lysozyme
LB	Lysogeny broth
MOPS	3-(N-morpholino)propanesulfonic acid
NanoLC–ESI–MS/MS	Nano-liquid chromatography-electrospray ionization-tandem mass spectrometry

NF-κB	Nuclear factor κB
NfuA	Fe-S biogenesis protein NfuA
NOD2	*Nucleotide-binding oligomerization domain containing 2*
OD_{600}	Optical density at 600 nm
PAGE	Polyacrylamide gel electrophoresis
PBS	Phosphate buffered saline
PCA	Principal component analysis
PCR	Polymerase chain reaction
PQ	Paraquat
qPCR	Quantitative real time polymerase chain reaction
Rcs	Regulation of the capsular synthesis
RNA	Ribonucleic acid
RNS	Reactive nitrogen species
ROS	Reactive oxygen species
ROX	Carboxy-X-rhodamine
Rpl13a	*Ribosomal protein L13A*
rrsA	16S ribosomal RNA
Rubps	Ruthenium II tris(bathophenanthroline disulfonate)
SDS	Sodium dodecyl sulphate
SUF	Sulphur mobilisation
T_a	Annealing temperature
Th cell	T helper cell
T_{reg}	Regulatory T cell
T-TBS	Tris-buffered saline containing Tween 20
TEMED	N, N, N', N'-tetramethylethylenediamine
TGFβ	Transforming growth factor-β
TLR	Toll-like receptor
TNBS	2,4,6-trinitrobenzenesulfonic acid
Tnf	*Tumor necrosis factor α*
Tris	Tris(hydroxymethyl)aminomethane
UC	Ulcerative colitis
UNC	University of North Carolina
wk	Weeks
wt	Wildtype
X-Gal	5-Bromo-4-chloro-indolyl-β-D-galactopyranoside
YggE	Uncharacterised protein YggE

V. ABSTRACT

Background: Increased numbers of intestinal *E. coli* are observed in inflammatory bowel disease, but the reasons for this proliferation and it exact role in intestinal inflammation are unknown. Aim of this PhD-project was to identify *E. coli* proteins involved in *E. coli*'s adaptation to the inflammatory conditions in the gut and to investigate whether these factors affect the host. Furthermore, the molecular basis for strain-specific differences between probiotic and harmful *E. coli* in their response to intestinal inflammation was investigated. **Methods:** Using mice monoassociated either with the adherent-invasive *E. coli* (AIEC) strain UNC or the probiotic *E. coli* Nissle, two different mouse models of intestinal inflammation were analysed: On the one hand, severe inflammation was induced by treating mice with 3.5% dextran sodium sulphate (DSS). On the other hand, a very mild intestinal inflammation was generated by associating interleukin 10-deficient (IL-10$^{-/-}$) mice with *E. coli*. Differentially expressed proteins in the *E. coli* strains collected from caecal contents of these mice were identified by two-dimensional fluorescence difference gel electrophoresis. **Results DSS-experiment:** All DSS-treated mice revealed signs of a moderate caecal and a severe colonic inflammation. However, mice monoassociated with *E. coli* Nissle were less affected. In both *E. coli* strains, acute inflammation led to a downregulation of pathways involved in carbohydrate breakdown and energy generation. Accordingly, DSS-treated mice had lower caecal concentrations of bacterial fermentation products than the control mice. Differentially expressed proteins also included the Fe-S cluster repair protein NfuA, the tryptophanase TnaA, and the uncharacterised protein YggE. NfuA was upregulated nearly 3-fold in both *E. coli* strains after DSS administration. Reactive oxygen species produced during intestinal inflammation damage Fe-S clusters and thereby lead to an inactivation of Fe-S proteins. *In vitro* data indicated that the repair of Fe-S proteins by NfuA is a central mechanism in *E. coli* to survive oxidative stress. Expression of YggE, which has been reported to reduce the intracellular level of reactive oxygen species, was 4- to 8-fold higher in *E. coli* Nissle than in *E. coli* UNC under control and inflammatory conditions. *In vitro* growth experiments confirmed these results, indicating that *E. coli* Nissle is better equipped to cope with oxidative stress than *E. coli* UNC. Additionally, *E. coli* Nissle isolated from DSS-treated and control mice had TnaA levels 4- to 7-fold higher than *E. coli* UNC. In turn, caecal indole concentrations resulting from cleavage of tryptophan by TnaA were higher in *E. coli* Nissle-associated control mice than in the respective mice associated with *E. coli* UNC. Because of its anti-inflammatory effect, indole is hypothesised to be involved in the extension of the remission phase in ulcerative colitis described for *E. coli* Nissle. **Results IL-10$^{-/-}$-experiment:** Only IL-10$^{-/-}$ mice monoassociated with *E. coli* UNC for 8 weeks exhibited signs of a very mild caecal inflammation. In agreement with this weak inflammation, the variations in the bacterial proteome were small. Similar to the DSS-experiment, proteins

downregulated by inflammation belong mainly to the central energy metabolism. In contrast to the DSS-experiment, no upregulation of chaperone proteins and NfuA were observed, indicating that these are strategies to overcome adverse effects of strong intestinal inflammation. The inhibitor of vertebrate C-type lysozyme, Ivy, was 2- to 3-fold upregulated on mRNA and protein level in *E. coli* Nissle in comparison to *E. coli* UNC isolated from IL-10$^{-/-}$ mice. By overexpressing *ivy*, it was demonstrated *in vitro* that Ivy contributes to a higher lysozyme resistance observed for *E. coli* Nissle, supporting the role of Ivy as a potential fitness factor in this *E. coli* strain. **Conclusions:** The results of this PhD-study demonstrate that intestinal bacteria sense even minimal changes in the health status of the host. While some bacterial adaptations to the inflammatory conditions are equal in response to strong and mild intestinal inflammation, other reactions are unique to a specific disease state. In addition, probiotic and colitogenic *E. coli* differ in their response to the intestinal inflammation and thereby may influence the host in different ways.

VI. ZUSAMMENFASSUNG

Hintergrund: Chronisch entzündliche Darmerkrankungen zeichnen sich unter anderem durch eine starke Proliferation intestinaler *E. coli* aus. Unbekannt ist jedoch, ob diese Vermehrung eine Ursache oder eine Folge der Erkrankung darstellt. Ziel der vorliegenden Doktorarbeit war es daher, *E. coli*-Proteine zu identifizieren, welche der Anpassung an die entzündlichen Bedingungen im Darmtrakt dienen und unter Umständen einen Effekt auf den Gesundheitszustand des Wirtes haben. Weiterhin sollten die molekularen Ursachen für stammesspezifische Unterschiede zwischen probiotischen und gesundheitsschädlichen *E. coli* näher untersucht werden. **Methoden:** In den tierexperimentellen Analysen wurden keimfreie Mäuse entweder mit dem probiotischen *E. coli* Nissle oder dem adhärent-invasiven *E. coli* UNC monoassoziiert und in zwei verschiedenen Entzündungsmodellen näher untersucht. Einerseits wurde eine starke Darmentzündung durch die Gabe von 3,5% Natrium-Dextransulfat (DSS) ausgelöst. Andererseits wurde in Interleukin 10-defizienten (IL-10$^{-/-}$) Mäusen eine sehr milde Form der Entzündung durch Besiedlung mit *E. coli* induziert. Die *E. coli* Bakterien wurden am Ende der Versuche aus den Caecuminhalten der Mäuse isoliert und die bakterielle Proteinexpression wurde mittels zwei-dimensionaler Gelelektrophorese analysiert. **Ergebnisse des DSS-Versuchs:** Alle Tiere des DSS-Versuchs entwickelten unabhängig vom *E. coli* Stamm, mit dem sie besiedelt waren, eine moderate Entzündung im Caecum und eine starke im Colon, wobei die Entzündungsreaktion durch die Monoassoziation mit *E. coli* Nissle leicht abgeschwächt wurde. In beiden *E. coli* Stämmen führte die Darmentzündung zu einer verringerten Expression von Enzymen des Kohlenhydratabbaus und der Energiegewinnung. In Folge dessen waren die intestinalen Konzentrationen bakterieller Fermentationsprodukte in den entzündeten Tieren geringer als in den gesunden Kontrolltieren. Weitere differentiell exprimierte Proteine umfassen das Fe-S-Cluster Reparaturprotein NfuA, die Tryptophanase TnaA und das uncharakterisierte Protein YggE. In beiden *E. coli* Stämmen, welche aus den DSS-Tieren isoliert wurden, war das NfuA Protein dreifach höher exprimiert. Eine Darmentzündung führt zu einer vermehrten Bildung reaktiver Sauerstoffspezies, welche die Fe-S-Cluster in Eisen-Schwefel-Proteinen zerstören und damit zu einer Inaktivierung dieser Proteine führen. *In vitro* Untersuchungen bestätigten, dass die Reparatur der Eisen-Schwefel-Proteine durch NfuA ein wichtiger Mechanismus ist um oxidativem Stress entgegenzuwirken. Das YggE Protein, welches laut Literaturangaben einen hemmenden Einfluss auf die Bildung reaktiver Sauerstoffspezies hat, war in *E. coli* Nissle 4- bis 8-fach erhöht (verglichen mit *E. coli* UNC unter Kontroll- und Entzündungsbedingungen). *In vitro* Versuche bestätigten diese Daten und zeigten, dass *E. coli* Nissle im Vergleich zu *E. coli* UNC eine erhöhte Resistenz gegenüber oxidativem Stress aufweist. Außerdem wurde im Vergleich *E. coli* Nissle vs. *E. coli* UNC (unter Entzündungs- und Kontrollbedingungen) ein 4- bis 7-fach erhöhter TnaA-Gehalt

nachgewiesen. Indol, das Produkt der TnaA-katalysierten Tryptophanspaltung wurde in erhöhten Mengen im Intestinaltrakt *E. coli* Nissle-assoziierter Kontrolltiere detektiert. Seit längerem werden entzündungshemmende Eigenschaften für Indol postuliert, die aufgrund der Ergebnisse dieser Doktorarbeit nun auch mit den gesundheitsfördenden Eigenschaften von *E. coli* Nissle in Zusammenhang gebracht werden können. **Ergebnisse des IL-10$^{-/-}$-Versuchs:** Nach einer 8-wöchigen Assoziationsdauer wurde nur in den mit *E. coli* UNC besiedelten IL-10$^{-/-}$ Tieren eine schwache Entzündungsreaktion nachgewiesen. Bedingt durch diese sehr schwach ausgeprägte Entzündungsantwort waren auch die Veränderungen im bakteriellen Proteom von *E. coli* UNC nur gering. Wie im DSS-Versuch waren Proteine des bakteriellen Energiestoffwechsels reprimiert, allerdings wurde keine Induktion von NfuA beobachtet. Daher scheint die Induktion von NfuA nur der Anpassung an eine starke Entzündung zu dienen. Weiterhin wurde nachgewiesen, dass *E. coli* Nissle aus IL-10$^{-/-}$ Tieren den Hemmer für das vertebrate C-Typ Lysozym (Ivy) sowohl auf mRNA- als auch auf Proteinebene stärker exprimiert als *E. coli* UNC. Überexpression von Ivy unter *in vitro* Bedingungen zeigte, dass es an der erhöhten Lysozymresistenz von *E. coli* Nissle beteiligt ist und somit eine Rolle als möglicher Fitnessfaktor von *E. coli* Nissle spielt. **Schlussfolgerungen:** In dieser Doktorarbeit wurde gezeigt, dass Darmentzündungen die Proteinexpression eines im Darm lebenden Bakteriums beeinflussen. Einige der aufgedeckten bakteriellen Anpassungsreaktionen werden sowohl bei einer starken als auch bei einer schwachen Entzündung ausgelöst; andere wiederum sind spezifisch für nur einen dieser Entzündungszustände. Weiterhin wurde deutlich, dass sich *E. coli*-Stämme hinsichtlich ihrer Reaktion auf eine Darmentzündung unterscheiden und damit möglicherweise den Wirt beeinflussen.

1 INTRODUCTION

1.1 Human inflammatory bowel disease (IBD)

1.1.1 Clinical manifestation of IBD

Inflammatory bowel disease is a chronic relapsing immunologically mediated disorder. Ulcerative colitis (UC) is one of the two major forms of IBD. It occurs mainly in the colon and rectum, while Crohn's disease (CD), the second form of IBD, can affect any part of the gastrointestinal tract (Fig. 1). The small intestine, in particular the terminal ileum, is involved in approximately 47% of all CD cases, while another 28% involve only the colon, and 21% involve both, the small intestine and the colon (reviewed in Baumgart & Sandborn, 2007). In UC patients, the inflammation is limited to the mucosa, whereas a transmural inflammation and the formation of granulomas are characteristic of CD (Lakatos *et al.*, 2006).

The clinical presentation of IBD depends on the form and the state of disease. Bloody diarrhoea and a destroyed crypt architecture are common to UC, while the presence of fistulae, skip lesions and intestinal obstruction are more characteristic of CD (reviewed in Baumgart & Sandborn, 2007).
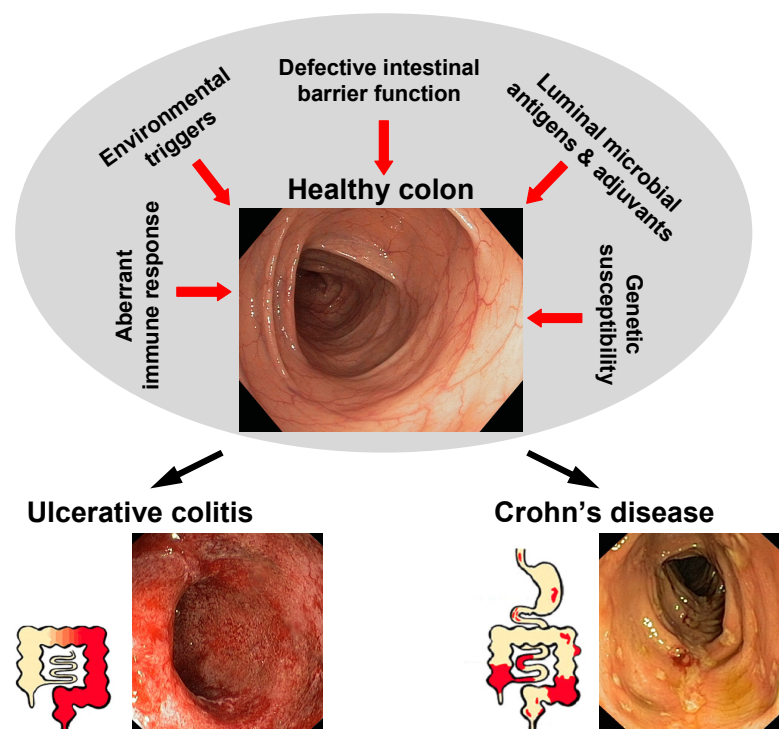
Fig. 1 Pathogenesis of inflammatory bowel disease
In genetically susceptible hosts, an altered immune response towards the luminal microbiota and a defective intestinal barrier function facilitate the conversion from a healthy to an inflamed intestine. Environmental factors promote this event. While the inflammation in UC patients is limited to the colon mucosa, the inflammation in CD patients transmurally affects any part of the gastrointestinal tract. The endoscopic pictures were downloaded from http://www.internetmedicin.se/dyn_main.asp?page=240.

The development of colitis-associated cancer is one complication, which can occur in patients with CD and UC. Meta-analysis of several population-based cohort studies indicated that patients suffering from UC have a 2.4-fold higher risk to develop colorectal cancer (CRC) than the general population (Jess *et al.*, 2012a). Crohn's disease patients with inflammation in the small intestine and the colon, have a 2.5-fold increased risk to generate CRC, while patients in whom the disease is restricted to the colon have a 4.5-fold higher risk. For patients suffering from isolated ileal CD, the risk for the development of CRC is not increased (Canavan *et al.*, 2006). However, a recent publication showed that diagnosis of IBD no longer seems to increase the risk of CRC, which might result from improved therapies (Jess *et al.*, 2012b).

1.1.2 Epidemiology of IBD

In Europe and North America, the incidence and prevalence of IBD have dramatically increased since the Second World War. A systematic review, analysing the data published between 1950 and 2010 claimed that incidence and prevalence rates are increasing with time and in different regions around the world, indicating that IBD is becoming a global disease. In Europe, the prevalence of UC is approximately 500 per 100.000 people and 320 per 100.000 people for CD (Molodecky *et al.*, 2012).

1.1.3 Pathology of IBD

IBD is a multifactorial disease and its onset is triggered by several factors (Fig. 1). It is hypothesised that a genetically predisposed host mounts an inordinate aggressive T cell-mediated immune response to a subset of commensal enteric bacteria. Several environmental factors are speculated to accelerate the onset of the disease (reviewed in Sartor, 2006).

1.1.3.1 Role of genetic factors

Familial aggregation and concordance rates between identical twins of 20 - 50% (for CD) and 14 - 19% (for UC) suggest that genetical factors may be involved in IBD pathogenesis (Halme *et al.*, 2006). Using genome-wide association studies, a number of genes have been identified that interact with the development of IBD. They have important functions in the regulation of the immune system, in mucosal barrier function and in the sensing of intestinal bacteria. A mutation or a dysregulation of these genes has disastrous consequences on gut function and therefore facilitates the onset of IBD.

The *NOD2* (*nucleotide-binding oligomerization domain containing 2*) gene was the first gene that was predicted to be associated with the onset of CD (Hugot *et al.*, 2001; Ogura *et al.*, 2001a). Thirty to forty percent of the CD patients in Western countries carry *NOD2* polymorphisms on at least one allele (reviewed in Kaser *et al.*, 2010). *NOD2* is a member of

the CED4/APAF1 superfamily of apoptosis regulators (Ogura *et al.*, 2001b), which are composed of two caspase recruitment domains, a nucleotide-binding domain and a leucine-rich repeat region (Hugot *et al.*, 2001). NOD2 plays a role in the immune response to intracellular bacteria by recognizing the muramyl dipeptide (Girardin *et al.*, 2003; Inohara *et al.*, 2003). After binding of muramyl dipeptide by the leucine-rich repeat region, the nuclear factor κB (NFκB) is activated, which in turn stimulates the transcription of several protective molecules, such as tumor necrosis factor-induced protein 3, cyclooxygenase 2, and β-defensins (reviewed in Sartor, 2006). *NOD2* knock out mice exhibit a dysregulated cytokine production and a reduced cryptdin expression (Kobayashi *et al.*, 2005). Therefore, mutations in *NOD2* may only promote CD through a defective regulation of the immune response against enteric bacteria, rather than acting as an initiating factor for the disease itself.

Further genes that are linked to CD include *autophagy related 16-like 1* (*ATG16L1*), *immunity-related GTPase family M* (*IRGM*) and *toll-like receptor 4* (*TLR4*). Genes that are linked to UC encode *cadherin 1* (*CDH1*), *extracellular matrix protein 1* (*ECM1*) and *interleukin 10* (*IL-10*) (reviewed in Kaser *et al.*, 2010; Thompson & Lees, 2010; Rogler, 2011).

1.1.3.2 Involvement of the immune system

The immunological dysregulation observed in the state of IBD is very complex and it is difficult to briefly sum up all factors. Therefore, this section will focus on the major events contributing to the onset of the disease. IBD is generally believed to be driven by an increased number of activated mucosal T helper cells (e. g. Th1, Th2, Th17) that lead to an uncontrolled production of proinflammatory cytokines, such as tumor necrosis factor α (Tnf), Interferon γ (Ifng), interleukin 12b (IL-12b), and interleukin 17 (IL-17) (reviewed in Round & Mazmanian, 2009). These proinflammatory T cell responses are usually suppressed by regulatory T cells (T_{reg}), which express anti-inflammatory cytokines such as IL-10 or the transforming growth factor β (TGFβ) (Vignali *et al.*, 2008). Due to a higher rate of apoptosis, the numbers of T_{reg} cells are significantly decreased in IBD patients (Veltkamp *et al.*, 2011), whereas the numbers of the T cell-stimulating dendritic cells are increased (Hart *et al.*, 2005). In total, these factors lead to an imbalance between pro- and anti-inflammatory stimuli that promote disease development (Fig. 2). Overwhelming proinflammatory cytokine production further stimulates a massive epithelial infiltration with polymorphonuclear and mononuclear phagocytic leukocytes. These produce large amounts of reactive oxygen species (ROS) and reactive nitrogen species (RNS) that exert a variety of physiological and pathophysiological actions (Harris *et al.*, 1992; Kruidenier *et al.*, 2003).
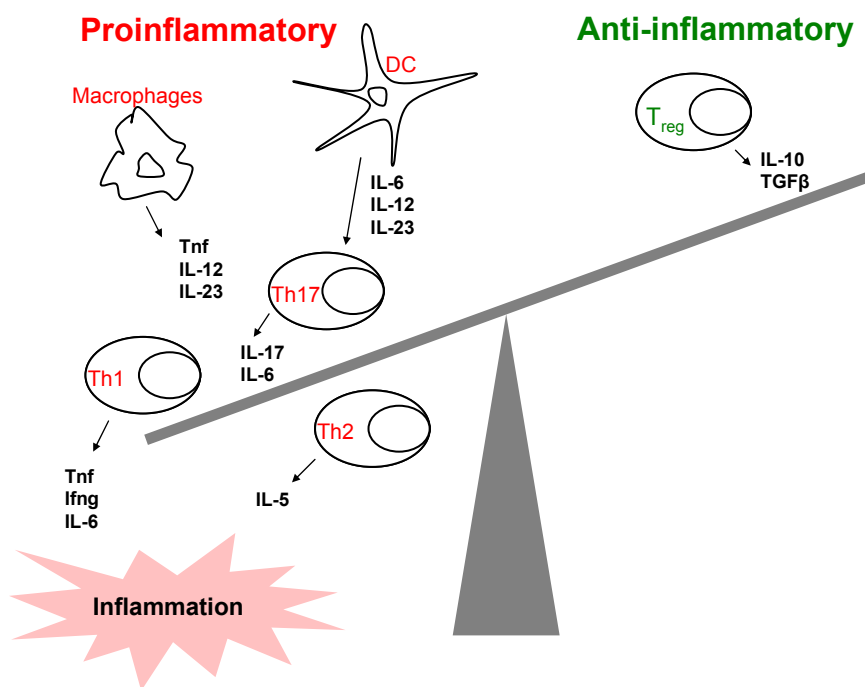
Fig. 2 Cytokine imbalance in IBD
The imbalance between effector (Th1, Th2 and Th17) and regulatory T cells leads to an overproduction of pro-inflammatory cytokines that facilitate the development of an intestinal inflammation. Th cells, T helper cells; IL, interleukin, DC, dentritic cells. Adapted from Sanchez-Munoz *et al.* (2008).

1.1.3.3 Intestinal barrier function in IBD

The intestinal epithelium lining the small intestine originates from multipotent stem cells present at the crypt ground. From these stem cells, five types of intestinal epithelial cells (IECs) differentiate as they migrate up to the villus tip: Absorptive enterocytes, goblet cells (mucus production), enteroendocrine cells (peptide hormone production) paneth cells (production of antimicrobial peptides) and the almost uncharacterised tuft cells (Cheng & Leblond, 1974; Gerbe *et al.*, 2011).

In healthy individuals, the intestinal epithelium provides an effective barrier against the invasion of luminal antigens. However, it is suggested that the continuous stimulation of the mucosal immune system observed in IBD is partly due to an increased epithelial permeability (Laukoetter *et al.*, 2008). In fact, several studies describe an increased intestinal permeability in CD patients and their relatives (May *et al.*, 1993; Peeters *et al.*, 1994; Peeters *et al.*, 1997).

The intestinal barrier encompasses luminal secretions such as mucins, defensins or lysozyme, a layer of IECs that allow a specific membrane transport, and a stromal compartment below the epithelial cells. During inflammatory processes, apoptosis of the IECs occurs. However, it has been shown that this alone does not account for the increased permeability (Bruewer *et al.*, 2003). Other discussed mechanisms include changes in paracellular transport, which is regulated by the tight junctions. In IBD, tight junction structure is altered, which decreases the epithelial barrier function (reviewed in Clayburgh *et al.*, 2004). Furthermore, IBD, especially CD, has been linked to Paneth cell dysfunction and a decreased secretion of antimicrobial peptides, such as defensins (reviewed in Wehkamp &

Stange, 2010; Kaser & Blumberg, 2011). Defensins are small cationic peptides with an antimicrobial activity against bacteria and fungi. They permeabilise microbial membranes and thereby protect the gastrointestinal tract against potentially pathogenic bacteria (Lehrer et al., 1993). Defensins are classified into α- and β-defensins based on the position of three intramolecular disulfide bridges (White et al., 1995). In ileal CD, the expression of α-defensins (HD-5, HD-6) and β-defensin 2 (hBD-2) is decreased, which is supposed to contribute to a defective antimicrobial barrier in these patients (Wehkamp et al., 2002; Wehkamp et al., 2004b; Wehkamp et al., 2005).

1.1.3.4 Role of intestinal bacteria

The human gastrointestinal tract harbours more than 10^{14} microorganisms of more than 1000 species (Gill et al., 2006; Turnbaugh et al., 2009). Over 500 bacterial phyla have been described to date, but the human gut microbiota is dominated by only two of them: the Bacteroidetes and the Firmicutes. Proteobacteria, Verrucomicrobia, Actinobacteria, Fusobacteria, and Cyanobacteria are present in minor proportions (reviewed in Sekirov et al., 2010). Studies using germ-free animals provide evidence that the intestinal microbiota contributes to the maturation and maintenance of the gut-associated immune system. In fact, germ-free animals exhibit defects in the gut-associated lymphoid tissues (Falk et al., 1998; Macpherson & Harris, 2004) and have decreased immunoglobulin A levels (Moreau et al., 1978). Furthermore, the expression of defensins and other antimicrobial proteins is defective in germ-free animals (reviewed in Round & Mazmanian, 2009).

In the healthy intestine a symbiotic mutualism exists between the commensal intestinal microbiota and the human host. As this symbiosis is impaired in the state of IBD, the immune system loses its tolerance to the commensal enteric bacteria (Duchmann et al., 1995). IBD patients exhibit higher antibody titres against indigenous bacteria than unaffected individuals (Macpherson et al., 1996) and respond favourably to antibiotic treatment (Guslandi, 2011). Several animal models of IBD also illustrate the importance of the intestinal microbiota: Human leukocyte antigen B27 (HLA-B27)-transgenic rats (Taurog et al., 1994) and IL-10-deficient (IL-10$^{-/-}$) mice (Sellon et al., 1998) stay disease-free when they are raised under germ-free conditions, but develop chronic colitis when they are raised under conventional conditions.

A disruption of the ecological balance between commensals and pathogens in the intestine is an important feature of IBD. Various studies assessing the intestinal microbiota reported a lower abundance of potentially beneficial bacteria, such as *Faecalibacterium prausnitzii*, in patients with IBD compared with healthy individuals (Sokol et al., 2009; Willing et al., 2009; Joossens et al., 2011). Furthermore, reductions in the relative abundance of Firmicutes and

concomitant increase in Proteobacteria have been observed in IBD patients (Gophna *et al.*, 2006; Frank *et al.*, 2011; Walker *et al.*, 2011).

Increased numbers of *Escherichia coli* (*E. coli*) are reported to be strongly associated with CD (Darfeuille-Michaud *et al.*, 1998; Darfeuille-Michaud *et al.*, 2004; Willing *et al.*, 2009). In ileal lesions of CD patients, *E. coli* account for more than 50% of total bacteria (Darfeuille-Michaud *et al.*, 1998). Since these *E. coli* strains display both, adherent and invasive properties that enable them to colonise the intestinal mucosa, they are referred to as adherent-invasive *E. coli* (AIEC) (Boudeau *et al.*, 1999). A correlation between higher intestinal *E. coli* levels and intestinal inflammation is also reported in animal studies (Heimesaat *et al.*, 2007; Wohlgemuth *et al.*, 2009). Wohlgemuth *et al.* (2009) observed a strong proliferation of *E. coli* in IL-10$^{-/-}$ mice simultaneously with a reduction in the overall microbial diversity. In this study, the *E. coli* population was represented by only one predominant strain with an O7:H7:K1 serotype, which was also able to outcompete other *E. coli* strains in di-association experiments. However, no evidence was found that this *E. coli* strain induces inflammation in IL-10$^{-/-}$ animals (Wohlgemuth *et al.*, 2009). In contrast, the AIEC strain from the University of North Carolina (*E. coli* UNC), previously referred to as *E. coli* NC101 (Patwa *et al.*, 2011), induced caecal inflammation in IL-10$^{-/-}$ mice within 3 weeks (wk) of monoassociation, which progressed to a more severe form of inflammation after 16 wk (Kim *et al.*, 2005a).

1.1.3.5 Environmental triggers of IBD

The effect of environmental triggers on the pathogenesis of IBD is controversially discussed. However, north-south, east-west, and urban-rural gradients for incidence rates of IBD have been identified worldwide (reviewed in Loftus, 2004). Moreover, the importance of environmental factors is supported by increasing incidence rates in previously less affected ethnic groups, such as Asians and Hispanics (reviewed in Hou *et al.*, 2009), and in immigrants moving from low incidence regions to areas with a traditionally high incidence (Joossens *et al.*, 2007). Many factors are discussed to stimulate the onset of IBD, some of which are: A reduced number of breastfeeding women (Barclay *et al.*, 2009), an improved domestic hygiene and sanitation (Gent *et al.*, 1994), the exposure to air pollution (Kaplan *et al.*, 2010), the consumption of a western diet rich in convenience foods (Hou *et al.*, 2011), and an increased tobacco use (Tuvlin *et al.*, 2007).

1.1.4 Treatment of IBD

1.1.4.1 The standard therapy for IBD

Mild to moderately active UC is treated orally or topically with 5-aminosalicylic acid compounds, such as mesalazine (5-aminosalicylic acid), sulfasalazine (5-aminosalicylic acid linked to sulfapyridine), olsalazine (5-aminosalicylic acid dimer)*,* and balsalazide (5-

aminosalicylic acid linked to 4-aminobenzoyl-β-alanine). For patients with CD, mesalazine treatment is controversially discussed, as its use is not evidence-based. Therefore, ileitis and colitis patients are usually treated with sulfasalazine (reviewed in Baumgart & Sandborn, 2007). Because several adverse side effects, such as interstitial nephritis and pancreatitis, are described after treatment with mesalazine (Ransford & Langman, 2002), alternative IBD therapies are under investigation.

1.1.4.2 Probiotics and their potential in IBD therapy

Probiotics are by definition living, non-pathogenic microorganisms that exert positive effects on the host when ingested in certain numbers (Guarner & Schaafsma, 1998). Since the normal gut microbiota is implicated in the pathogenesis of IBD, probiotics are thought to influence the host microbiota by eliminating pathogenic bacteria. The proposed mechanisms underlying this probiotic effect include the production of antimicrobials, such as bacteriocins (reviewed in Dobson *et al.*, 2012) or lactic acid. The latter lowers the local pH and thereby inhibits the growth of bacteria sensitive to acidic conditions (reviewed in Wohlgemuth *et al.*, 2010). Other probiotics block the attachment of pathogenic bacteria to IECs and thereby prevent their invasion (Resta-Lenert & Barrett, 2003). Furthermore, probiotics have been shown to exhibit important immunoregulatory activities: They modulate the balance between T_{reg} and Th cells, increase the production of anti-inflammatory cytokines, and decrease the level of proinflammatory cytokines (Di Giacinto *et al.*, 2005; Lin *et al.*, 2008).

The *E. coli* Nissle 1917 (active substance of Mutaflor[®] [Ardeypharm GmbH, Germany]) is one of the best characterised probiotic strains. It is successfully used for the treatment of IBD, particularly for the remission maintenance of UC patients (Kruis *et al.*, 1997; Rembacken *et al.*, 1999; Kruis *et al.*, 2004; Henker *et al.*, 2008; Matthes *et al.*, 2010). Alfred Nissle isolated this *E. coli* strain in 1917 from the faeces of a soldier, who was immune against infectious diarrheal diseases. Serologically, *E. coli* Nissle belong to the *E. coli* O6 group with an O6:K5:H1 serotype (Grozdanov *et al.*, 2004). *E. coli* Nissle express several fitness factors, such as microcins, adhesins, and at least six different iron-uptake systems that enable this *E. coli* to compete with other strains in the ecological system of the gut. Moreover, *E. coli* Nissle lack prominent virulence genes, such as α-hemolysin and P-fimbrial adhesins (summarised in Grozdanov *et al.*, 2004). Besides the inhibition of IEC-invasion by potentially pathogenic bacteria (Altenhoefer *et al.*, 2004), *E. coli* Nissle possess several immunomodulatory properties: In various cell culture models, *E. coli* Nissle reduce the secretion of proinflammatory cytokines (Ifng, Tnf), while the secretion of the anti-inflammatory cytokine IL-10 is increased (Sturm *et al.*, 2005). By upregulating the zona occludens protein 1, *E. coli* Nissle directly modulate the function of the intestinal epithelial barrier (Ukena *et al.*, 2007). In addition, Wehkamp *et al.* (2004a) demonstrated that *E. coli* Nissle induce the expression of the β-defensin, hBD-2, via NF-κB and c-Jun N-terminal

kinase, which was later shown to be mediated by *E. coli* Nissle's specific flaggelin (Schlee *et al.*, 2007). Important in this context is the finding that hBD-2 expression in the remission state is low and induction may prevent a bacterially induced relapse (Wehkamp *et al.*, 2003), which is in agreement with the use of *E. coli* Nissle in remission maintenance.

1.2   Animal models of IBD

Although it was recently shown that the genomic responses of mouse models to inflammatory stresses correlate poorly with that in humans (Seok *et al.*, 2013), various animal models have been developed that mimic several aspects of human IBD. They are classified into five different groups: (1) antigen-induced colitis and colitis induced by microbials, (2) other inducible forms of colitis, such as chemical, immunological or physical forms of stress, (3) genetic models of colitis, (4) adaptive transfer models, and (5) spontaneous colitis models (reviewed in Hoffmann *et al.*, 2002). In the present work, intestinal inflammation was induced either chemically by dextran sodium sulphate (DSS) or genetically through knock out of the anti-inflammatory cytokine IL-10.

1.2.1   Chemically-induced colitis: The DSS-induced colitis model

DSS is a heparin-like polysaccharide containing up to three sulphate groups per glucose molecule. Oral application of DSS to rodents (hamsters, mice, rats, and guinea-pigs) induces intestinal inflammation restricted to the large intestine, especially to the distal part of the colon (Cooper *et al.*, 1993), displaying similarities to human UC. As different therapeutic agents for human IBD are also effective for the treatment of DSS-induced colitis in rodents, this model seems to be adequate for studying IBD (Melgar *et al.*, 2008).

Generally it is believed that DSS is directly toxic to IECs. It destroys the integrity of the mucosal barrier and allows the entry of luminal antigens and microorganisms into the mucosa resulting in an overwhelming inflammatory response characterised by an induction of proinflammatory cytokines (such as Tnf, IL-1β, Ifng, and IL-12) (Yan *et al.*, 2009). Depending on the concentration, the duration, and the frequency of DSS administration, the animals develop an acute or chronic colitis. However, mice differ in their susceptibility and responsiveness to DSS-induced colitis depending on genetic (strain, gender) and microbiological factors.

Differences in the susceptibility to DSS-induced colitis among different mouse strains have been identified by Mähler *et al.* (1998): While C3H/HeJ and NOD/LtJ inbred strains are very susceptible to DSS-induced lesions, C57BL/6J, 129/SvPas and DBA/2J inbred mice are less susceptible. The impact of the intestinal microbiota on the development of DSS-induced colitis in mice is not so clear, since antibiotic treatment improves the symptoms of acute

DSS-induced colitis, but has no effect on chronic DSS-induced colitis (Hans *et al.*, 2000). Hudcovic *et al.* (2001) observed further that germ-free immunocompetent BALB/c mice are less susceptible to DSS-treatment, while germ-free immunodeficient SCID mice died after application of 2.5% DSS. Similar results were published by Kitajima *et al.* (2001): Administration of 5% DSS to germ-free and conventional IQI/Jic mice resulted in the deaths of the germ-free mice within 3 days, whereas none of the conventional mice died until the end of the experiment after 7 days. A histopathological examination three days after DSS administration did not reveal any colitic lesions in the intestine of the germ-free mice, while conventional mice were moderately inflamed. Hence, the toxicity of DSS to germ-free mice with an impaired immune system is not the result of an intestinal inflammation.

1.2.2 Genetically-induced colitis: The interleukin 10-deficient mouse model

IL-10 is probably the most important anti-inflammatory cytokine involved in the pathogenesis of IBD since it inhibits the activity of T helper cells (Th1, Th2) and thereby limits the production of proinflammatory cytokines (reviewed in Louis *et al.*, 2009). To study the effect of IL-10 in inflammation, IL-10$^{-/-}$ mice were generated by Kühn *et al.* (1993). Phenotypic characterisation revealed, that IL-10$^{-/-}$ mice maintained under conventional conditions develop discontinuous transmural lesions affecting both, the upper and lower gastrointestinal tract (Kühn *et al.*, 1993). The intestines of inflamed IL-10$^{-/-}$ mice are infiltrated by a large number of macrophages and other immune cells, which produce large amounts of numerous cytokines, such as IL-1α, IL-6, Tnf, IL-17, and Ifng. These abnormally high cytokine levels lead to an uncontrolled immune response, which is speculated to be the reason for the onset of inflammation in IL-10$^{-/-}$ mice (Berg *et al.*, 1996; Gomes-Santos *et al.*, 2012).

While specific monoassociation with distinct bacteria induces to the onset of the disease, IL-10$^{-/-}$ mice maintained under germ-free conditions remain disease-free and have no evidence of an immune system activation. In fact, monoassociation of IL-10$^{-/-}$ mice with either *Enterococcus faecalis* or *E. coli* UNC resulted in differences in the localisation and in the kinetic onset of the inflammation. *Enterococcus faecalis*-monoassociated mice developed distal intestinal inflammation within 12 wk, whereas IL-10$^{-/-}$ mice monoassociated with *E. coli* UNC developed a predominantly caecal inflammation with a more rapid onset (3 wk) but a less intense manifestation than observed for the *Enterococcus faecalis*-monoassociated IL-10$^{-/-}$ mice (Kim *et al.*, 2005a). Other potentially pathogenic bacteria, such as *Pseudomonas fluorescens*, which has been implicated in CD pathogenesis (Wei *et al.*, 2002), failed to induce inflammation in IL-10$^{-/-}$ mice, suggesting that only certain bacterial species are capable of inducing colitis in this animal model (Kim *et al.*, 2005a).

Besides environmental factors, also inheritable genetic factors are important for the disease development in IL-10$^{-/-}$ mice: More severe intestinal inflammation, characterised by an earlier

onset and higher histopathological score, was observed in IL-10^{-/-} mice with a 129/SvEv, a BALB/c or a C3H/HeJBir background compared to IL-10^{-/-} mice with a C57BL/6 background (Berg *et al.*, 1996; Bristol *et al.*, 2000).

1.3 Host – microbe interactions

While the influence of the intestinal microbiota on the physiology and pathophysiology of the mammalian host is studied in detail, little is known about the impact of host derived factors on the intestinal microbiota. First indications for a cross-talk between the gut microbiota and the mammalian host came from the studies by Hooper *et al.* (1999). Using mice monoassociated with *Bacteroides thetaiotaomicron*, they identified the bacterial signal that stimulates the host to produce fucosylated glycoconjugates. In turn, the presence of L-fucose induces the expression of fucose-utilising enzymes in *B. thetaiotaomicron*, enabling the bacterium to use it as a carbon source. Vogel-Scheel *et al.* demonstrated that *E. coli* specifically adapt to the conditions in the mouse intestine by changes in protein expression. Especially proteins needed for purine and pyrimidine synthesis were upregulated in *E. coli* isolated from caecal contents in comparison to *E. coli* grown *in vitro* under conditions mimicking the murine intestine (Vogel-Scheel *et al.*, 2010). In fact, it was shown that the intestinal concentrations of purines and pyrimidines are low and therefore *E. coli*'s colonisation efficiency depends on the ability to synthesise nucleotides. Rothe *et al.* (2012) demonstrated the impact of nutritional factors on the bacterial protein expression in the murine gut. In mice fed a lactose-rich diet, intestinal *E. coli* induce the Leloir pathway enzymes, which are required for the utilisation of lactose-derived galactose. Hence, host-derived and dietary factors influence the bacterial protein expression in the intestine, which may affect the host.

As mentioned above, intestinal inflammation leads to changes in the gut microbiota composition, which is characterised by a decrease in obligate anaerobic bacteria and an increased relative abundance of facultative anaerobic bacteria belonging to the family of Enterobacteriaceae (such as *E. coli*), which are supposed to fuel the inflammatory process (Darfeuille-Michaud *et al.*, 2004; Kim *et al.*, 2005a; Wohlgemuth *et al.*, 2009). Therefore, the identification of inflammation-associated environmental factors that influence intestinal microbiota composition may help to develop new strategies for IBD therapy. Recently, it was shown that *E. coli*, unlike obligate anaerobic members of the gut microbiota, can utilise host-derived nitrate as terminal electron acceptor for anaerobic respiration, which enables *E. coli* to edge out other bacteria (Winter *et al.*, 2013). Furthermore, Patwa *et al.* (2011) investigated the adaptation of intestinal *E. coli* UNC to the gut inflammation in IL-10^{-/-} mice. *E. coli* UNC invade IECs and macrophages, and thereby stimulate the production of proinflammatory cytokines. Due to the lack of the anti-inflammatory cytokine IL-10, these mice are unable to

counteract this proinflammatory response and a perpetuating intestinal inflammation develops. During this process ROS and RNS, as well as several antimicrobial peptides are produced to restrict the bacterial invasion (Fig. 3). Patwa *et al.* demonstrated that the intestinal inflammation mostly induces *E. coli*'s stress-response genes (*ibpB*, *ibpA*, *oxyS*), which generally are believed to help the bacteria in dealing with ROS and RNS. However, in contrast to these findings, deletion of the small heat shock proteins *ibpA* and *ibpB* resulted in higher bacterial cell numbers under both, control and inflammatory conditions in comparison to the *E. coli* wildtype strain, an effect, which could not be explained by the authors. Nevertheless, this study clearly demonstrates that intestinal inflammation causes bacterial stress, which is compensated by an induction of stress response proteins.
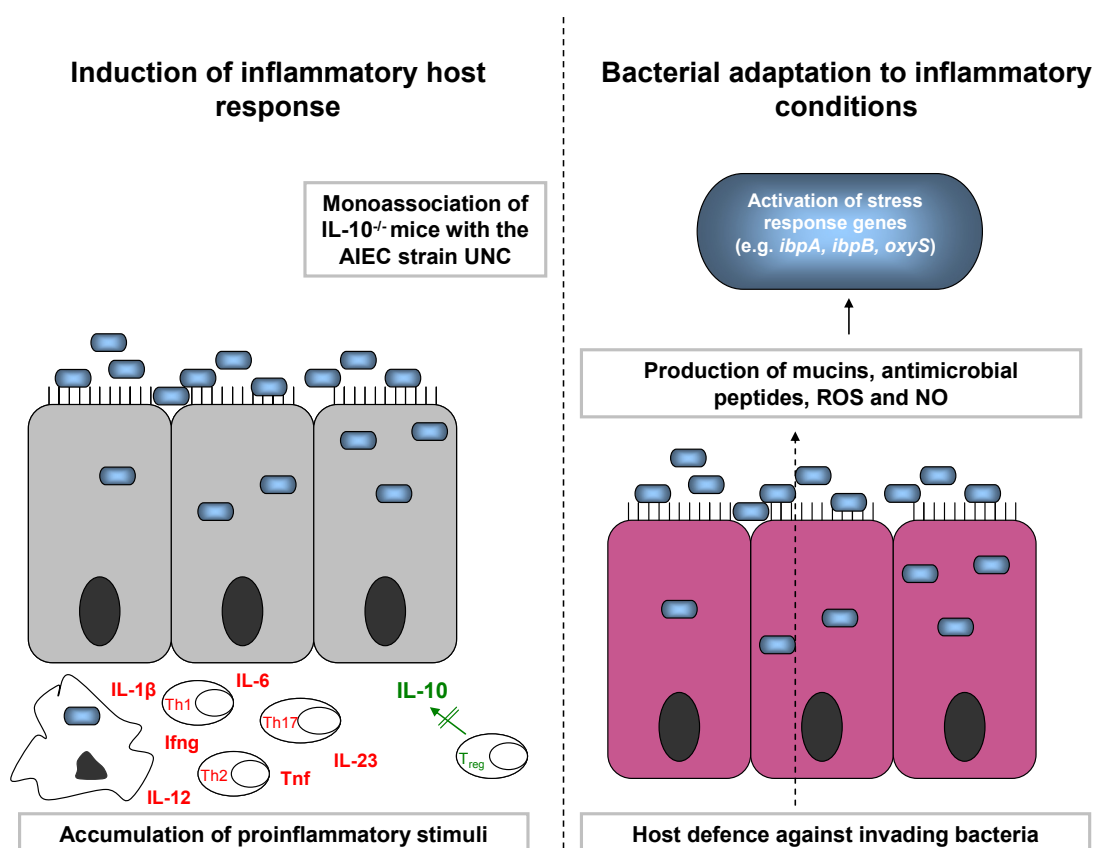
Fig. 3   Host - microbe interactions in IL-10$^{-/-}$ mice monoassociated with *E. coli* UNC
Mice lacking the anti-inflammatory cytokine IL-10 were monoassociated with the adherent-invasive *E. coli* (AIEC) strain UNC. This *E. coli* strain has the ability to adhere and invade intestinal epithelial cells as well as macrophages leading to a production of proinflammatory stimuli. Due to the lack of IL-10, the proinflammatory host response prevails and an intestinal inflammation develops. During this process, the host produces several "antimicrobials", such as reactive oxygen species (ROS) and nitric oxide (NO), mucins, and antimicrobial peptides that stress the bacteria and activate the bacterial stress response regulons.

2 OBJECTIVES

The prevalence of IBD is dramatically increasing in western countries and it is becoming a global disease. A common feature of IBD is the strong proliferation of intestinal *E. coli* (Darfeuille-Michaud *et al.*, 1998; Swidsinski *et al.*, 2002; Baumgart *et al.*, 2007; Kotlowski *et al.*, 2007; Sasaki *et al.*, 2007). Even though the identification of inflammation-associated *E. coli*-derived factors may help to develop new strategies for IBD therapy, the exact role of this species in the disease development is far from being understood. Until today, only few publications investigated *E. coli*'s adaptation to the inflammatory conditions in the intestine and also the strain-specific differences between probiotic and potentially pathogenic *E. coli* have been insufficiently studied.

Therefore, this PhD-thesis aimed to identify *E. coli* proteins that influence the health status of the host. Since the spectrum of pathology in IBD patients ranges from a chronic indolent state of disease to an acute fulminant disease, two different mouse models of intestinal inflammation were used. In the first model, *E. coli*'s response to a severe DSS-induced inflammation was studied, while IL-10$^{-/-}$ mice were used to elucidate the bacterial response to a mild form of an intestinal inflammation. To study the molecular basis for strain-specific differences between probiotic and potentially pathogenic *E. coli*, all mice were monoassociated either with the probiotic *E. coli* Nissle or the AIEC strain UNC.

Using a proteomic-based approach it was intended to analyse if:

- Intestinal inflammation leads to changes in the proteome of intestinal *E. coli*

- The bacterial adaptation differs between the state of a severe and a mild intestinal inflammation

- *E. coli*'s response influences the health status of the host

- The probiotic nature of *E. coli* Nissle and the potentially pathogenic behaviour of *E. coli* UNC are based on differences in their proteome

3 MATERIAL AND METHODS

3.1 Bacterial strains

The colitogenic *E. coli* strain UNC was a kind gift from Dirk Haller (Technical University Munich, Germany). The commercial product Mutaflor (Ardeypharm, Germany) served as the source for *E. coli* Nissle. *E. coli* K-12 MG1655 (CGSC 6300) was kindly provided by K. Schnetz (University of Cologne, Germany). For association of germ-free mice with *E. coli*, the strains were freshly grown in LB-Lennox medium (10 g/liter tryptone, 5 g/liter yeast extract, 5 g/liter NaCl) at 37°C to an optical density at 600 nm (OD_{600}) of 0.5 to 0.7 (SmartSpec Plus; Bio-Rad). Bacteria were collected by centrifugation (10.000 x g, 5 min, 4°C). The pellet was resuspended in sterile phosphate-buffered saline (PBS; 37 mM NaCl, 2.7 mM KCl, 4.3 mM Na_2HPO_4, 1.47 mM KH_2PO_4 [pH 7.4]) and *E. coli* were administered by oral gavage.

3.2 Animal experiments

3.2.1 DSS-induced intestinal inflammation

3.2.1.1 Animals and study procedure

To investigate the effect of a severe intestinal inflammation on the proteome of intestinal *E. coli*, the DSS-induced colitis model was used. Germ-free male and female 129/SvEv mice were housed within sterile Trexler type isolators until they were 6 to 10 wk old. To confirm the germ-free status of the animals, faecal material was Gram-stained and analysed by microscopic inspection. Furthermore, fresh faecal material was plated on Columbia sheep blood agar (bioMérieux, Germany) and incubated overnight under aerobic and anaerobic conditions at 37°C.

Each mouse was orogastrically inoculated with 1 x 10^7 cells of *E. coli* Nissle or *E. coli* UNC and kept in individually ventilated cages for the duration of the experiment. During this time, the mice had free access to radiated (50 kGy) feed (Altromin fortified type 1310; Altromin, Germany) and autoclaved water.

The mice of the control group were kept under these conditions over 21 days. Seven days after association, the mice of the DSS-group were treated for 7 days with 3.5% (wt/vol) DSS (MP Biomedicals, France) in the drinking water, followed by 2 days with sterile drinking water without DSS. At the end of the experiment, all mice were killed by cervical dislocation. To determine the disease severity, animal weight and colon length were determined. Furthermore, caecal and colonic tissues were collected for histopathology or alternatively for

the isolation of IECs. Caecal and colonic contents were collected for the isolation of intestinal *E. coli*.

3.2.1.2 Histopathology scoring

Caecum and colonic swiss rolls were fixed in 10% neutral buffered formalin, embedded in paraffin and sectioned at a thickness of 4 μm. The slices were stained with hematoxylin and eosin (H&E) or with an anti-CD3 antibody (Dako, Germany) in order to quantify intraepithelial lymphocytes. The severity of inflammation was assessed on blinded samples according to the method of Burich *et al.* (2001), using a scale of 0 (no inflammation) to 28 (severe inflammation). Each section was scored for the following categories: cellular infiltration, crypt hyperplasia, goblet cell depletion, edema, architectural distortion, and the area involved. The scoring was performed by Susanne Mauel (Freie Universität Berlin, Department of Veterinary Medicine).

3.2.1.3 Isolation of intestinal epithelial cells

To determine the caecal and colonic cytokine gene expression as an additional marker for disease severity, IECs were isolated from animals that had not been used for the histopathological scoring. Caecum and colon were opened longitudinally and washed in Dulbecco's PBS (PAA, Austria). The tissues were cut into pieces and incubated for 15 min under continuous shaking at 37°C in 20 ml of Dulbecco's Modified Eagle's Medium (DMEM; PAA, Austria) containing 1 mM dithiothreitol (DTT, GE Healthcare, Sweden). After filtration through a tea strainer, the remaining tissue was incubated in 20 ml of PBS containing 1.5 mM ethylenediaminetetraacetic acid (EDTA; Fluka, Germany) for additional 10 min at 37°C under continuous shaking. The cell suspension was again filtered and the resulting filtrate was combined with that from the first filtration. The obtained filtrate was centrifuged (300 x g, 7 min, 4°C) and the cells were resuspended in 5 ml of DMEM. Finally, the IEC suspension was purified by centrifugation (600 x g, 30 min, 4°C) through a 20 - 40% discontinuous Percoll (Sigma-Aldrich, Germany) gradient. The upper layer containing the IECs was collected for the isolation of ribonucleic acid (RNA) and protein by centrifugation (300 x g, 5 min, 4°C) and subsequent resuspension in either 300 μl of RLT® buffer (RNeasy Mini Kit, Qiagen, Germany) for the isolation of RNA or 200 μl of lysis buffer (8 M urea, 2 M thiourea, 4% CHAPS, 25 mM Tris; pH 8.0) for the isolation of proteins.

The IECs of the control animals were isolated from combined caecum and colon tissue, while IECs from the DSS-treated animals were isolated separately for caecal and colonic tissue. Western blot analysis was performed to confirm the purity of IECs and the absence intraepithelial lymphocytes (3.3.3).

3.2.1.4   Isolation of intestinal *E. coli* and determination of *E. coli* cell numbers

To isolate intestinal *E. coli* for proteome analysis, caecal and colonic contents were collected, weighed, and diluted 1:10 (wt/vol) with PBS containing a protease inhibitor mixture (100-fold dilution; GE Healthcare, Sweden), which inhibits serine, cysteine, and calpain proteases. After homogenisation of intestinal contents by agitation with a Uniprep 24 gyrator (speed 2; UniEquip, Germany) in the presence of glass beads (diameter 2.85 to 3.33 mm), the samples were centrifuged (300 x g, 5 min, 4°C) to remove coarse particles originating from the feed. Cell numbers in the supernatants were determined by plating serial dilutions on LB-Lennox agar (Roth, Germany) and incubating them aerobically overnight at 37°C.

The remaining supernatants were centrifuged (10.000 x g, 5 min, 4°C) and the bacterial pellets were resuspended in 500 µl of washing buffer (10 mM Tris; pH 8, 5 mM magnesium acetate, 30 mg/ml chloramphenicol, protease inhibitor mix [diluted 1:100]). The resulting supernatants were collected for the determination of bacterial fermentation products and dietary substrates (3.5). The bacterial cells were subsequently isolated by Nycodenz gradient centrifugation as follows: 500 µl of 40% (wt/vol) Nycodenz solution (Axis-shield, Norway) was overlayed with 500 µl of the bacterial cell suspension and centrifuged for 15 min at 186.000 x g and 4°C. The resulting *E. coli* interphase was collected and washed 4 times with washing buffer; the washed cells were stored at -80°C.

3.2.2   Intestinal inflammation in IL-10$^{-/-}$ mice

3.2.2.1   Animals and study procedure

To investigate the bacterial response towards a very mild intestinal inflammation, the IL-10$^{-/-}$ mouse model was used. Germ-free 7 to 10 wk old male IL-10$^{-/-}$ and wildtype mice (both C3H background) were orogastrically inoculated with 1 x 10^7 *E. coli* cells (either *E. coli* Nissle or *E. coli* UNC). During the whole experiment, the animals had free access to radiated (50 kGy) feed (Altromin fortified type 1310; Altromin, Germany) and autoclaved water. Five animals per group were killed by cervical dislocation 3 or 8 wk after monoassociation (wildtype mice only after 8 wk). The experiments with gnotobiotic IL-10$^{-/-}$ animals were conducted at the Central Animal Facility of the Hannover Medical School, while the experiments with the wildtype mice were performed at the Max-Rubner-Laboratory of the German Institute of Human Nutrition Potsdam-Rehbruecke. Animal weight was determined at the end of the experiment and tissue samples from caecum were taken for histopathological analyses. Furthermore, caecal mucosa was scraped for the preparation of RNA. To isolate caecal *E. coli* for the preparation of RNA, approximately 50 mg of freshly harvested caecal contents were resuspended in 500 µl of AquaStool (MoBiTec, Germany). After centrifugation (300 x g, 5 min, 4°C) the resulting supernatant containing the *E. coli* cells was collected and stored at

-80°C. The remaining caecal contents were used for the isolation of *E. coli* for proteome analysis as described under 3.2.1.4.

3.2.2.2   Histopathology scoring

Caecal tissues were fixed in 10% neutral buffered formalin, embedded in paraffin, sectioned at 4 µm and stained with H&E. The disease severity was assessed on blinded samples according to a modified protocol based on Burich et al. (2001) using a scale of 0 (no inflammation) to 12 (severe inflammation). The following categories were evaluated: degree of lamina propria and submucosal mononuclear cellular infiltration, crypt hyperplasia, goblet cell depletion, architectural distortion and edema. The scoring was performed by Prof. Robert Klopfleisch (Freie Universität Berlin, Department of Veterinary Medicine).

3.3   Protein biochemical methods

3.3.1   Bradford protein assay

The protein concentrations of the bacterial and the murine samples were determined in a 96-well plate-format using the method described by Bradford (1976). Ten µl of the sample was mixed with 200 µl of the 1:5 diluted Bradford solution (Coomassie Brilliant Blue G 250 dye, Bio-Rad, Spain). After 15 min incubation at room temperature, the absorbance was measured at 595 nm (Tecan Infinite F200 Pro microplate reader, Tecan Group Ltd., Switzerland) and the protein concentration of the sample was calculated from a standard curve using 20 to 300 µg/ml of bovine albumin fraction (Roth, Germany).

3.3.2   Two-dimensional gel electrophoresis

The proteome of intestinal *E. coli* was determined by 2D gel electrophoresis, which is a powerful method for the analysis of complex protein mixtures extracted from various biological samples. In the first dimension, the isoelectric focusing (IEF), the proteins are separated according to their isoelectric points. In the second dimension, the sodium dodecyl sulphate-polyacrylamide gel electrophoresis (SDS-PAGE), the proteins are separated according to their molecular weights. Thus, theoretically each spot of the resulting 2D gel potentially corresponds to a single protein. Differentially expressed proteins can be identified by mass spectrometry.

3.3.2.1   Preparation of bacterial protein extracts

Bacterial protein extracts were obtained from caecal bacteria isolated as described under 3.2.1.4. Frozen cells were thawed on ice and resuspended in 800 µl of lysis buffer containing 8 M urea, 30 mM Tris, and 4% (wt/vol) CHAPS (pH 8.5). After 5 min incubation on ice, the cells were mechanically disrupted with 1.2 g zirconia-silica beads (0.1 mm; Roth, Germany)

in an FP120 FastPrep cell disruptor (speed: 4.0 m/s; Thermo Scientific, USA). Intact cells were removed by centrifugation (14.000 x g, 20 min, 4°C). To eliminate deoxyribonucleic acid (DNA) and RNA, the samples were incubated with 125 U of Benzonase (Novagen, Germany) at 37°C for 5 min. In addition, components interfering with the proteomic analysis were removed by selective precipitation using the 2D Clean-Up Kit (GE Healthcare, Sweden) according to the manufacturer's protocol. The pH of the protein solution was adjusted to pH 8.5 using 50 mM NaOH for an optimal reaction with the CyDyes in the following step (3.3.2.2). The protein concentrations were determined with the Bradford protein assay (3.3.1).

3.3.2.2   Sample preparation for the isoelectric focusing

Different procedures were used for the detection and the identification of differentially expressed proteins: Analytical gels were prepared for the detection, whereas preparative gels were run for the identification of proteins by mass spectrometry.

Analytical gels took advantage of the 2D fluorescence difference gel electrophoresis (2D-DIGE) technique. Prior to the electrophoresis, the proteins were labelled with different fluorescent cyanine minimal dyes (CyDyes), enabling an accurate analysis of differences in the protein abundance between the samples. Furthermore, with this method it is possible to analyse up to three different samples within the same 2D gel, which reduces the gel to gel variation (Fig. 4).

According to the manufacturer's protocol, two different samples containing 50 µg of protein were labelled either with the Cy5 or the Cy3 working solution (400 pmol/µl; GE Healthcare, Sweden). Furthermore, equal amounts of each sample were mixed and labelled with Cy2 to be used as an internal standard that is present in each gel. Each labelling reaction was incubated on ice for 30 min in the dark before the reaction was stopped by adding 1 µl of 10 mM lysine. The three labelled samples were mixed and adjusted to a final volume of 450 µl using rehydration buffer (7 M urea, 2 M thiourea, 4% [wt/vol] CHAPS, 1% [vol/vol] IPG buffer, 0.002% [wt/vol] bromophenol blue, and 130 mM DTT). These preparations were simultaneously separated on the same 2D gel.
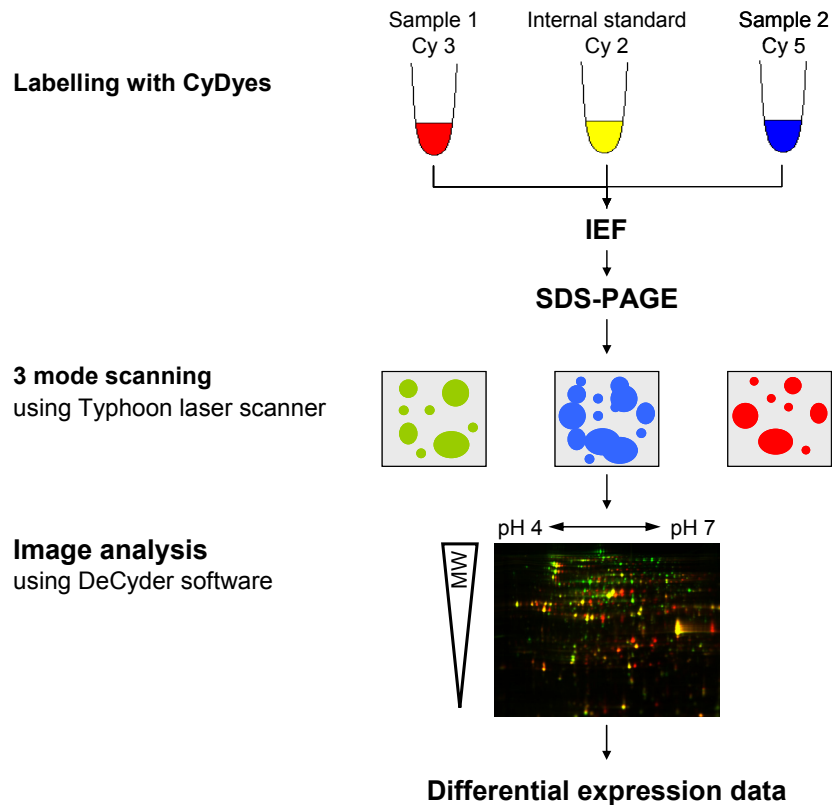
Fig. 4   Outline of the 2D-DIGE workflow
Protein samples that are to be compared are labelled either with Cy3 or Cy5; the internal standard is prepared by labelling equal amounts of each sample with Cy2. Two samples and the internal standard are mixed and separated collectively by IEF and SDS-PAGE. Proteins labelled with different CyDyes exhibit distinct excitation and emission wavelengths, enabling a separate detection on the same gel. Using the DeCyder software, the relative ratios of individual sample spots to the spots of the internal standard are used to accurately compare the protein abundance between the samples. The resulting differentially expressed protein spots are picked from a preparative gel and analysed by mass spectrometry.

For preparative gels, 500 µg of protein were dissolved in a final volume of 450 µl using the rehydration buffer without a preceding labelling step. The proteins were visualised by staining with ruthenium II tris(bathophenanthroline disulfonate) (Rubps) after the SDS-PAGE as described under 3.3.2.5.

3.3.2.3   Isoelectric focusing (First dimension)

Protein separation was performed using the immobilized pH-gradient strips with a linear pH range from 4 to 7 (length: 24 cm). For the analytical gels, active rehydration and IEF were performed in an Ettan IPGphor 3 (GE Healthcare, Sweden) at 20°C according to the following protocol: 30 V for 10 h (active rehydration), 500 V for 1 h, 1.000 V for 1 h, 10.000 V until a total of 61.045 Vhs was reached. For the preparative gels, active rehydration and IEF were performed similarly with minor modifications: 30 V for 10 h (active rehydration), 500 V for 2 h, 1.000 V for 1 h, 10.000 V until a total of 71.544 Vhs was reached. After IEF, the stripes were directly used for the second dimension or stored at -80°C.

3.3.2.4 SDS-PAGE (Second dimension)

To ensure complete polymerisation, 12.5% polyacrylamid gels were casted one day before the run and polymerised overnight. The frozen IEF-stripes were thawed and incubated 15 min in equilibration buffer (6 M urea, 29.3% [vol/vol] glycerol, 2% [wt/vol] SDS, 0.002% [wt/vol] bromophenol blue, and 75 mM Tris; pH 8.8) containing 1% (wt/vol) DTT. Then the solution was replaced by an equilibration buffer containing 2.5% (wt/vol) iodoacetamide and incubated for 15 min with agitation. The stripes were placed on the gel surface and sealed with 0.5% (wt/vol) agarose. The second dimension was run in an Ettan-Dalt II apparatus (GE Healthcare, Sweden) at 1 W per gel for 45 min, followed by 17 W per gel for 3.5 h.

3.3.2.5 Spot visualisation and image analysis

Preparative gels were stained with Rubps (Rabilloud *et al.*, 2001) according to the following procedure: First, the gels were fixed for 1 h in 500 ml fixing solution (30% [vol/vol] ethanol and 10% [vol/vol] acetic acid). Then, this solution was removed and 500 ml fresh fixing solution, containing 0.04 nM Rubps, was added; the gels were incubated overnight at room temperature with agitation.

For the analytical gels, no further treatment is necessary after the SDS-PAGE. Therefore, proteins were directly visualised with a Typhoon Trio laser scanner (GE Healthcare, Sweden) using different excitation (Cy2: 488 nm, Cy3: 532 nm, Cy5: 633 nm) and emission (Cy2: 520 nm, Cy3: 580 nm, Cy5: 670 nm) wavelengths. Image analysis, the matching of analytical and preparative gels, and the generation of pick lists were performed using the DeCyder software, version 6.5 (GE Healthcare, Sweden).

3.3.2.6 Tryptical digestion and NanoLC–ESI–MS/MS

The proteins of interest were excised automatically from the preparative gels using an Ettan-Dalt spot picker (GE Healthcare, Sweden) and subsequently subjected to tryptic digestion by the following procedure: Using a 96-well plate, gel plugs were equilibrated twice with 50 mM NH_4HCO_3 and 50% (vol/vol) methanol for 30 min. Then, the spots were equilibrated with 100% acetonitrile for 10 min. After dehydrating the spots, proteins were digested overnight with 50 ng of trypsin (Promega, USA) in 20 mM NH_4HCO_3 at 37°C. Peptides were extracted from the gel plugs with 50% (vol/vol) acetonitrile and 0.1% (vol/vol) trifluoroacetic acid for 20 min. The tryptically digested proteins were dried by vacuum centrifugation.

Protein identification was carried out using nano-liquid chromatography-electrospray ionization-tandem mass spectrometry (NanoLC–ESI–MS/MS). ProteinLynx Global Server software, version 2.3 (Waters Corporation, Germany), and Swiss-Prot, version 57.2 (http://www.expasy.org/sprot/), were used for processing of MS/MS data and subsequent data bank searching. To eliminate false-positive results, a second search was performed

using a randomised protein database. The NanoLC–ESI–MS/MS and the spot identification were performed by Wolfram Engst (German Institute of Human Nutrition, Analytical group).

3.3.3 SDS-PAGE and Western Blot analysis

To ensure the purity of the IECs isolated under 3.2.1.3, IECs were analysed for CD3$^+$-T cell contamination by Western Blot. The corresponding aliquot collected for the isolation of proteins was thawed on ice and treated with 10 ultrasonic impulses (amplitude 35, Cycle 0.5). After incubating the cell suspension for 30 min on ice, cellular debris was sedimented by centrifugation (14.000 x g, 30 min, 4°C) and the protein concentration was determined in the supernatant with the Bradford assay (3.3.1). Using 5 x Laemmli buffer (0.313 M Tris; pH 6.8, 50% [wt/vol] glycerol, 10% [wt/vol] SDS, 12.5% [vol/vol] β-mercaptoethanol, and 0.0063% [wt/vol] bromophenol blue), protein lysates were adjusted to a concentration of 1 x Laemmli buffer and the proteins were denatured by heating the samples for 5 min to 95°C.

Polyacrylamide gels were casted according to Table 1, and 25 µg of total protein was subjected to electrophoresis (Biometra, Germany; Amperage: 15 mA per gel) in 1 x electrophoresis buffer (25 mM Tris, 192 mM glycine, 3.4 mM SDS, pH 8.5). The separated proteins were subsequently transferred to a nitrocellulose membrane using the Hoefer SemiPhor^{TM} (USA) blotting system. First, the gels, the membranes, and the filter paper were incubated in blotting buffer (25 mM Tris, 100 mM glycine, 15% [vol/vol] methanol, pH 8.3), then the proteins were blotted to the membrane for 2 h and 1.2 mA/cm^2 gel at 4°C.

Table 1   Composition of stacking and resolving gel for SDS-PAGE

	Stacking gel 5.5% AA	Resolving gel 12.5% AA
Aqua bidest	1.53 ml	2.44 ml
40% Acrylamide/Bis-Acrylamide	0.32 ml	1.87 ml
Tris-HCl (0,5 M; pH 6,8)	0.63 ml	-
Tris-HCl (1,5 M; pH 8,8)	-	1.5 ml
10% (wt/vol) SDS	25 µl	60 µl
10% (wt/vol) APS	25 µl	60 µl
10% (vol/vol) TEMED	25 µl	60 µl

AA: Acrylamide/Bis-Acrylamide; APS: Ammonium persulfate;
TEMED: N, N, N', N'-tetramethylethylenediamine

The membranes were subsequently incubated for 1 h in 5% milk powder in Tris-buffered saline containing Tween 20 (T-TBS; 50 mM Tris, 150 mM NaCl, 0.1% [vol/vol] Tween 20, pH 7.5). After blocking, the membranes were washed three times with T-TBS and incubated overnight with the primary antibody at 4°C with agitation. The dilution of the primary antibody in T-TBS was optimised ranging from 1:1.000 (Anti-CD3; Santa Cruz, Germany) to 1:15.000 (Anti-β-actin; Abcam, UK). The membranes were washed 2 to 3 times with T-TBS and

incubated for 1 h with an anti-mouse- or anti-rabbit-detection antibody that was coupled to horseradish peroxidase. Detection was performed using the Supersignal West Dura Chemiluminescent Substrate (Thermo Fisher Scientific, Germany) and the Fuji LAS3000 camera system. To analyse more than one antibody on one membrane, the membranes were stripped using Restore Western Blot Stripping Buffer (Perbio, Germany) followed by blocking with 5% milk powder as described above. As indicated in Fig. 5, IECs were free from contaminating CD3$^+$-T cells.
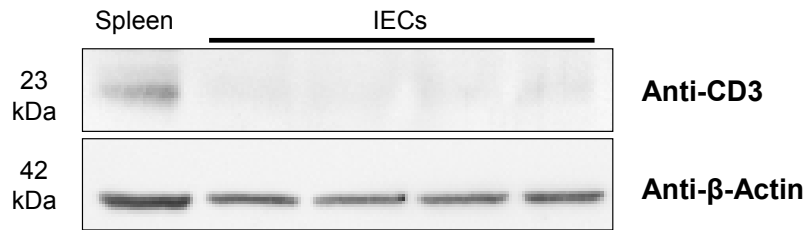
Fig. 5   Purity control of murine intestinal epithelial cells (IECs)
IECs were isolated and purified from mouse intestine. Total protein (25 µg) was subjected to SDS-PAGE and immunoblotting with Anti-CD3 antibody. Murine spleen lysate was used as a positive control, β-actin was used as loading control. The image is representative for all animals.

3.4   Molecular biological methods

3.4.1   Standard PCR and agarose gel electrophoresis

If not mentioned in the text, polymerase chain reaction (PCR) was performed using Dream*Taq* Green DNA Polymerase$^®$ (Fermentas, Germany). One 25 µl reaction contained 1 µl template DNA, 2.5 µl of 10 x Dream*Taq* Green Buffer, 0.4 µl of each 12.5 mM dNTP, 2.5 µl of each 20 µM primer, and 0.25 µl of Dream*Taq*. Amplification was performed in a Thermo Hybaid thermocycler (Thermo Fisher Scientific, Germany) according to the manufacturer's protocol using PCR-specific annealing temperatures and extension times. Since the Dream*Taq* Green buffer includes a density reagent and two tracking dyes, the PCR products were directly separated according to their size using 1 to 2.5% (wt/vol) agarose gels. For that purpose, the respective amount of agarose was dissolved by heating in 1x TAE buffer (40 mM Tris, 0.2 M EDTA, 20 mM acetic acid, pH 8.3). After ethidium bromide staining, the DNA was visualised in the ChemiDoc (Bio-Rad, Germany).

3.4.2   RNA isolation from intestinal epithelial cells

To determine the cytokine gene expression in IECs, the corresponding aliquot for the RNA isolation (see section 3.2.1.3) was thawed on ice and total RNA was isolated using the RNeasy Mini Kit (Qiagen, Germany) according to the manufacturer's instructions. Briefly, one volume of 70% (vol/vol) ethanol was added to the homogenised cell suspension. Then, the sample was transferred to an RNeasy spin column and centrifuged (15 sec, 8.000 x g).

Contaminating DNA was eliminated by on-column DNase digestion for 15 min at room temperature using the RNase-Free DNase Set (Qiagen, Germany). After washing the column twice with RW1$^®$ and RPE$^®$ buffer (both supplied by Qiagen, Germany), the RNA was isolated in diethylpyrocarbonate (DEPC) containing H_2O (0.05% [vol/vol]) and RNA concentrations were determined using the Nanodrop 1000 spectrophotometer (Peqlab, Germany).

3.4.3 RNA isolation from caecal mucosa

To measure the cytokine expression in caecal mucosa of IL-10$^{-/-}$ and wildtype mice (3.2.2.1), total RNA was prepared using peqGOLD TriFast™ (Peqlab, Germany) according to the manufacturer's protocol. The mucosa was ground and a portion of 100 mg was mixed with 1 ml of TriFast reagent. The cells were mechanically disrupted in an FP120 FastPrep cell disruptor (speed: 4.0 m/s) and 200 µl of chloroform was mixed with the cell suspension. After 3 min incubation at room temperature, phase separation was obtained by centrifugation (12.000 x g, 5 min). The upper phase was transferred into a new Eppendorf tube and the RNA was precipitated using 500 µl of isopropyl alcohol followed by centrifugation (12.000 x g, 10 min, 4°C). Subsequently, the RNA pellet was washed two times with 75% (vol/vol) ethanol and then dissolved in 50 µl of DEPC-H_2O (0.05% [vol/vol]). Contaminating DNA was eliminated by TURBO DNA-free™ DNase treatment (Ambion, UK) for 30 min at 37°C. After inactivating the DNase, RNA concentrations were determined using the Nanodrop 1000 spectrophotometer. RNA was stored at -80°C and RNA gels were performed to determine RNA integrity.

3.4.4 RNA preparation from *E. coli*

To confirm *E. coli*'s proteome data, additional bacterial RNA was prepared from *E. coli* isolated from the IL-10$^{-/-}$ and wildtype animals (3.2.2.1). Cells were disrupted with 1.2 g zirconia-silica beads (0.1 mm; Roth, Germany) in a FP120 FastPrep cell disruptor (speed: 4.0 m/s). Cellular debris was removed by centrifugation (14.000 x g, 5 min, 4°C). RNA was precipitated after addition of isopropyl alcohol at a 1:2 ratio, followed by centrifugation (14.000 x g, 5 min, 4°C). The resulting pellet was washed three times with 70% (vol/vol) ethanol and subsequently air-dried. RNA samples from 5 animals per group were pooled by resuspending the respective pellets in 350 µl of RA1 buffer (Macherey-Nagel, Germany). RNA was further purified using the RNA Isolation Kit II (Macherey-Nagel, Germany) according to the manufacturer's protocol, followed by DNase treatment (TURBO DNA-free™).

To verify the *in vivo* results, *E. coli* were grown *in vitro* under conditions mimicking the high ROS levels and the low iron concentrations in the inflamed intestine (3.10.1). The RNA

preparation from these *in vitro* samples was performed similar to the *in vivo* samples, except that the RNA was purified with the RNA Isolation Kit II only, followed by a double treatment with DNase (TURBO DNA-free™).

Absence of DNA contamination was checked by PCR using the purified RNA as a template and 5'-GCGGATCGTCACGTCTACAG-3' as forward primer and 5'-ATGGCGAGCAGTAC AAGCTG-3' as reverse primer; genomic DNA served as a positive control. *E. coli* RNA samples obtained from the *in vivo* samples were analysed for integrity on Agilent Bioanalyzer chips according to manufacturer's instructions (Agilent Technologies, USA), whereas the integrity of the *in vitro* samples was determined using an RNA gel.

3.4.5 RNA gel

To verify the integrity of the isolated RNA, RNA prepared as described under 3.4.3 and 3.4.4 were analysed using horizontal gel electrophoresis. Gels (1.2% [wt/vol] agarose) were prepared by boiling 0.72 g RNase-free agarose (Fermentas, Germany) with 54 ml sterile aqua bidest. After cooling to 70°C, 6 ml of previously autoclaved 10-fold concentrated 3-(N-morpholino)propanesulfonic acid (MOPS) buffer (400 mM MOPS, 100 mM sodium acetate, 10 mM EDTA disodium salt dihydrate, pH 7.2) were added and the gels were casted. Different amounts of RNA, ranging from 2 µg (mucosa) to 200 ng (*E. coli*) were mixed with 2 x RNA loading dye (Fermentas, Germany). After heating to 70°C for 10 min, the RNA was applied to the gel and subjected to electrophoresis using 1 x MOPS buffer (1 h, 100 V). The rRNA bands were visualised after ethidium bromide staining in the ChemiDoc (Fig. 6).
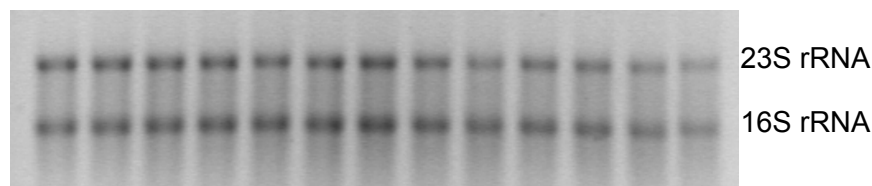
Fig. 6   Representative picture of an RNA gel
RNA was isolated from *E. coli* K-12 and genomic DNA was digested twice by DNase. RNA integrity was confirmed on an RNA gel, showing the presence of an intact 23S and 16S rRNA band (28S and 18S rRNA for murine RNA samples).

3.4.6 Reverse transcription of RNA into cDNA

For complementary DNA (cDNA) synthesis of the murine samples, 0.1 µg (IECs) or 1 µg (mucosa) of RNA were reversely transcribed using RevertAid® H Minus First Strand cDNA Synthesis Kit (Fermentas, Germany). At first, the appropriate volume of RNA was adjusted to 12 µl using 1 µl of 100 µM oligo (dT)18 primer and aqua bidest. This mixture was heated for 5 min to 65°C and then cooled to 4°C. Afterwards, the master mix, containing 1 µl of Ribolock® ribonuclease inhibitor (20 U/µl), 4 µl of 5 x reaction buffer®, 2 µl of 10 mM dNTP,

and 1 µl of RevertAid™ H Minus M MuLV Reverse Transcriptase (200 U/µl), was added and reverse transcription was performed for 1 h at 42°C and 5 min at 70°C in a Thermo Hybaid thermocycler.

For *E. coli* samples, reverse transcription was done similarly but with the following modifications: 1 µg (*in vitro* samples) or 0.1 µg (*in vivo* samples) of RNA were reversely transcribed using 100 pmol Random Hexamer primer instead of oligo (dT) primer. After addition of the master mix, the 20 µl reaction mixture was heated for 5 min to 25°C, 1 h to 42°C and 5 min to 70°C.

3.4.7 Quantitative real time PCR (qPCR)

Murine primers were designed with the program PerlPrimer 1.1.14 (Marshall, 2004), with at least one primer spanning an intron-exon boundary to prevent amplification of genomic DNA. *E. coli* primers were designed with the Vector NTI Suite 9 software according the NCBI gene sequence of the K-12 strain. All primers used for qPCR analysis are listed in Table 2. The primer specificity was first tested by standard PCR followed by agarose gel electrophoresis. The resulting PCR product was isolated from the PCR reaction using High Pure PCR Product Purification Kit (Roche, Germany). qPCR standards were prepared for every gene by diluting these purified PCR products to final concentrations ranging from 1×10^8 to 1×10^2 copies/5 µl. The standard curves were tested for linearity and specificity in the melt curve analysis. The standards were then used for the relative quantification of the samples.

For qPCR, the cDNA samples (obtained as described under 3.4.6) were diluted either 1:5 (IECs) or 1:10 (mucosa and *E. coli*) and 5 µl of each sample was used for quantification in a 7500 Fast Real-Time PCR System (Applied Biosystems, Germany). Each 20 µl reaction mixture contained in addition: 2 µl of 10 x reaction buffer, 4.4 µl of 25 mM $MgCl_2$, 0.8 or 0.4 µl of each 5 µM primer, 0.4 µl of each 12.5 mM dNTP, 0.2 µl of 10 x SYBR Green I, 0.04 µl of 50 nM carboxy-X-rhodamine (ROX), and 0.1 µl of 5 U/µl innu*Taq* HOT-A DNA polymerase®. SYBR Green I (Sigma-Aldrich, Germany) was used as a fluorescence dye, while ROX (Affymetrix, USA) served as a reference. PCR was performed in 96-well PCR plates (Sigma-Aldrich, Germany) according to the standard protocol: 95°C for 2 min, followed by 40 cycles of 94°C for 15 sec, T_a (see Table 2) for 15 sec and 72°C for 15 sec. At the end of the protocol, a melt curve was determined to check PCR specificity. Per PCR run, three replicates per sample were measured. A standard curve and a no template control were included on each plate.

qPCRs of murine samples were normalised to the geometrical mean of the amplification reactions obtained from *Hprt1* (*hypoxanthine guanine phosphoribosyl transferase*) and *Rpl13a* (*ribosomal protein L13A*) as described by Vandesompele *et al.* (2002). qPCRs of *E. coli* samples were normalised to the reference gene *rrsA* (*16S ribosomal RNA*). The

corresponding reference genes were selected because of their constant expression level under the conditions used. Furthermore they were expressed at high levels, ensuring a reliable quantification. Not all samples that were to be compared were analysed on the same PCR plate. Therefore, the same calibrator was included on plates with samples that were meant to be compared, and the gene expression level was always calculated relative to that calibrator.

Table 2   Primer sequences used for qPCR analysis

Gene	Gene ID	Primer sequence (5' → 3')	Product size (bp)	Annealing temperature (T$_a$; °C)
Mus musculus				
Cxcl10	15945	fwd TGGGACTCAAGGGATCCCTC rev TGGCAATGATCTCAACACGTGG	142	62
Hprt1	15452	fwd CGTTGGGCTTACCTCACTGCT rev CATCATCGCTAATCACGACGCT	134	62
Ifng	15978	fwd GCCAAGTTTGAGGTCAACAACCC rev CCGAATCAGCAGCGACTCCT	124	62
Rpl13a	22121	fwd GTTCGGCTGAAGCCTACCAG rev TTCCGTAACCTCAAGATCTGCT	158	60
Tnf	21926	fwd CCTCACACTCAGATCATCTTCTC rev GTCTTTGAGATCCATGCCGT	141	60
E. coli				
ibpA[1]	948200	fwd TTGCTGAGAGCGAACTGGAA rev TCGGCGTGAGCACCTTTC	67	60
ibpB[1]	948192	fwd CGCGCCTGAGCGTAAAAG rev CCTTGATGCAGCCATTTTTTC	64	60
ivy	946530	fwd GGTCATCGCCACCAGTGCAA rev TCACCCAGGCAGGCAGCTTA	122	55
nfuA	947925	fwd CTGGCACGCCTAACGCTGAA rev GGAACCCAACTGGTCGGTAAC	168	55
rrsA[1]	948332	fwd GAATGCCACGGTGAATACGTT rev ACCCACTCCCATGGTGTGA	64	60

[1] Primers and PCR conditions were published by Patwa *et al.* (2011)

3.5 Enzymatic assays

Enzymatic test kits (R-Biopharm, Germany) were used for the determination of dietary substrates (glucose, galactose) and bacterial fermentation products (succinate, formate, and lactate) in the caecal supernatants. The analysis was performed according to the manufacturer's protocol, except that a 96-well plate format was used, which allowed a 20-fold volume reduction of all test components in comparison to the original protocol. Absorption was measured at 340 nm and the concentration was calculated using respective standard curves.

3.6 Determination of caecal indole concentrations

Since the tryptophanase (TnaA) was upregulated in *E. coli* Nissle isolated from control and DSS-treated animals compared to *E. coli* UNC from the respective animals, the TnaA

product, indole, was determined in the caecal supernatants of these animals. The procedure for the determination of indole was based on the method of Mattivi *et al.* (1999), with major modifications: Caecal supernatants were centrifuged (20.000 x g, 5 min, 4°C). For high-performance liquid chromatography, 20 µl of the liquid phase was used. Samples were separated on a LiChrospher 100 RP-18 column (length, 250 mm; inner diameter, 4 mm; particle size, 5 µm; Merck, Germany) at 20°C and at a flow rate of 0.5 ml/min. Solvent A was 1% acetic acid (vol/vol), and solvent B was methanol. The elution was performed using the following gradient: 45 to 72% B in 10 min, 72 to 76% B in 10 min, 76 to 80% B in 3 min, and 80 to 100% B in 5 min. Fluorescence was detected at an excitation wavelength of 225 nm and an emission wavelength of 365 nm with a 100-fold gain (821-FP fluorescence detector; Jasco, Japan). Indole standards (Sigma-Aldrich, Germany) ranging from 0.05 µM to 10 µM were used to calculate the indole concentration in the caecal samples.

3.7 Luciferase reporter gene analysis

Proteomic analysis of both *E. coli* strains isolated from DSS-treated mice, revealed an induction of the Fe-S cluster repair protein NfuA, while the uncharacterised protein YggE was always more highly expressed in *E. coli* Nissle than in *E. coli* UNC. To investigate the role of these proteins in more detail, luciferase reporter gene mutants were generated.

3.7.1 Generation of luciferase reporter gene constructs

Luciferase reporter gene constructs were generated using the pKEST06 vector, which carries the bacterial *luxAB* genes from *Photorhabdus luminescens* (Fig. 7). The *bglB-bglG* homology region was excised from the vector by digestion with the restriction enzymes EcoRI and XbaI (both from Fermentas, Germany). To prevent a recircularisation, the plasmid was incubated after each digestion for 1 h at 37°C with 5 U Antarctic Phosphatase (New England Biolabs, USA). The vector was gel purified, and the DNA was extracted using the InnuPREP Gel Extraction Kit (Analytik Jena, Germany).

Promoter regions of *nfuA* and *yggE* were amplified by PCR from *E. coli* K-12, Nissle or UNC using high fidelity Platinum *Pfx* DNA polymerase[®] (Invitrogen, USA), which was originally isolated from *Pyrococcus* sp. strain KOD1 (Takagi *et al.*, 1997). The 5' end of the primers were flanked by the sequences for the restriction enzymes EcoRI and XbaI and two nucleotides in addition to improve the digestion (Table 3). One 48 µl PCR reaction contained 4.8 µl of 10 x *Pfx* amplification buffer[®], 0.96 µl of 50 mM $MgSO_4$, 0.72 µl of each 20 µM primer, 1.15 µl of each 12.5 mM dNTP, and 0.4 µl of 2.5 U/µl *Pfx* DNA polymerase[®]. Amplification was performed in a Thermo Hybaid thermocycler using the following protocol: 94°C for 5 min and 35 cycles of 94°C for 15 sec, 55°C for 30 sec, and 68°C for 1 min.
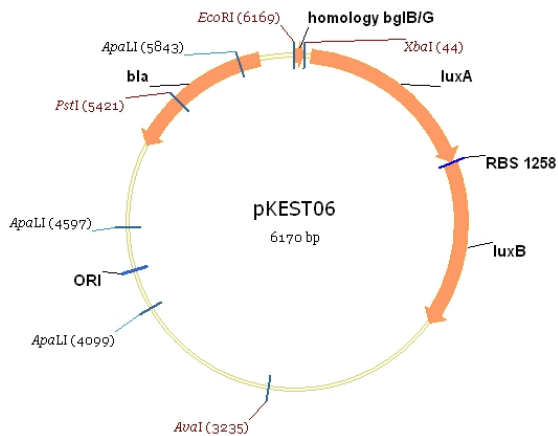
Fig. 7   Schematic representation of the pKEST06 vector
The *bglB-bglG* homology region was excised and replaced by the promoter region of *nfuA* or *yggE* originating either from *E. coli* K-12, Nissle or UNC. The resulting plasmid was then transformed in the corresponding *E. coli* strain.

After the specific amplification was confirmed by agarose gel electrophoresis, the purified PCR products were digested using EcoRI and XbaI according to the manufacturer's instructions (Fermentas, Germany). The amplified fragments were again purified using the High Pure PCR product purification kit and DNA concentrations were determined with the NanoDrop ND-1000 spectrophotometer.

Ligation was performed using 400 U of T4 DNA ligase (New England BioLabs, USA) and 25 ng of vector DNA. The required amount of insert was calculated to reach a plasmid/insert ratio of 1:5 and the ligation mixture was incubated overnight at 4°C. For transformation, 50 µl of electrocompetent *E. coli* K-12, Nissle or UNC were treated with 5 µl of the respective ligation mixture in a Gene Pulser apparatus (Bio-Rad, Germany) (Dower *et al.*, 1988). To select the right clones, the transformed cells were plated on LB-Lennox agar containing 50 µg/ml carbenicillin (Roth, Germany). Positive clones were verified by sequencing (Eurofins MWG Operon, Germany) using plasmid-specific primers (pKEST fwd/rev; Table 3).

Table 3   Primer sequences used for the generation of luciferase reporter gene constructs

Code	Primer sequence (5' → 3')[a]	Restriction enzyme	Annealing temperature (°C)	Product size (bp)
nfuA fwd	CG**GAATTC**ACGTACACGGGCCACTGCGA	EcoRI	55	381
nfuA rev	GC**TCTAGA**GCGTGCCAGGGTTAATCACA	XbaI		
yggE fwd	CG**GAATTC**CAGCGCATTATCAATCTGGT	EcoRI	55	285
yggE rev	GC**TCTAGA**TGACAATATGCGGTCCATCC	XbaI		
pKEST fwd	AAAGTGCCACCTGACGT	-	46	545 (*nfuA*) 449 (*yggE*)
pKEST rev	GGGTTGGTATGTAAGCAA	-		

[a] Boldface letters indicate recognition sites of the respective restriction enzymes

3.7.2 Luciferase reporter gene assay

To determine the activity of the *yggE* and *nfuA* promoters under conditions simulating the inflammatory environment, all three *E. coli* strains containing the respective pKEST06 construct were diluted 1:10 from overnight cultures. They were grown aerobically for 1 h in LB-Lennox medium containing 50 µg/ml carbenicillin and aliquots of 8 ml were transferred to 6-well plates. The cells were stimulated for 1 h with 250 µM 2,2'-dipyridyl (DP; Sigma-Aldrich, Germany) or 300 µM H_2O_2 (Roth, Germany); control cells were left untreated. After incubating the cells at 37°C under continuous shaking (215 rpm), the bacteria were harvested by centrifugation (10.000 x g, 3 min, 4°C) and the pellet was resuspended in 200 µl of ice-cold PBS containing 30 mg/ml chloramphenicol.

The luminescence measurements were carried out in a Luminoscan Ascent plate luminometer (Labsystems, Finland). In a 96-well plate, 5×10^9 bacterial cells were analysed per well after addition of 100 µl of 2% (vol/vol) decanal (Sigma-Aldrich, Germany). Luminescence was measured in triplicates immediately after the addition of the substrate and the results were expressed as relative light units. To calculate the relative luminescence, the luminescence signal of the stimulated bacterial cells was normalised to the luminescence of the controls.

3.8 *nfuA* deletion mutants

The role of NufA in *E. coli*'s adaptational response to the inflammatory process was studied in more detail by generating *nfuA* deletion mutants.

3.8.1 Generation of *nfuA* deletion mutants

Deletion mutants were generated according to the method of Datsenko and Wanner (Datsenko & Wanner, 2000). Briefly, the kanamycin resistance cassette was PCR-amplified from the pKD13 plasmid using primers flanking both, the kanamycin resistance cassette (P1, P2) and the *nfuA* gene (H1, H2) as listed in Table 4. Electrocompetent *E. coli* K-12 cells carrying the pKD46 λ-Red recombinase plasmid were transformed with the purified PCR-product. The Red recombinase catalyses the homologous recombination between the H1/H2 sequences of the PCR product and the genomic sequence. Thereby, the target gene (*nfuA*) is replaced by the kanamycin resistance cassette (Fig. 8). Mutant candidates were tested for the loss of the target gene by PCR with kanamycin- and locus-specific primers (Kt/K2; Table 4). In addition, the genotype of each mutant was confirmed by sequencing (Eurofins MWG Operon, Germany).

1. **Amplification of kanamycin resistance cassette**

2. **Transformation of *E. coli* K-12 with pKD46 plasmid** carrying the λ-Red Recombinase system

3. **λ-Red catalysed recombination**

4. **Replacement of *nfuA* gene by the kanamycin resistance cassette**
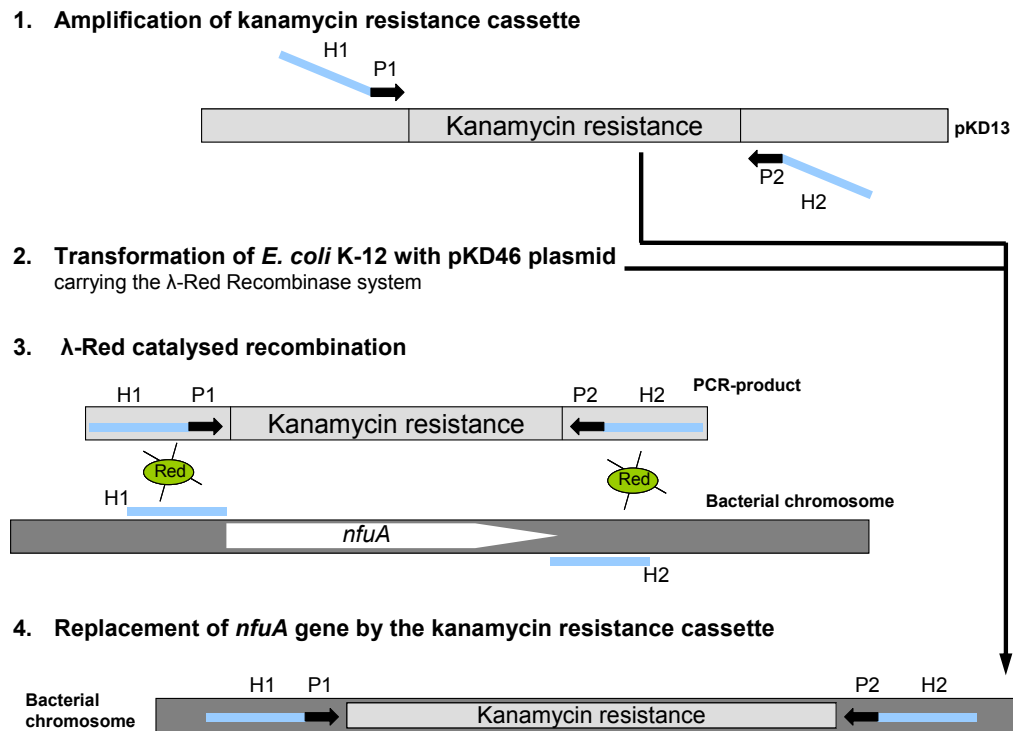
Fig. 8   Procedure for the generation of *nfuA* deletion mutants
H1/H2 refers to the homology extensions or regions, P1/P2 refers to the priming sites.

3.8.2 Growth experiments

Wildtype and Δ*nfuA* cells were inoculated 1:100 from an overnight culture into LB-Lennox medium alone (control) or LB-Lennox medium supplemented with 300 µM paraquat (Sigma-Aldrich, Germany). The cultures were incubated aerobically at 37°C and 215 rpm for 8 h. Growth was monitored by measuring the OD_{600} (SmartSpec Plus, Bio-Rad). The effect of 250 µM 2,2'-dipyridyl was tested in the same way, except that 350 µM $FeSO_4$ (Merck, Germany) was added after 16 h of incubation and growth was monitored for additional 12 h.

3.8.3 Complementation of *nfuA* deletion

To confirm that the differences in the growth phenotype originate from the *nfuA* knock out, *nfuA* was re-introduced into the *nfuA*-deficient cells through the low-copy-number plasmid pSU19 or by insertion of *nfuA* into the chromosomal *lacZ* gene.

The *nfuA* gene was PCR-amplified from *E. coli* K-12 using the primers Comp. fwd and Comp. rev (Table 4), which contain restriction sites for HindIII and BamHI, respectively. The digestion was performed according to the manufacturer's protocol (Fermentas, Germany) and the purified product was cloned into the pSU19 plasmid (Bartolome *et al.*, 1991). The insert including both promoter regions of *nfuA* was verified by sequencing (Eurofins MWG Operon, Germany) and transformed into both, the *E. coli* K-12 wildtype and the Δ*nfuA* strain. In addition, a 1.070 nt HindIII-KpnI fragment of the *nfuA* region was recovered from the

pSU19 construct, inserted into pBRINTs-Cat2, and recombined into the chromosomal *lacZ* gene of the Δ*nfuA* strain as described by Le Borgne *et al.* (2001) resulting in K-12Δ*nfuA lacZ::(nfuA cat)*.

For the growth experiments, *E. coli* cells were grown to the exponential growth phase in LB-Lennox medium (with 20 µg/ml chloramphenicol), collected by centrifugation, and resuspended in fresh medium. The cell suspensions were adapted to equal optical densities (OD$_{600}$) and serially diluted. Five µl of each dilution was spotted onto LB-Lennox plates containing 20 µg/ml chloramphenicol and either 375 µM 2,2'-dipyridyl or 300 µM paraquat.

Table 4   Primers used for the generation and complementation of Δ*nfuA* mutants

Code	Primer sequence (5' → 3')	Short description
DW fwd[a]	ATCGGGCAATCTACAAAAGAGGGGATAACTTA GTAGTAGGAGTGTTCGCCtgtaggctggagctgcttcg	The primers were used for the generation of the *nfuA* knock out.
DW rev[a]	TGGGCGTATTATAACCAACTAAAATAGTCAAC TATTAGGCCATTACTATGattccggggatccgtcgacc	
K2[b]	GCAGTTCATTCAGGGCACCG	The primers were used to test the loss of *nfuA*.
Kt[b]	CGGCCACAGTCGATGAATCC	
Comp. fwd	CG**AAGCTT**ACGTACACGGGCCACTGCGA	The primers were used to clone *nfuA* gene into the pSU19 plasmid.
Comp. rev	GC**GGATCC**TGCGGCACCACGACTGATAC	

[a] Boldface letters indicate the recognition sites for the restriction enzymes; lowercase letters indicate the priming sites P1 and P2. The nomenclature for homology and priming sites is based on the Keio database (http://www.shigen.nig.ac.jp/ecoli/strain/nbrp/explanation/keioCollection.jsp).
[b] Primers were published by Datsenko and Wanner (2000).

3.9   *E. coli* clones overexpressing *ivy*

In *E. coli* obtained from IL-10^{-/-} mice, the inhibitor of vertebrate lysozyme, Ivy, was upregulated in *E. coli* Nissle in comparison to *E. coli* UNC. To investigate the role of Ivy for *E. coli*'s lysozyme sensitivity, *E. coli* overexpressing *ivy* were generated.

3.9.1   Sequencing of the *ivy* gene and its promoter region

High fidelity Platinum *Pfx* Polymerase[®] (Invitrogen, USA) and 5'-CGCGCCCGGTA ATACCTTCCAG-3' as forward primer and 5'-CCGGAAGAGCTGGCGACGAA-3' as reverse primer were used to PCR-amplify the *ivy* promoter and gene regions from *E. coli* K-12, Nissle and UNC as described under 3.7.1. Ten µg of the purified PCR product was sent out for sequencing (Eurofins MWG Operon, Germany).

3.9.2   Generation of clones overexpressing *ivy*

As sequence differences in the coding region of *ivy* were observed between *E. coli* K-12 and *E. coli* Nissle, but not between *E. coli* K-12 and *E. coli* UNC, the corresponding gene sequences of *ivy* were amplified from *E. coli* Nissle and the common lab strain K-12 using 5 U LongAmp *Taq* DNA Polymerase[®] (New England BioLabs, USA) for the generation of dA-

overhangs at the 3'-end. 5'-TAGGAGGTTAATAACATGGGCA-3' was used as forward primer and 5'-CTCCGTTTCTTTATCCGCTAAT-3' as reverse primer. One 50 µl reaction contained 5 µl of 5 x LongAmp *Taq* reaction buffer®, 0.75 µl of each 10 mM dNTP, 1 µl of each 10 µM primer, and 1 µl of LongAmp *Taq*® (5 U). The amplification was performed in a Thermo Hybaid thermocycler using the following protocol: 94°C for 30 sec, 30 cycles of 94°C for 30 sec, 50°C for 60 sec, and 65°C for 50 sec. The amplification was completed by a final step at 65°C for 10 min.

The purified PCR products were ligated into the pGEM-T Easy Vector at a 3:1 ratio and transformed into *E. coli* KRX (both supplied by Promega, USA). After plating on LB-Lennox agar (supplemented with 1 mM isopropyl β-D-1-thiogalactopyranoside [IPTG], 40 µg/ml 5-bromo-4-chloro-indolyl-β-D-galactopyranoside [X-Gal] and 50 µg/ml carbenicillin), the transformed white colonies were tested for the correct insert size by PCR using vector specific T7 (5'-TAA TAC GAC TCA CTA TAGG G-3') and SP6 (5'-GAT TTA GGT GAC ACT ATA G-3') primers. The PCR product was verified by sequencing (Eurofins MWG Operon, Germany).

The correct clones were grown in LB-Lennox medium plus carbenicillin (50 µg/ml) for 4 h at 37°C and shaking at 180 rpm. Ivy was induced by addition of 0.1% rhamnose (Promega, USA). The cultures were incubated overnight at 25°C and 180 rpm and protein expression was controlled by SDS-PAGE as described under 3.3.3 (Fig. 9).
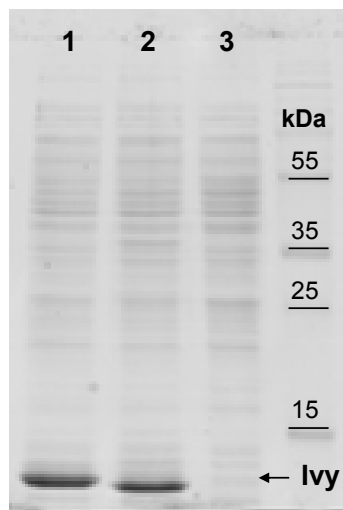
Fig. 9   Induction of Ivy by addition of 0.1% rhamnose
E. coli carrying the pGEM-T-*ivy*EcN **(1)**, the pGEM-T-*ivy*K12 **(2)** or the empty the pGEM-T Easy vector **(3)** were grown overnight at 25°C in LB-Lennox medium supplemented with 50 µg/ml carbenicillin and 0.1% rhamnose to induce *ivy* expression. Cells were harvested by centrifugation and the proteins were isolated. For SDS-PAGE, 10 µg of protein were used per well.

3.9.3   Growth experiments

For growth experiments, overnight cultures of *E. coli* containing the pGEM-T-*ivy*EcN, pGEM-T-*ivy*K12 or the empty pGEM-T Easy vector were diluted 1:33 into fresh LB-Lennox medium supplemented with 50 µg/ml carbenicillin and 0.1% rhamnose. Subsequently, 1 ml aliquots were transferred to 12-well plates and grown aerobically for 2.45 h in the Tecan Infinite F200 Pro microplate reader at 30°C and shaking at 218 rpm. OD_{600} was measured

every 15 min. Cells were treated with 2.5 mg/ml lysozyme (Sigma-Aldrich, Germany) in Tris-EDTA-buffer (final concentration: 2.44 mM Tris, 1.22 mM EDTA, pH 7.2). Growth was monitored over 11 h and OD_{600} (transformed) was calculated as described previously (Rothe *et al.*, 2013). Briefly, OD_{600} values were calculated to 1 cm path length using the following formula: OD_{600} (transformed) = OD_{600} / 0.1069.

3.9.4 Radial diffusion assay

Radial diffusion assay was performed as described by Möndel *et al.* (2009). Briefly, 10^7 bacterial CFU of *E. coli* KRX carrying either the pGEM-T-*ivy*K12, pGEM-T-*ivy*EcN or the empty pGEM-T vector were inoculated from overnight cultures into 10 ml of warm (~42°C), sterile underlay agar containing 0.03% trypticase soy broth (Merck, Germany), 10 mM sodium phosphate (pH 7.4), 1% SeaKem LE agarose (Cambrex, USA), 0.02% Tween 20 (Promega, USA), 0.1% rhamnose and 50 µg/ml carbenicillin. The bacteria were dispersed by vortexing and the liquid agar was poured into Petri dishes. Small wells were punched into the solidified agar and the following test substances were added to the wells: One µg of lysozyme or 0.5 µg of hBD-2 (Biotrend, USA) dissolved alone or in combination in 5 µl of 10 mM acetic acid; acetic acid (10 mM) served as vehicle control. The plates were incubated for 3 h at 30°C and subsequently overlayed with 10 ml of previously autoclaved warm (~42°C) top agar (6% trypticase soy broth, 1% SeaKem LE agarose, 0.1% rhamnose and 50 µg/ml carbenicillin) and incubated for 3 days at 30°C. Bacterial cells were visualised using the ChemiDoc.

3.10 Growth experiments using wildtype *E. coli*

3.10.1 Growth experiments for RNA isolation

To isolate RNA from *E. coli* grown under different *in vitro* conditions (3.4.4), overnight cultures of *E. coli* K-12, Nissle and UNC were 10-fold diluted. The cells were grown aerobically for 1 h in LB-Lennox medium and 5 ml aliquots of the cultures were transferred to 6-well plates. The cells were treated for 30 min either with 300 µM paraquat, 300 µM H_2O_2 or 250 µM 2,2'-dipyridyl; control cells were left untreated. After incubation at 37°C and shaking at 215 rpm, 5 x 10^8 bacterial cells were sedimented by centrifugation (10.000 x g, 3 min, 4°C) and immediately resuspended in RA1® buffer.

3.10.2 Determination of ROS sensitivity

To check, whether the *E. coli* strains differ in their sensitivity to ROS, *E. coli* wildtype strains (K-12, Nissle, and UNC) were precultured aerobically overnight in LB-Lennox medium. The cells were subsequently 1:100 diluted using LB-Lennox medium alone or in combination with

300 µM paraquat. The cultures were grown aerobically at 37°C and 215 rpm for 8 h, and growth was monitored by measuring the OD_{600} in a SmartSpec Plus photometer.

3.10.3 Determination of lysozyme sensitivity

To determine the sensitivity of different *E. coli* strains to lysozyme, overnight cultures of *E. coli* K-12, Nissle and UNC were 100-fold diluted with fresh LB-Lennox medium. Subsequently, 1 ml aliquots of this cell suspension were transfered to 12-well plates and the cells were grown aerobically for 3 h in the Tecan Infinite F200 Pro microplate reader at 37°C and 218 rpm; OD_{600} was measured every 15 min. Cells were then treated either with 2.5 mg/ml lysozyme (Sigma-Aldrich, Germany) in Tris-buffer (final Tris concentration: 2.44 mM, pH 7.2) or with 2.5 mg/ml lysozyme in a Tris-buffer containing 1.22 mM EDTA. As a control, Tris-EDTA buffer without lysozyme was added to the cells. The OD_{600} was measured over 11 h every 15 min and OD_{600} (transformed) was calculated as described under 3.9.3.

3.11 Statistics

Data were analysed using GraphPad Prism Version 5 software (GraphPad, USA). Data were tested for Gaussian distribution by the D'Agostino and Pearson omnibus normality test and the Kolmogorow-Smirnow test. Significance of difference was analysed as indicated in each legend with the Mann-Whitney U-test, the Kruskal Wallis H test or One-way ANOVA. Differences were considered as statistically significant, if $p \leq 0.05$.

4 RESULTS

4.1 The DSS-induced colitis model

4.1.1 Assessment of intestinal inflammation

To evaluate the disease severity in the DSS-treated animals several parameters were determined. First, the weight of the control and DSS-treated animals was measured at the end of the experiment. Independent from the associated *E. coli* strain, the body weight of the DSS-treated animals was approximately 40% lower compared to the respective control mice (Fig. 10A). Furthermore, the weight loss of the DSS-treated animals was calculated from the difference between the weight at the beginning and the weight at the end of the experiment. The results obtained reveal in tendency ($p = 0.06$) a 4-fold higher body weight reduction in the DSS-treated animals monoassociated with *E. coli* UNC compared to the DSS-treated mice associated with *E. coli* Nissle (Fig. 10B).
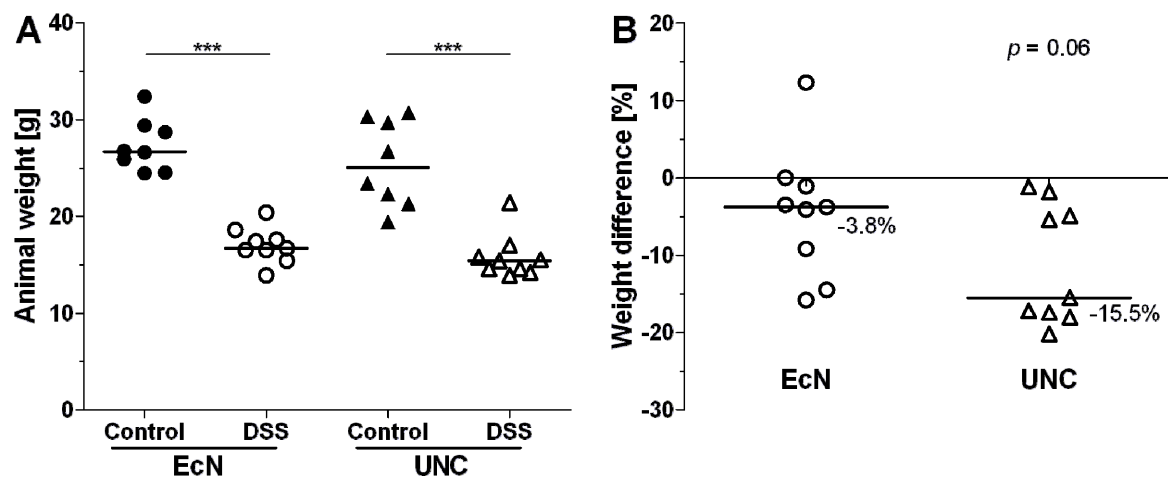
Fig. 10   Influence of DSS-treatment on the animal weight
Germ-free mice (129/SvEv) were monoassociated with *E. coli* Nissle (EcN) or UNC. Mice of the DSS group received 3.5% DSS in sterile drinking water for 7 days, control mice received sterile drinking water without DSS. **(A)** Body weights at the end of the experiment. **(B)** Differences in the body weights of DSS-treated animals calculated from the weight at the beginning and the weight at the end of the experiment. Data are expressed as medians. Mann-Whitney U Test was used for statistical analysis; ***, $p \leq 0.001$.

Morphological changes in the intestinal crypt architecture were examined by histopathological analyses. Fig. 11A shows a representative thin section of the healthy colon from a control mouse monoassociated with *E. coli* Nissle. The epithelial layer and the crypt architecture are intact, and the dimensions of mucosa and submucosa are normal. In comparison to that, the colonic crypt architecture was completely destroyed after DSS administration (Fig. 11B/C). Loss of the epithelial layer, extension of mucosa and

submucosa, as well as infiltration of immune cells were characteristic for the inflamed intestine of the DSS-treated animals. Histopathological scoring revealed a moderate inflammation of the caecum and a severe inflammation of the colon in the DSS group. No differences in disease severity were observed between animals monoassociated with *E. coli* Nissle or that with *E. coli* UNC, neither in caecum nor in colon of DSS-treated mice (Fig. 11D/E). The caecal tissue of the control animals displayed a mild inflammation when they were associated with *E. coli* UNC, but not when they were monoassociated with *E. coli* Nissle.
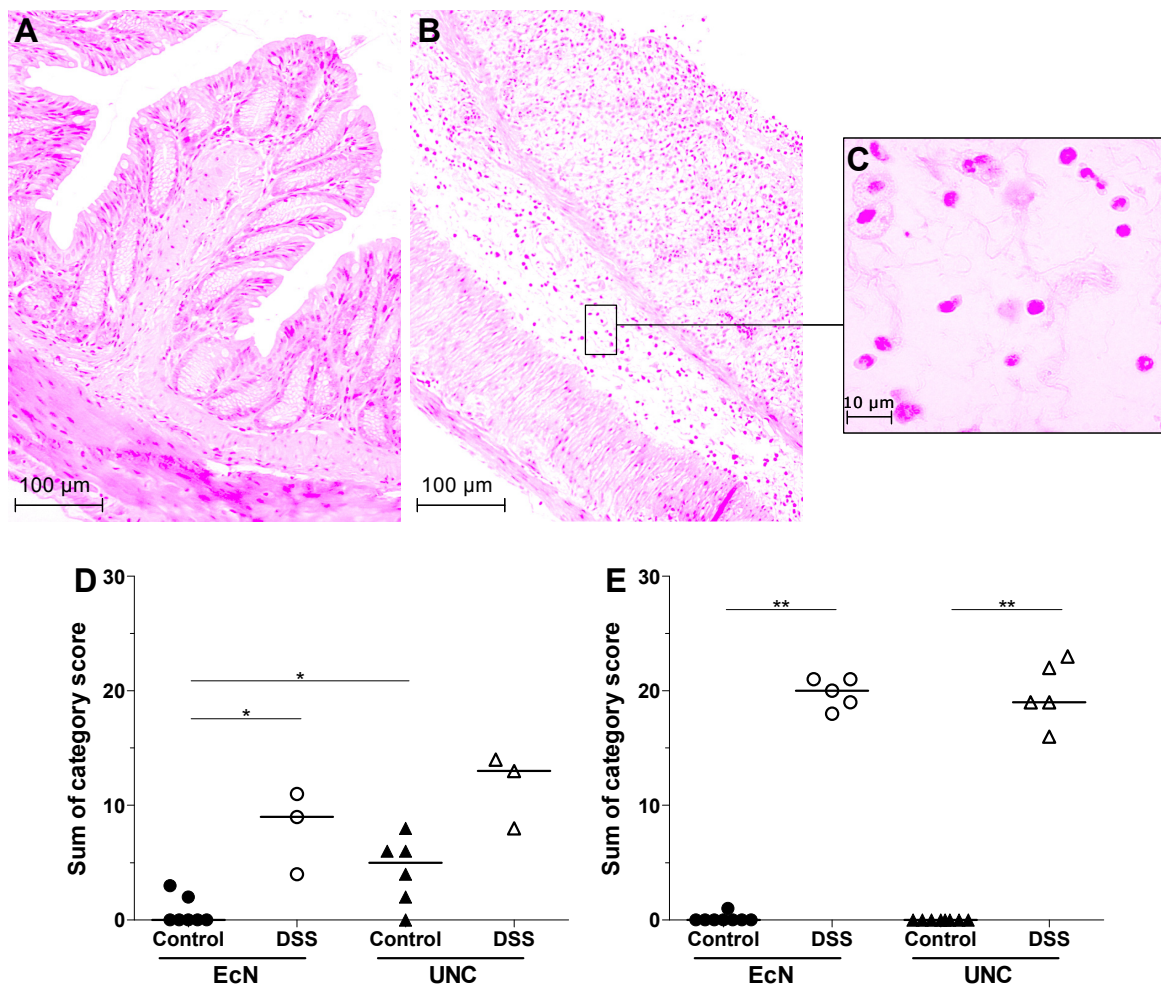
Fig. 11   Histopathology of caecal and colonic tissue from control and DSS-treated mice
Germ-free mice (129/SvEv) were monoassociated with *E. coli* Nissle (EcN) or UNC. Mice of the DSS group received 3.5% DSS in sterile drinking water for 7 days, control mice received sterile drinking water without DSS. **(A)** Light microscopic H&E picture of a healthy distal colon obtained from control mice monoassociated with *E. coli* Nissle. **(B)** Severe inflammation in the distal colon of DSS-treated mice monoassociated with *E. coli* Nissle. **(C)** Infiltration of immune cells in the colonic submucosa of DSS-treated animals. **(D/E)** Sum of histopathology scores (0, no inflammation; 28, severe inflammation) from caecum **(D)** and colon **(E)**. Data are expressed as medians. Mann-Whitney U Test was used for statistical analysis; *, $p \leq 0.05$; **, $p \leq 0.01$.

To evaluate the disease state in more detail, the gene expression of three important proinflammatory cytokines was determined by qPCR. In agreement with the histopathological scoring, *Tnf* and *Ifng* were increased in caecal epithelial cells isolated from *E. coli* UNC associated DSS-animals in comparison to the control group by factors of 8 and 3, respectively. On the contrary, DSS-treated animals monoassociated with *E. coli* Nissle had no increased proinflammatory cytokine expression in the caecum when compared with the respective control animals. In both *E. coli* groups, the colonic epithelial cells isolated from the DSS-treated animals displayed a higher cytokine expression than that of the respective control animals: DSS-treated animals associated with *E. coli* UNC had 39, 10 and 30-fold higher mRNA levels of *Tnf, Ifng* and *Cxcl10* compared to control mice, while DSS-treated mice associated with *E. coli* Nissle had 17, 9, or 15-fold higher mRNA levels than the control mice.
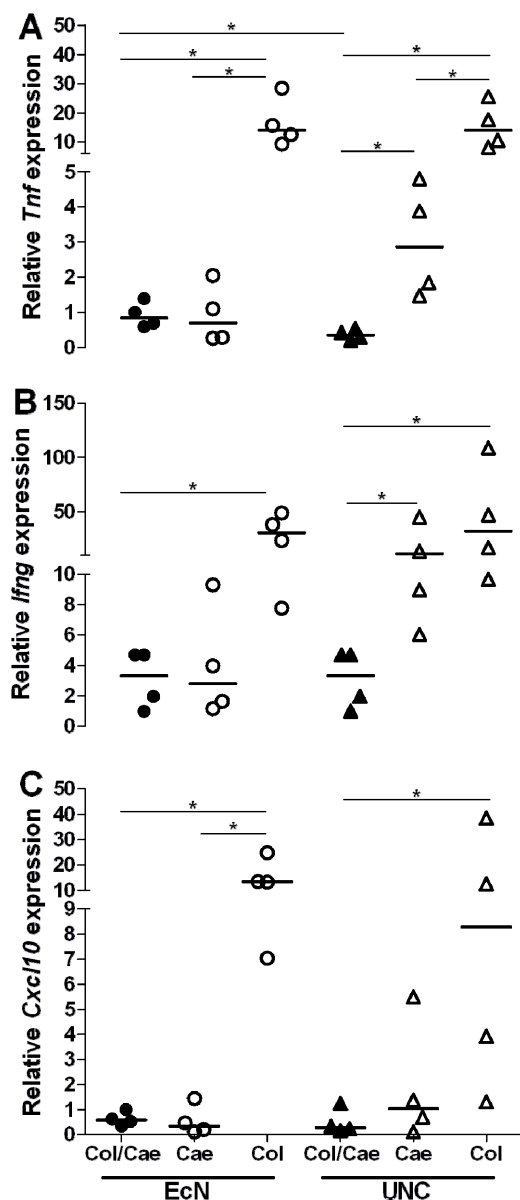
Fig. 12 Proinflammatory cytokine gene expression in control and DSS-treated mice
Germ-free mice (129/SvEv) were monoassociated with *E. coli* Nissle (EcN) or UNC. Mice of the DSS group received 3.5% DSS in sterile drinking water for 7 days, control mice received sterile drinking water without DSS. Epithelial cells isolated from caecal and colonic (Col/Cae) tissues of control mice were combined (filled symbols). Epithelial cells from DSS-treated mice (open symbols) were kept separately from caecum (Cae) and colon (Col). Total RNA was extracted and reversely transcribed into cDNA. Gene expression of proinflammatory cytokines was measured by quantitative real time PCR. Results were normalised to the geometrical means of the amplification reactions with *Hprt1* and *Rpl13a*. **(A)** *Tnf (tumor necrosis factor α)*; **(B)** *Ifng (interferon γ)*; **(C)** *Cxcl10 (chemokine (C-X-C motif) ligand 10)*. Data are expressed as medians. Mann-Whitney U Test was used for statistical analysis; *, $p \leq 0.05$.

Taken together, DSS-treatment resulted in moderate caecal inflammation and in a severe colonic inflammation in animals monoassociated with both, *E. coli* Nissle or *E. coli* UNC. In accordance with the slightly reduced weight loss and the unchanged caecal proinflammatory cytokine expression, DSS-treated animals monoassociated with the probiotic *E. coli* Nissle tended to be less inflamed than animals associated with the AIEC strain UNC.

4.1.2 Bacterial adaptation to acute intestinal inflammation

The primary objective of this PhD-thesis was to investigate the bacterial response towards the host factor intestinal inflammation. In order to check whether acute intestinal inflammation has an impact on the bacterial survival in the gut, the numbers of *E. coli* in the caecum and colon of control and DSS-treated mice were compared. While the cell numbers of *E. coli* Nissle were not affected by intestinal inflammation, bacterial numbers of *E. coli* UNC decreased by approximately 4% and 6% in caecum and colon, respectively (Fig. 13A/B).
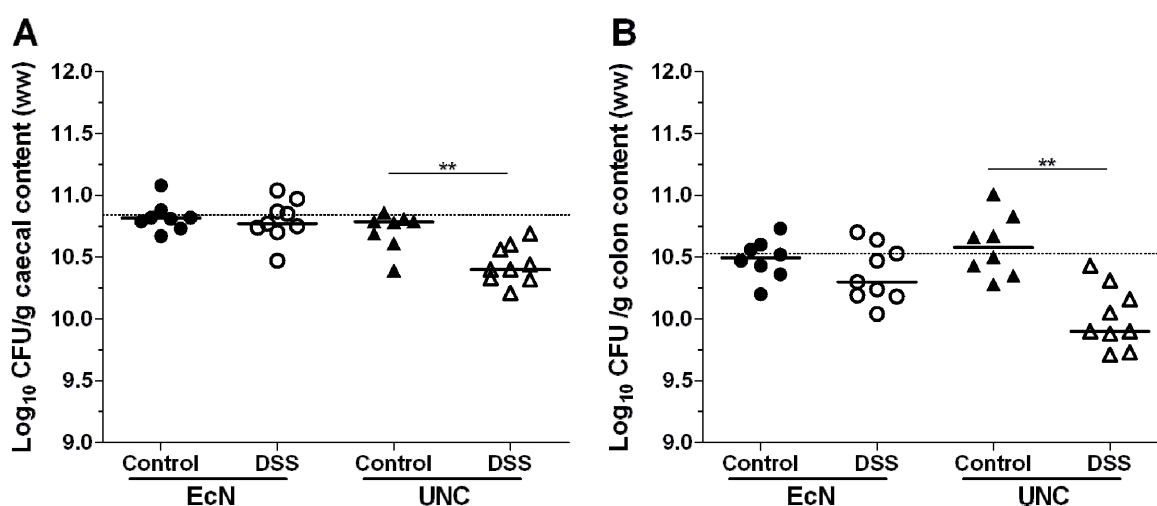
Fig. 13   Determination of intestinal bacterial numbers
Germ-free mice (129/SvEv) were monoassociated with *E. coli* Nissle (EcN) or UNC. Mice of the DSS group received 3.5% DSS in sterile drinking water for 7 days, control mice received sterile drinking water without DSS. *E. coli* were isolated from the caecal contents of control and DSS-treated animals. Bacterial colony-forming units (CFU) in caecal **(A)** and colonic **(B)** contents were determined by plating on LB-Lennox agar. Data are expressed as medians. Mann-Whitney U Test was used for statistical analysis; **, $p \leq 0.01$; ww, wet weight.

To identify bacterial proteins involved in *E. coli*'s adaptation to intestinal inflammation, the expression of caecal *E. coli* proteins was analysed by 2D-DIGE. The principal component analysis (PCA) in Fig. 14 displays a distinct separation between the proteomes of *E. coli* isolated from healthy control mice and from the inflamed DSS-treated animals. Differences between the proteome of the probiotic *E. coli* Nissle and the AIEC strain UNC were also observed.
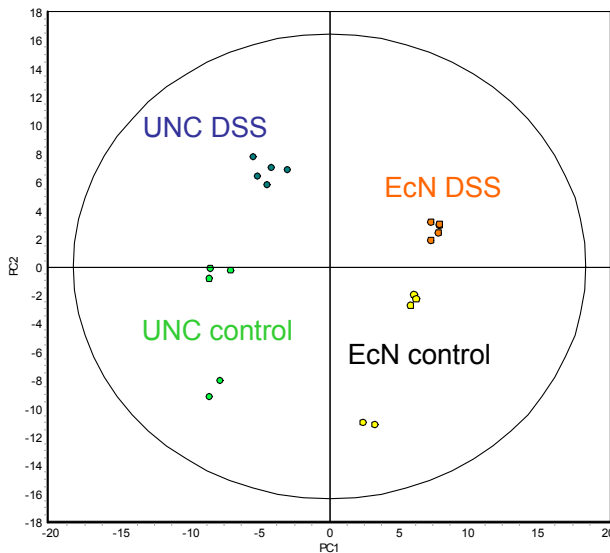
Fig. 14 Principal component analysis (PCA) of the *E. coli* proteome obtained from control and DSS-treated animals.

Germ-free mice (129/SvEv) were monoassociated with *E. coli* Nissle or UNC. Mice of the DSS group received 3.5% DSS in sterile drinking water for 7 days, control mice received sterile drinking water without DSS. *E. coli* were isolated from the caecal contents of control and DSS-treated animals. Proteins were extracted from 4 to 5 animals per group and the bacterial proteome was analysed by 2D-DIGE. PCA was performed using the Extended Data Analysis module of the DeCyder software; EcN, *E. coli* Nissle.

The comparison of *E. coli* isolated from DSS-treated animals vs. *E. coli* isolated from control animals, revealed in *E. coli* Nissle 35 differentially expressed proteins (≥ 3, ≤ -3; $p \leq 0.05$), 24 were downregulated, while 11 were upregulated. In the AIEC strain UNC, 35 proteins were repressed, while 16 were induced by DSS administration (Table 10, Appendix). In both *E. coli* strains, the upregulated proteins are mainly stress response proteins, while the majority of downregulated proteins belong to the carbohydrate metabolism.

Important key enzymes of glycolysis, such as glyceraldehyde-3-phosphate dehydrogenase A and triosephosphate isomerase were downregulated in both *E. coli* strains in response to acute intestinal inflammation. Furthermore, other downregulated enzymes of carbohydrate metabolism are involved in the conversion of carbohydrates (transketolase 1), fermentation (formate acetyltransferase 1), gluconeogenesis (phosphoenolpyruvate carboxykinase), and the metabolism of carbohydrates (Table 5).

Table 5   Downregulation of proteins belonging to the carbohydrate metabolism
Germ-free mice (129/SvEv) were monoassociated with *E. coli* Nissle or UNC. Mice of the DSS group received 3.5% DSS in sterile drinking water for 7 days, control mice received sterile drinking water without DSS. Bacterial proteins were isolated from caecal contents and proteome analysis was performed using the 2D-DIGE technique.

Swiss Prot accession no.	Gene	Protein description	Fold change[a] DSS vs. control
E. coli **Nissle**			
P0A9B2	*gapA*	Glyceraldehyde-3-phosphate dehydrogenase A	-7.06
P0A858	*tpiA*	Triosephosphate isomerase	-4.03
P27302	*tktA*	Transketolase 1	-3.97
P06720	*melA*	Alpha-galactosidase	-3.82
P22259	*pckA*	Phosphoenolpyruvate carboxykinase [ATP]	-3.46
P09373	*pflB*	Formate acetyltransferase 1	-3.15
E. coli **UNC**			
P0A9B2	*gapA*	Glyceraldehyde-3-phosphate dehydrogenase A	-8.41
P0AB71	*fbaA*	Fructose-bisphosphate aldolase class 2	-6.92
P0A858	*tpiA*	Triosephosphate isomerase	-6.10
P09148	*galT*	Galactose-1-phosphate uridylyltransferase	-5.05
P0A6P9	*eno*	Enolase	-4.5; -3.38
P0A6T3	*galK*	Galactokinase	-3.81
P0A799	*pgk*	Phosphoglycerate kinase	-3.61; -3.46
P04982	*rbsD*	D-ribose pyranase	-3.55
P0A9J6	*rbsK*	Ribokinase	-3.46

[a] n = 4/5 per group; fold change ≤ -3, $p ≤ 0.05$

To check whether the downregulation of proteins belonging to the carbohydrate metabolism resulted in a modified carbon catabolism, the concentrations of the bacterial fermentation products were measured in intestinal contents. In agreement with an inhibition of glycolysis and fermentation, the concentrations of the bacterial fermentation products succinate, formate, and lactate were decreased in the DSS-treated animals compared to the control mice (Fig. 15A/B/C). While the concentrations of succinate and formate in the control animals were in the low mM range, almost no fermentation products were detectable in the intestines of the DSS-treated animals (Fig. 15A/B). Lactate was detected only at low concentrations in the caecum of control animals associated with *E. coli* Nissle, but not with *E. coli* UNC (Fig. 15C). In contrast, the caecal carbohydrate levels (glucose and galactose) were not affected by intestinal inflammation (Fig. 15D/E), indicating that a decreased availability of fermentable

substrates was not the cause for the lower concentrations of the bacterial fermentation products in the inflamed animals.
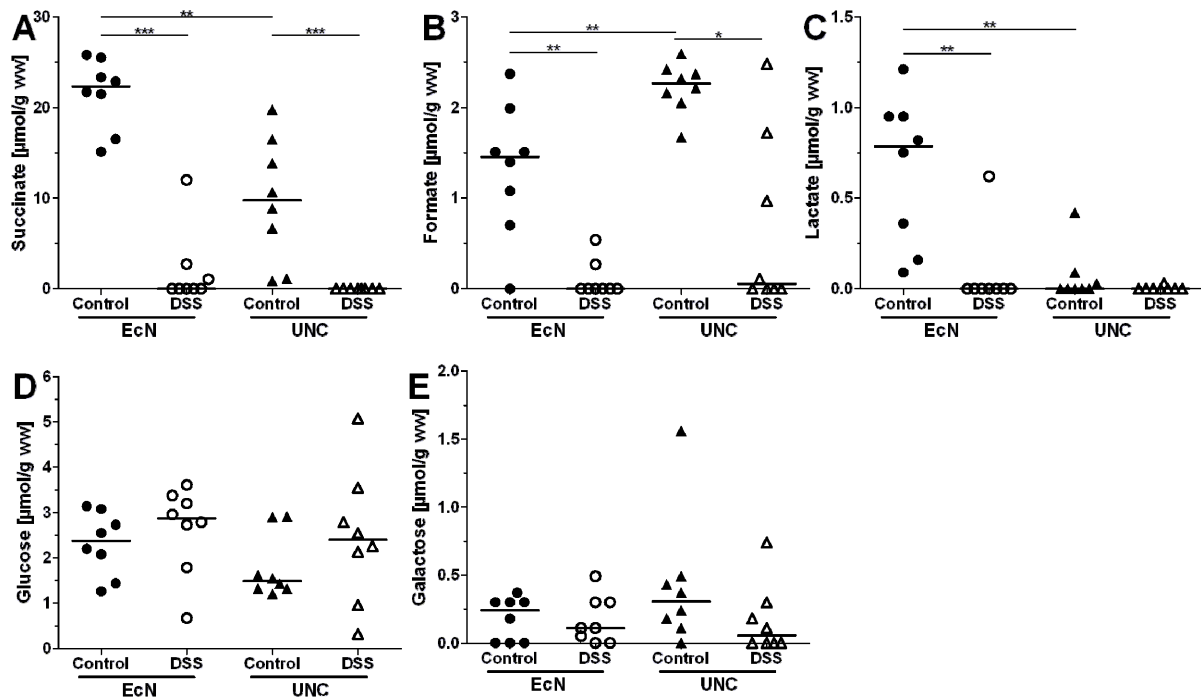
Fig. 15   Concentrations of bacterial fermentation products and dietary substrates
Germ-free mice (129/SvEv) were monoassociated with *E. coli* Nissle (EcN) or UNC. Mice of the DSS group received 3.5% DSS in sterile drinking water for 7 days, control mice received sterile drinking water without DSS. The concentrations of bacterial fermentation products succinate **(A)**, formate **(B)**, and lactate **(C)**, as well as the dietary substrates glucose **(D)** and galactose **(E)** were measured by enzymatic assays in the caecal supernatants of control and DSS-treated animals. Data are expressed as medians. Mann-Whitney U Test was used for statistical analysis; *, $p \leq 0.05$; **, $p \leq 0.01$; ***, $p \leq 0.001$; ww, wet weight.

Both *E. coli* strains replied to intestinal inflammation with an induction of stress response proteins. While the induction of protein RecA, 60 kDa chaperonin, transcription elongation protein NusA, chaperone protein ClpB, alkyl hydroperoxide reductase subunit F, and thiol peroxidase was detected either in *E. coli* Nissle or in *E. coli* UNC, the upregulation of Fe-S biogenesis protein NfuA by factors of 3 (*E. coli* UNC) and 4 (*E. coli* Nissle) was equal for both *E. coli* strains (Table 6).

Table 6 Induction of stress response proteins in the state of acute inflammation
Germ-free mice (129/SvEv) were monoassociated with *E. coli* Nissle or UNC. Mice of the DSS group received 3.5% DSS in sterile drinking water for 7 days, control mice received sterile drinking water without DSS. Bacterial proteins were isolated from caecal contents and proteome analysis was performed using the 2D-DIGE technique.

Swiss Prot accession no.	Gene	Protein description	Fold change[a] DSS vs. control
***E. coli* Nissle**			
P0A7G6	*recA*	Protein RecA	4.46
P0A6F5	*groL*	60 kDa chaperonin	4.13
P63020	*nfuA*	Fe-S biogenesis protein NfuA	3.75
***E. coli* UNC**			
P0AFF6	*nusA*	Transcription elongation protein NusA	6.38
P63284	*clpB*	Chaperone protein ClpB	3.31
P63020	*nfuA*	Fe-S biogenesis protein NfuA	3.13
P35340	*ahpF*	Alkyl hydroperoxide reductase subunit F	3.03
P0A862	*tpx*	Thiol peroxidase	3.00

[a] n = 4/5 per group; fold change ≥ 3, $p \leq 0.05$

4.1.3 Induction of NfuA in response to strong intestinal inflammation

The Fe-S biogenesis protein NfuA, which was upregulated in both, *E. coli* Nissle and UNC isolated from DSS-treated animals (Fig. 16) was selected for further analysis. NfuA plays an important role in the adaptation of *E. coli* K-12 MG1655 to oxidative stress and iron starvation under *in vitro* conditions (Angelini *et al.*, 2008). These factors are also crucial in the state of intestinal inflammation (Harris *et al.*, 1992; Loetscher *et al.*, 2012) and bacteria have to cope with them to survive. A general role of NfuA in the adaptation to intestinal inflammation was therefore hypothesised.
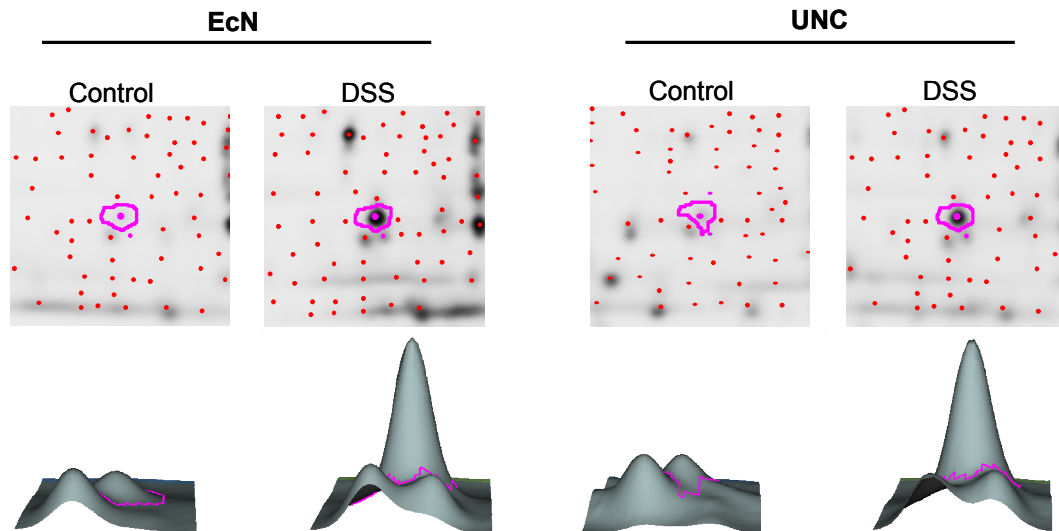
Fig. 16 NfuA protein expression in *E. coli* Nissle (EcN) and UNC
Germ-free mice (129/SvEv) were monoassociated with *E. coli* Nissle or UNC. Mice of the DSS group received 3.5% DSS in sterile drinking water for 7 days, control mice received sterile drinking water without DSS. Bacterial protein samples obtained from the caecal contents of control and DSS-treated mice were analysed using 2D gel electrophoresis. Differences in the spot expression pattern from *E. coli* isolated from control and DSS-treated animals were detected in the gel image as well as in the 3D presentation of the NfuA spot.

To assess the promoter activity of the *nfuA* gene in different *E. coli* strains, luciferase reporter gene constructs were designed using *E. coli* K-12, Nissle, and UNC as template for the *nfuA* promoter region. Fig. 17 reveals a general induction of the *nfuA* promoter in all tested *E. coli* strains by the iron chelator 2,2'-dipyridyl (250 µM), which simulates the conditions of iron limitation in the inflamed gut. However, incubation of the three *E. coli* strains with 300 µM H_2O_2 that induces oxidative stress, did not lead to an induction of *nfuA* promoter activity (data not shown).
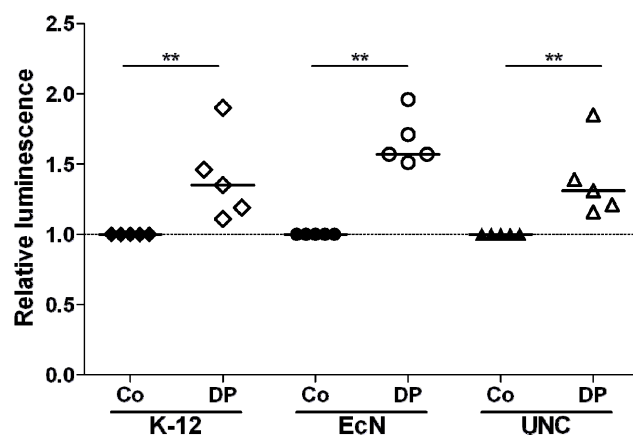
Fig. 17 Activation of the *nfuA* promoter by 2,2'-dipyridyl
Luciferase reporter gene constructs of the *nfuA* promoters were generated for *E. coli* K-12, Nissle (EcN), and UNC. Cells were grown aerobically in LB-Lennox medium to early-exponential phase. After incubating the cells for 60 min with 250 µM 2,2'-dipyridyl (DP) luciferase activity was measured. Control cells (Co) remained untreated. Data are expressed as medians. Mann-Whitney U Test was used for statistical analysis; **, $p \leq 0.01$.

To further investigate *nfuA* expression in response to different stressors, *nfuA* mRNA levels in the three *E. coli* strains were determined by qPCR after incubating the cells for 30 min either with 250 µM 2,2'-dipyridyl or 300 µM paraquat. mRNA levels of *nfuA* significantly increased 1.7- and 1.9-fold in *E. coli* K-12 and *E. coli* UNC, respectively, when the cells were treated with 2,2'-dipyridyl. Although the effect was not significant, superoxide stress induced by paraquat increased *nfuA* expression in all tested *E. coli* strains in comparison to the control cells. Strain-specifically, *E. coli* K-12 exhibited the highest *nfuA* expression in the basic and in the stimulated state, while *E. coli* Nissle expressed *nfuA* to the lowest extent.
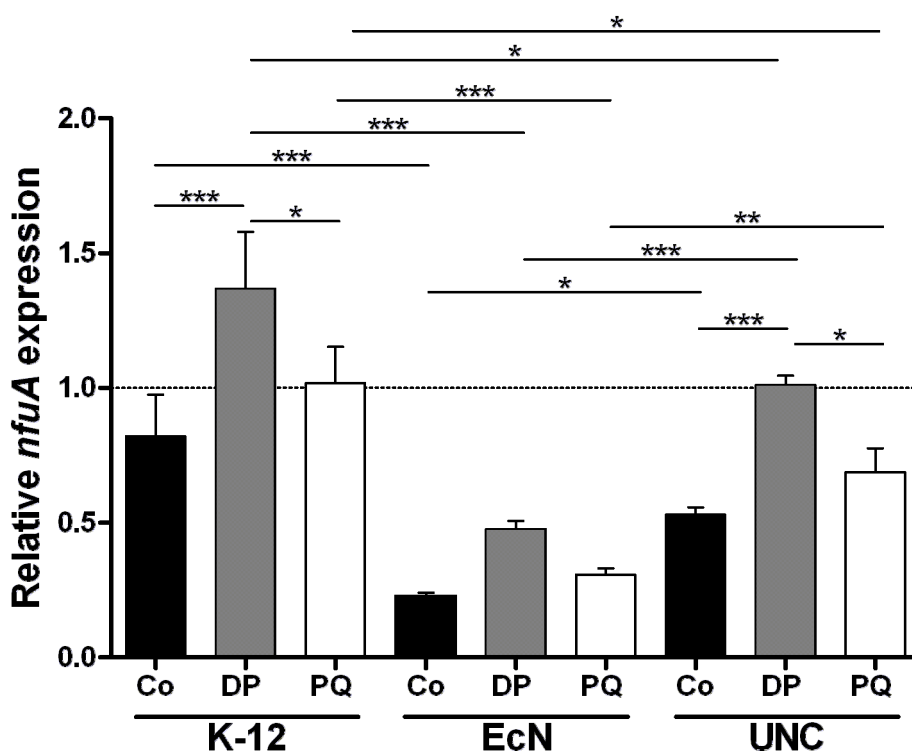
Fig. 18   Relative *nfuA* mRNA level in different *E. coli* strains in response to various stressors
E. coli K-12, Nissle (EcN), and UNC were grown aerobically to early exponential phase. Total RNA was isolated after treating the culture for 30 min either with 250 µM 2,2'-dipyridyl (DP) or with 300 µM paraquat (PQ). Control cells (Co) remained untreated. After reverse transcription, relative *nfuA* gene expression was analysed by quantitative real time PCR using *rrsA* as a reference gene. Data are expressed as means ± SD from 3 independent replicates per group. Expression was calculated relative to a calibrator sample. One-way ANOVA and Bonferroni's multiple comparison test were used for statistical analysis; *, $p \leq 0.05$; **, $p \leq 0.01$; ***, $p \leq 0.001$.

Since all tested *E. coli* strains reacted similarly in the luciferase reporter gene assay, *nfuA* deletion mutants were generated only for *E. coli* K-12. In presence of paraquat, the deletion of *nfuA* led to a strong growth retardation. The maximal OD_{600} after 8 h was only 22% of that reached by the untreated Δ*nfuA* culture (Fig. 19A). In presence of 250 µM 2,2'-dipyridyl, growth of *E. coli* K-12 wildtype and the Δ*nfuA* strain was strongly inhibited after 16 h (Fig. 19B) and growth was slightly delayed after the addition of 350 µM $FeSO_4$ in Δ*nfuA* cells

(Fig. 19B). Complementation of *nfuA* restored the growth of the *nfuA* deletion strain in presence of either paraquat or 2,2'-dipyridyl, indicating that the growth defect was due to the deletion of *nfuA* (Fig. 34, Appendix).

In summary, all tested *E. coli* strains displayed an increased *nfuA* expression or an enhanced *nfuA* promoter activity in the state of superoxide stress or iron starvation. In addition, growth of the *E. coli* K-12 *nfuA* deletion mutant was delayed in presence of these two stressors.
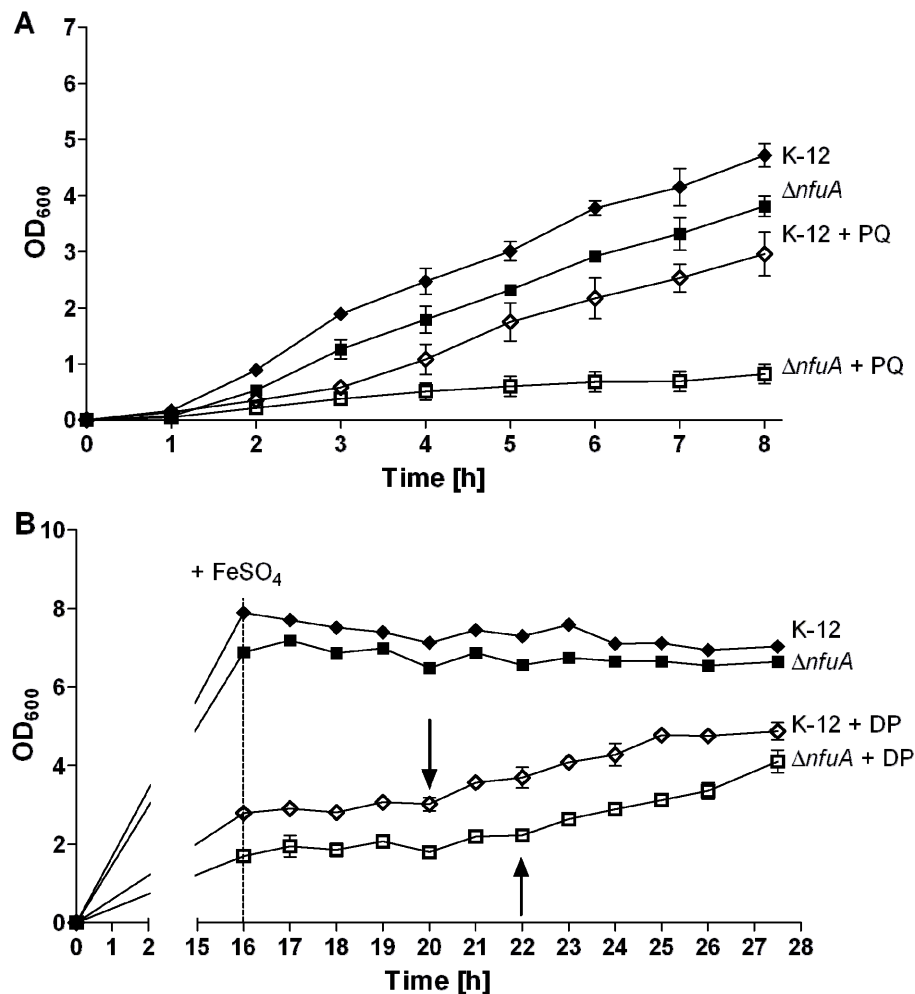
Fig. 19   Growth retardation of a *ΔnfuA* mutant by superoxide stress and iron starvation
Deletion mutants of *nfuA* (*ΔnfuA*) were generated for *E. coli* K-12. **(A)** Cells were grown aerobically in LB-Lennox medium with or without 300 µM paraquat (PQ) for 24 h. **(B)** Cells were grown aerobically in LB-Lennox medium with or without 250 µM 2,2'-dipyridyl (DP) for 16 h. Subsequently, 350 µM $FeSO_4$ was added and growth was monitored for another 12 h. Arrows indicate the starting points of growth for the different genotypes after the addition of 350 µM $FeSO_4$. Experiments were run in triplicates. Data are expressed as means ± SD.

4.1.4   Role of *YggE* as a potential fitness factor in *E. coli* Nissle

The proteomic data were also analysed for differences in protein expression between the two *E. coli* strains under both, control and inflammatory conditions. In the control group (no DSS), 26 proteins were upregulated and 39 proteins were downregulated in *E. coli* UNC versus *E. coli* Nissle, while in the DSS group, 21 proteins were upregulated and 32 proteins were downregulated in *E. coli* UNC (Table 11, Appendix). The uncharacterised protein YggE was upregulated in *E. coli* Nissle compared to *E. coli* UNC by factors of 4.4 (control group) and 8.1 (DSS group) (Fig. 20).
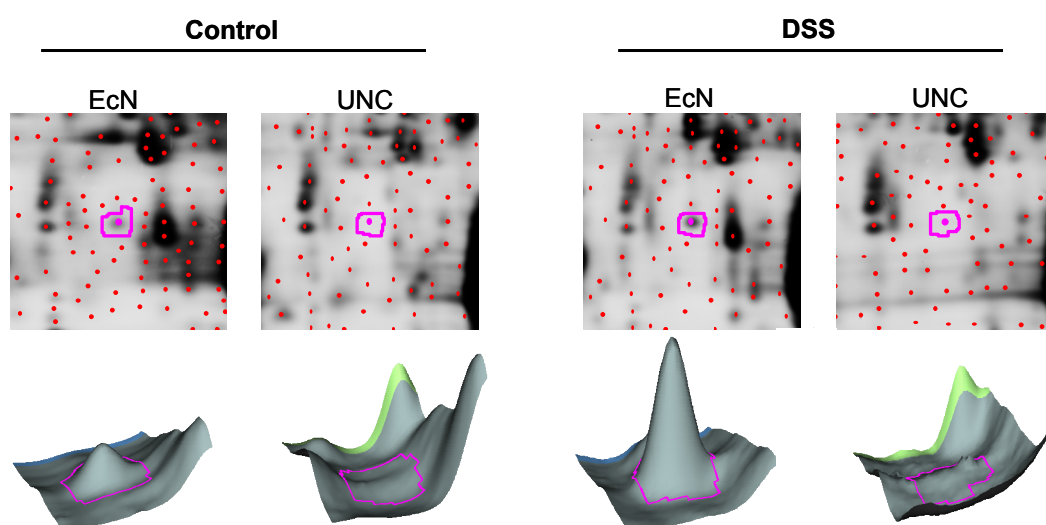
Fig. 20   YggE protein expression in *E. coli* Nissle (EcN) and UNC
Germ-free mice (129/SvEv) were monoassociated with *E. coli* Nissle or UNC. Mice of the DSS group received 3.5% DSS in sterile drinking water for 7 days, control mice received sterile drinking water without DSS. Bacterial protein samples obtained from caecal contents were analysed using 2D gel electrophoresis. Differences in the spot expression pattern from *E. coli* isolated from control and DSS-treated mice were detected in the gel image and in the 3D presentation of the YggE spot.

Since YggE has been predicted to represent an additional defence system against oxidative stress (Kim *et al.*, 2005b), YggE was hypothesised to be a potential fitness factor in *E. coli* Nissle. To test this assumption, luciferase reporter gene constructs were generated for *E. coli* K-12, Nissle, and UNC. The activation of the *yggE* promoter was tested using different stressors that simulate the inflammatory conditions in the intestine. While the *yggE* promoter activity in *E. coli* K-12 and UNC was not affected by 300 µM H_2O_2, the *yggE* promoter in *E. coli* Nissle was slightly activated (Fig. 21A). Also the effect was small, a similar activation of the *yggE* promoter was observed for iron starved cells of *E. coli* Nissle (Fig. 21B).
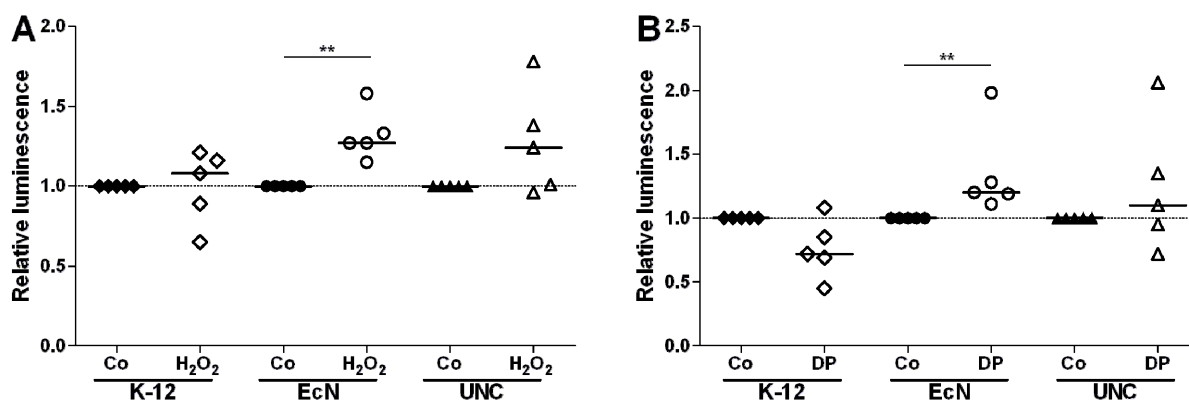
Fig. 21 *yggE* **promoter activity in** *E. coli* **after treatment with** H_2O_2 **or 2,2'-dipyridyl**

Luciferase reporter gene constructs of the *yggE* promoters were generated for *E. coli* K-12, Nissle (EcN), and UNC. Cells were grown aerobically in LB-Lennox medium to early-exponential phase. Luciferase activity was measured 60 min after stimulation with **(A)** 300 µM hydrogen peroxide (H_2O_2) or **(B)** 250 µM 2,2'-dipyridyl (DP). Control cells (Co) remained untreated. Data are expressed as medians. Mann-Whitney U Test was used for statistical analysis; **, $p \leq 0.01$.

To check if the tested *E. coli* strains differ in their sensitivity to oxidative stress, growth experiments in presence of the superoxide generator paraquat were performed. As indicated in Fig. 22, *E. coli* Nissle was less sensitive to superoxide stress than *E. coli* K-12 and UNC. The maximal OD_{600} after 8 h was reduced in *E. coli* Nissle by only 19%, whereas paraquat reduced the maximal OD_{600} of *E. coli* K-12 and UNC by 48% and 56%, respectively.

Taken together, these results indicate that *E. coli* Nissle has higher YggE expression levels, which might contribute to the increased resistance of this strain towards oxidative stress.
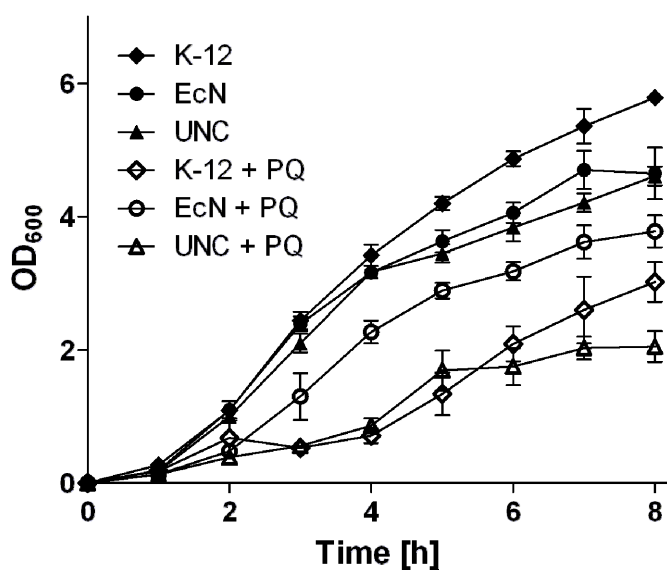
Fig. 22   Growth of different *E. coli* **strains in presence of superoxide stress**

E. coli K-12, Nissle (EcN), and UNC were grown aerobically in LB-Lennox medium with or without 300 µM paraquat (PQ). OD_{600} was measured every 60 min. Experiments were run in triplicates. Data are expressed as means ± SD.

4.1.5 Differences in *E. coli* tryptophanase expression

Besides differences in the YggE protein expression, the comparison between *E. coli* Nissle and *E. coli* UNC isolated from control and DSS-treated animals revealed several differentially expressed proteins belonging to the central energy metabolism, such as carbohydrate, fatty acid, and amino acid metabolism (Table 11, Appendix). TnaA expression was highly increased in *E. coli* Nissle compared to *E. coli* UNC in control (7-fold) and DSS-treated (4-fold) animals (Fig. 23).
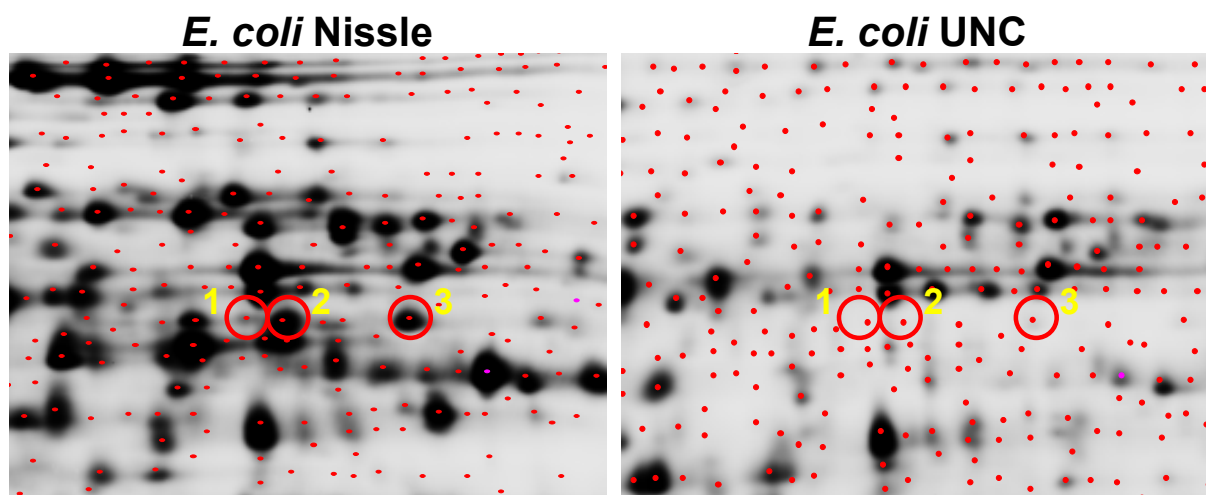
Fig. 23   TnaA protein expression in *E. coli* Nissle and UNC
Germ-free mice (129/SvEv) were monoassociated with *E. coli* Nissle (EcN) or UNC. Mice of the DSS group received 3.5% DSS in sterile drinking water for 7 days, control mice received sterile drinking water without DSS. Bacterial protein samples obtained from the caecal contents were analysed using 2D gel electrophoresis. Three spots representing TnaA (1, 2 and 3) were upregulated in *E. coli* Nissle in comparison to *E. coli* UNC.

Indole, the product of TnaA reaction, was identified as an anti-inflammatory agent (Bansal *et al.*, 2007; Bansal *et al.*, 2010). The higher TnaA levels detected in *E. coli* Nissle led to the speculation that mice associated with *E. coli* Nissle have elevated intestinal indole concentrations, which contribute to an attenuation of intestinal inflammation. In order to clarify this assumption, indole concentrations in caecal supernatants were determined. The observed indole concentrations were 36% higher in the control mice monoassociated with *E. coli* Nissle than in control mice associated with *E. coli* UNC. However, the indole concentrations decrease in both DSS groups and therefore these differences were not observed in the state of intestinal inflammation (Fig. 24).
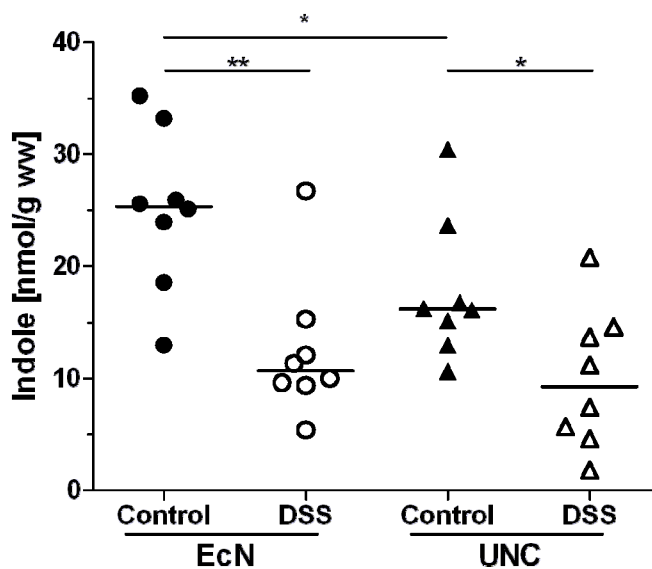
Fig. 24   Indole concentrations in the caecal supernatants
Germ-free mice (129/SvEv) were monoassociated with *E. coli* Nissle (EcN) or UNC. Mice of the DSS group received 3.5% DSS in sterile drinking water for 7 days, control mice received sterile drinking water without DSS. Caecal indole concentrations were measured in control and DSS-treated animals. Data are expressed as medians. Mann-Whitney U Test was used for statistical analysis; *, $p \leq 0.05$;   **, $p \leq 0.01$; ww, wet weight.

4.2   The interleukin 10-deficient mouse model

4.2.1   Assessment of intestinal inflammation in IL-10^{-/-} mice

In a second animal experiment, IL-10^{-/-} mice were monoassociated either with the probiotic *E. coli* Nissle or with the AIEC strain UNC. *E. coli* UNC is known to induce caecal inflammation in gnotobiotic IL-10^{-/-} mice within 3 wk (Kim *et al.*, 2005a; Patwa *et al.*, 2011), while IL-10^{-/-} animals associated with *E. coli* Nissle are hypothesised to remain disease-free.

Several parameters were used to assess the inflammatory host response. First, the animal weights at the end of the experiments were compared, revealing a 17% and 16% lower body weight of the IL-10^{-/-} animals monoassociated with *E. coli* Nissle for 3 and 8 wk, respectively, compared to the corresponding wildtype animals (Fig. 25A). IL-10^{-/-} mice monoassociated with *E. coli* UNC for 3 and 8 wk had 20% and 28%, respectively, lower body weights than the corresponding wildtype mice. Histopathological scoring of the caecal tissues did not reveal any significant morphological differences. However, the histopathological scores of IL-10^{-/-} mice associated with *E. coli* UNC tended to be higher than the scores of the respective wildtype mice (Fig. 25B). These changes were not observed in IL-10^{-/-} mice monoassociated with *E. coli* Nissle.
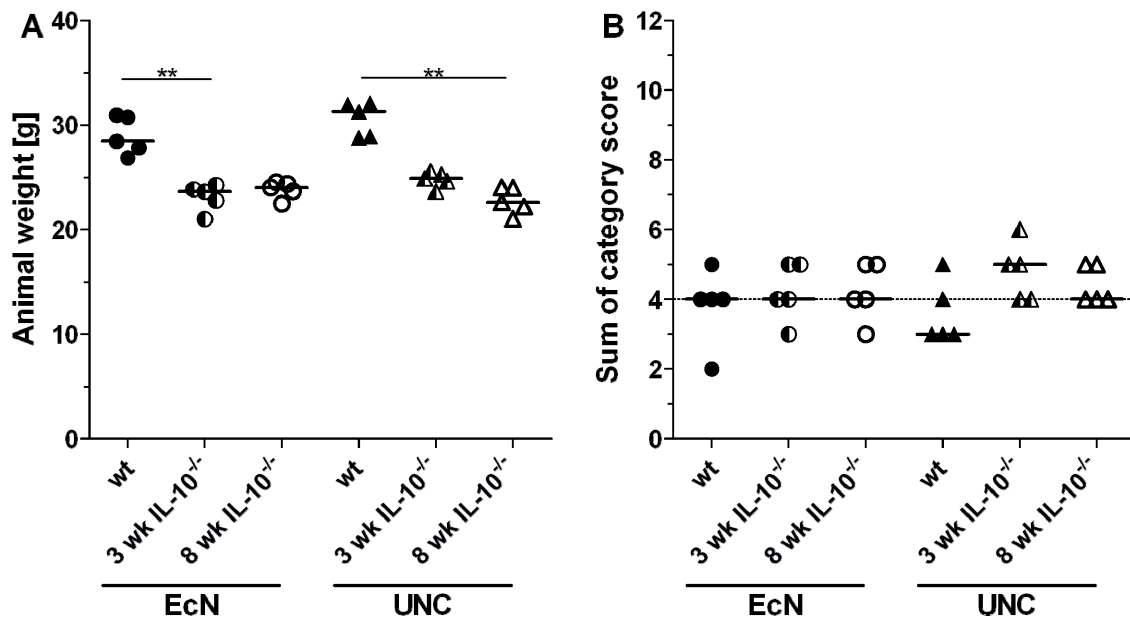
Fig. 25   Body weight and histopathological scores of IL-10$^{-/-}$ and wt mice
Germ-free IL-10$^{-/-}$ mice were monoassociated with *E. coli* Nissle (EcN) or *E. coli* UNC for 3 or 8 wk.
Wildtype (wt) mice were monoassociated for 8 wk with either EcN or UNC. **(A)** Body weights at the
end of the experiment. **(B)** Sum of histopathology scores (0, no inflammation; 12, severe inflammation)
for caecal tissue. Data are expressed as medians. Kruskal-Wallis H Test and Dunn's multiple
comparison test were used for statistical analysis; **, $p \leq 0.01$.

To assess the inflammatory host response in more detail, gene expression of several
proinflammatory cytokines was measured in caecal mucosa by qPCR. At 8 wk, IL-10$^{-/-}$ mice
monoassociated with *E. coli* UNC had 7.3, 3.9, and 2.6-times higher mRNA levels of *Tnf*,
Ifng, and *Cxcl10*, respectively, compared to *E. coli* UNC associated wildtype animals (Table
7). In tendency, the proinflammatory cytokine levels were increased similarly in IL-10$^{-/-}$ mice
associated for 3 wk with *E. coli* UNC. In IL-10$^{-/-}$ mice monoassociated with *E. coli* Nissle, no
significant induction of the proinflammatory cytokine expression was observed.

Taken together, these findings indicate that only the AIEC strain UNC induces signs of a very
mild caecal inflammation by elevating proinflammatory cytokine expression in IL-10$^{-/-}$, but not
in wildtype mice, within 8 wk of monoassociation, while the probiotic *E. coli* Nissle did not do
so.

Table 7   mRNA levels of proinflammatory cytokines in IL-10$^{-/-}$ and wildtype mice
Germ-free IL-10$^{-/-}$ mice were monoassociated with *E. coli* Nissle (EcN) or *E. coli* UNC for 3 or 8 wk. Wildtype (wt) animals were monoassociated for 8 wk with either EcN or UNC. RNA was extracted from caecal mucosa and reversely transcribed into cDNA. Gene expression of proinflammatory cytokines was measured by quantitative real time PCR. Results were normalised to the geometrical means of the amplification reactions with *Hprt1* and *Rpl13a*. Relative expression levels are expressed as medians (25th : 75th percentile). Kruskal-Wallis H Test and Dunn's multiple comparison test were used for statistical analysis.

	EcN wt	EcN 3 wk IL-10$^{-/-}$	EcN 8 wk IL-10$^{-/-}$	UNC wt	UNC 3 wk IL-10$^{-/-}$	UNC 8 wk IL-10$^{-/-}$
Relative expression of *tumor necrosis factor α*						
Median (25th : 75th percentile)	0.60 (0.25 : 1.40)	1.50 (0.75 : 1.90)	1.80 (1.20 : 2.75)	0.30 (0.25 : 0.85)	1.00 (0.60 : 2.50)	**2.20^a** (0.90 : 3.45)
Relative expression of *interferon γ*						
Median (25th : 75th percentile)	1.60 (1.10 : 2.15)	2.30 (1.40 : 5.75)	4.00 (2.10 : 5.50)	1.40 (1.20 : 1.65)	4.90 (1.95 : 5.60)	**5.40^a** (3.65 : 16.70)
Relative expression of *chemokine (C-X-C motif) ligand 10*						
Median (25th : 75th percentile)	1.80 (0.90 : 2.60)	3.80 (2.90 : 6.35)	3.80 (2.40 : 5.50)	1.60 (1.00 : 2.05)	3.90 (2.85 : 5.00)	**4.10^{aa}** (3.25 : 8.95)

^{a} Indicates significant differences between wt mice monoassociated with *E. coli* UNC and the corresponding IL-10$^{-/-}$ mice monoassociated for 8 wk; ^{a}, $p \leq 0.05$; ^{aa}, $p \leq 0.01$.

4.2.2   Adaptation of *E. coli* to mild caecal inflammation

To elucidate the effects of a very mild inflammatory host response on the proteome of intestinal bacteria, the proteome of caecal *E. coli* isolated from IL-10$^{-/-}$ mice was compared to that of *E. coli* from wildtype mice. Since only IL-10$^{-/-}$ animals associated with *E. coli* UNC exhibit a distinct increase in the proinflammatory cytokine expression, IL-10$^{-/-}$ and wildtype mice monoassociated with *E. coli* UNC were compared. In agreement with the observation of only minor inflammatory symptoms, differences in the *E. coli* proteomes between the two animal groups were small. In *E. coli* UNC isolated from 8 wk monoassociated IL-10$^{-/-}$ mice, 13 proteins were differentially expressed by a factor of ± 1.5 ($p \leq 0.01$), seven were downregulated and 6 were upregulated in comparison to *E. coli* UNC from wildtype animals. Interestingly, despite minor changes inflammatory host response, the number of differentially expressed proteins detected in *E. coli* UNC from IL-10$^{-/-}$ mice compared to *E. coli* UNC from wildtype mice was higher at 3 wk than at 8 wk: In total, 22 proteins were identified: 18 were repressed, while 4 were upregulated in comparison to *E. coli* UNC isolated from wildtype animals (Table 12, Appendix). In concordance with the DSS-experiment, in particular glycolytic proteins were downregulated in *E. coli* UNC isolated from IL-10$^{-/-}$ animals at 8 wk in comparison to *E. coli* UNC from wildtype animals (Table 8).
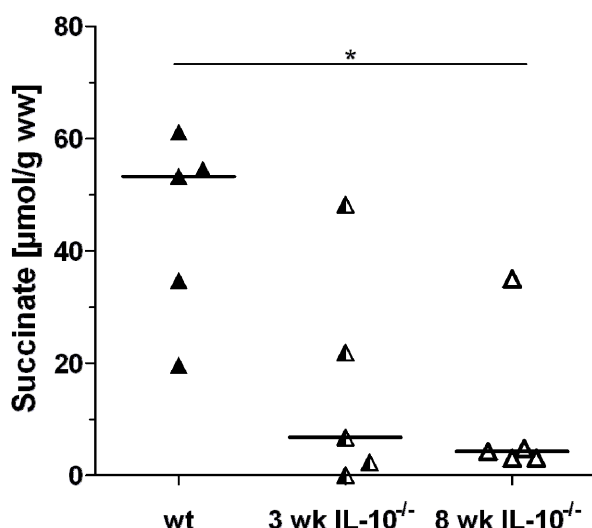
Table 8   Glycolytic proteins downregulated in mild caecal inflammation in *E. coli* UNC
Wildtype (wt) and IL-10$^{-/-}$ mice were monoassociated with *E. coli* UNC for 3 (only IL-10$^{-/-}$) or 8 wk. After isolation of the caecal bacterial proteins, proteome analysis was performed using the 2D-DIGE technique.

Swiss Prot accession no.	Gene	Protein description	Fold change[a] 3 wk IL-10$^{-/-}$ vs. wt	Fold change[a] 8 wk IL-10$^{-/-}$ vs. wt
P0AB71	*fbaA*	Fructose-bisphosphate aldolase class 2	-1.53	-1.60
P0A6P9	*eno*	Enolase	-2.05; -2.52	-1.69
P0AD61	*pykF*	Pyruvate kinase I	-2.02	-1.57
P0A9B2	*gapA*	Glyceraldehyde-3-phosphate dehydrogenase A	-1.75	
P62707	*gpmA*	2,3-bisphosphoglycerate-dependent phosphoglycerate mutase	-1.85; -2.25	

[a] Proteins downregulated by a factor ≤ -1.5 ($p ≤ 0.01$); n = 4-5 per group

To check if the downregulation of important glycolytic enzymes such as fructose-bisphosphate aldolase class 2, enolase, pyruvate kinase I, and glyceraldehyde-3-phosphate dehydrogenase A led to changes in the metabolism, the concentrations of the bacterial fermentation product succinate were determined in the caecal supernatants of wildtype and IL-10$^{-/-}$ animals. The succinate concentrations were significantly decreased by 92% in IL-10$^{-/-}$ animals associated for 8 wk with *E. coli* UNC compared to the respective wildtype animals (Fig. 26) suggesting a strong influence of the proteomic changes on bacterial metabolism.

Fig. 26   Succinate concentrations in caecal supernatants of IL-10$^{-/-}$ and wildtype mice
Germ-free wildtype (wt) and IL-10$^{-/-}$ mice were monoassociated with *E. coli* UNC for 3 (only IL-10$^{-/-}$) or 8 wk and succinate concentrations were measured in the caecal water. Data are expressed as medians. Mann-Whitney U test was used for statistical analysis; *, $p ≤ 0.05$; ww, wet weight.

Recently, Patwa *et al.* (2011) reported the induction of the small heat shock proteins *ibpA* and *ibpB* in *E. coli* UNC and proposed it to be an adaptive response to intestinal inflammation in IL-10$^{-/-}$ mice. Since the present study design of the IL-10 experiment was similar to that of Patwa *et al.*, the *ibpAB* expression was analysed in more detail. Proteomic

analysis did not detect differences in IbpAB protein expression. However, *ibpAB* gene expression was significantly lower in caecal *E. coli* Nissle and *E. coli* UNC when isolated from IL-10$^{-/-}$ animals than when isolated from wildtype animals (Fig. 27A/B). *E. coli* K-12, Nissle, and UNC were tested *in vitro* for their expression of *ibpAB* in response to oxidative stress generated by 300 µM paraquat (Fig. 27C/D) or 300 µM H_2O_2 (data not shown). However, neither paraquat nor H_2O_2 had an impact on *ibpAB* expression in any of the tested strains, suggesting that factors other than oxidative stress influenced *ibpAB* expression.
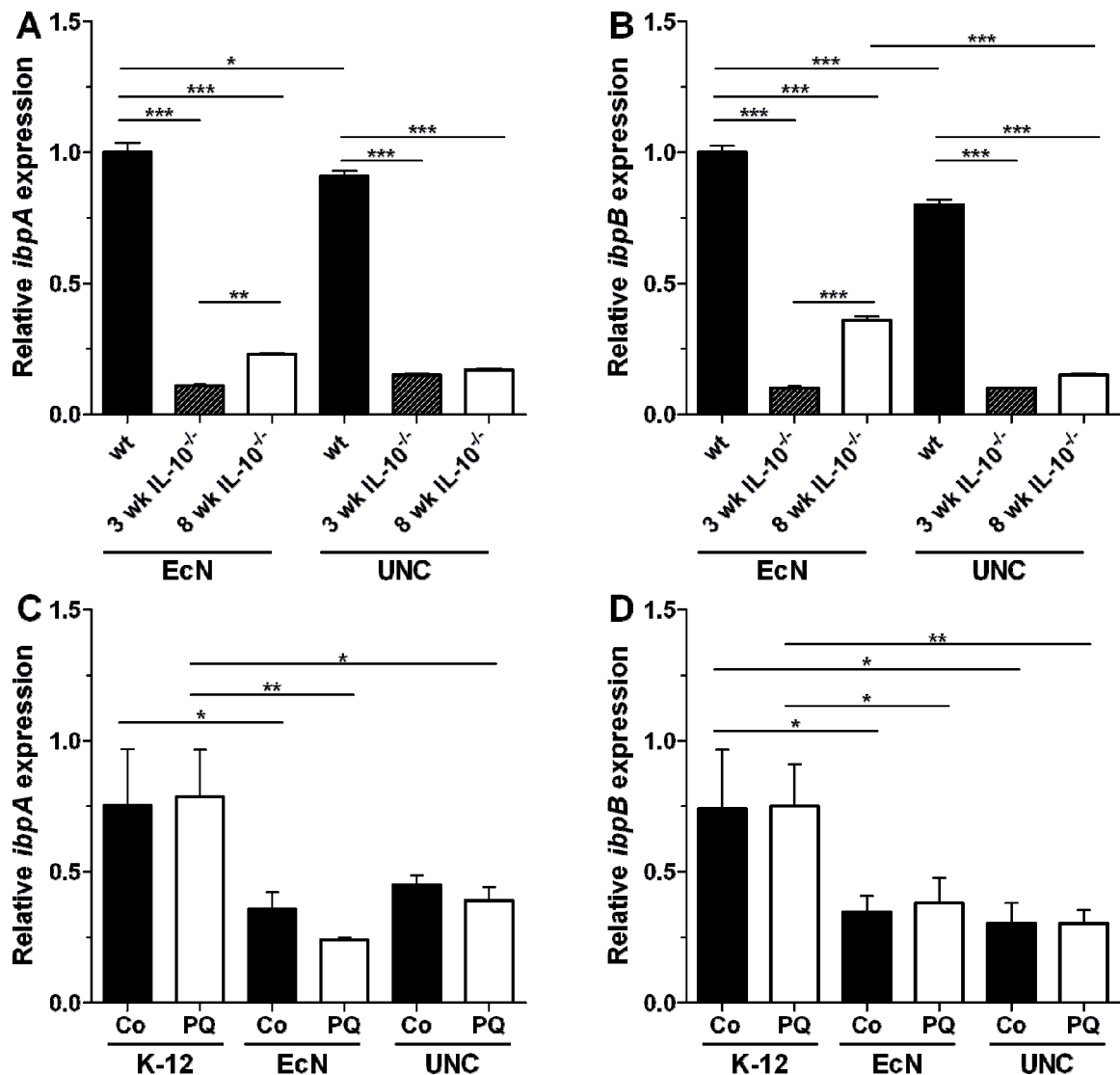
Fig. 27   mRNA levels of the heat shock chaperones *ibpAB in vivo* and *in vitro*
(A/B) Wildtype (wt) and IL-10$^{-/-}$ mice were monoassociated with either *E. coli* Nissle (EcN) or *E. coli* UNC for 3 (only IL-10$^{-/-}$) or 8 wk. *ibpAB* were quantified by real time PCR using bacterial RNA isolated from caecal contents (n = 5, pooled; real time PCR measurement in triplicates). Data are expressed as means ± SD. **(C/D)** Cells were grown aerobically in LB-Lennox medium to early exponential phase. Subsequently, *E. coli* cells were incubated for 30 min with 300 µM paraquat (PQ). Control cells remained untreated. Cells were harvested and *ibpAB* were quantified by real time PCR. Data are expressed as means (n = 3) ± SD. Results were normalised to *rrsA*. One-way ANOVA and Bonferroni's multiple comparison test were used for statistical analysis; *, $p \leq 0.05$; **, $p \leq 0.01$; ***, $p \leq 0.001$.

4.2.3 Ivy expression in different *E. coli* strains

In addition to the identification of bacterial proteins needed for the adaptation to a very mild caecal inflammation, the second aim of this PhD-study was to identify proteins differentially expressed between the probiotic *E. coli* Nissle and the AIEC strain UNC. These proteins may contribute to differences between *E. coli* Nissle and *E. coli* UNC in their potential to induce intestinal inflammation in IL-10$^{-/-}$ mice.

One of the differentially expressed proteins was the inhibitor of vertebrate C-type lysozyme (Ivy), which was upregulated in *E. coli* Nissle isolated from IL-10$^{-/-}$ mice in comparison to *E. coli* UNC, from IL-10$^{-/-}$ mice (Table 9). Expression of Ivy was also higher in *E. coli* Nissle from IL-10$^{-/-}$ mice than in *E. coli* Nissle from wildtype mice. Owing to their outer membrane, Gram-negative *E. coli* are usually less sensitive to lysozyme. Therefore, the role of Ivy in *E. coli* Nissle is not clear.

Table 9 Ivy protein expression in caecal *E. coli*
Wildtype (wt) and IL-10$^{-/-}$ mice were monoassociated with either *E. coli* Nissle or *E. coli* UNC for 3 (only IL-10$^{-/-}$) or 8 wk. After protein isolation from caecal *E. coli*, the proteomes were analysed by 2D-DIGE.

Arrangement	Fold change[a]
***E. coli* Nissle**	
8 wk IL-10$^{-/-}$ vs. wt	1.78
3 wk IL-10$^{-/-}$ vs. wt	1.93
8 wk IL-10$^{-/-}$ vs. 3 wk IL-10$^{-/-}$	n.s.
***E. coli* UNC**	
8 wk IL-10$^{-/-}$ vs. wt	n.s.
3 wk IL-10$^{-/-}$ vs. wt	n.s.
8 wk IL-10$^{-/-}$ vs. 3 wk IL-10$^{-/-}$	n.s.
***E. coli* UNC vs. Nissle**	
8 wk IL-10$^{-/-}$	-2.02
3 wk IL-10$^{-/-}$	-1.68
wt	n.s.

[a] Expression factor ≥ 1.5, ≤ -1.5 (p ≤ 0.01) in caecal samples (n = 4/5); n.s., not significant

Nevertheless, upregulation of Ivy on protein level in *E. coli* Nissle vs. UNC corresponded with its induction on mRNA level. Expression of *ivy* was 2-fold (3 wk) and 3-fold (8 wk) higher in *E. coli* Nissle isolated from IL-10$^{-/-}$ animals than in *E. coli* UNC from IL-10$^{-/-}$ mice (Fig. 28A). To test the hypothesis that *ivy* plays a role in *E. coli* Nissle's response to oxidative stress as caused during intestinal inflammation, *ivy* mRNA levels were determined *in vitro* for *E. coli* K-12, Nissle, and UNC after incubating the cells with 300 µM paraquat. In absence of paraquat, *ivy* gene expression was 2- and 3-fold increased in *E. coli* Nissle compared to *E. coli* K-12 and UNC, respectively (Fig. 28B). However, the superoxide generator paraquat

did not significantly affect *ivy* gene expression. Hence, the increased *ivy* expression appears to be a specific feature of *E. coli* Nissle and not a general response to intestinal inflammation.
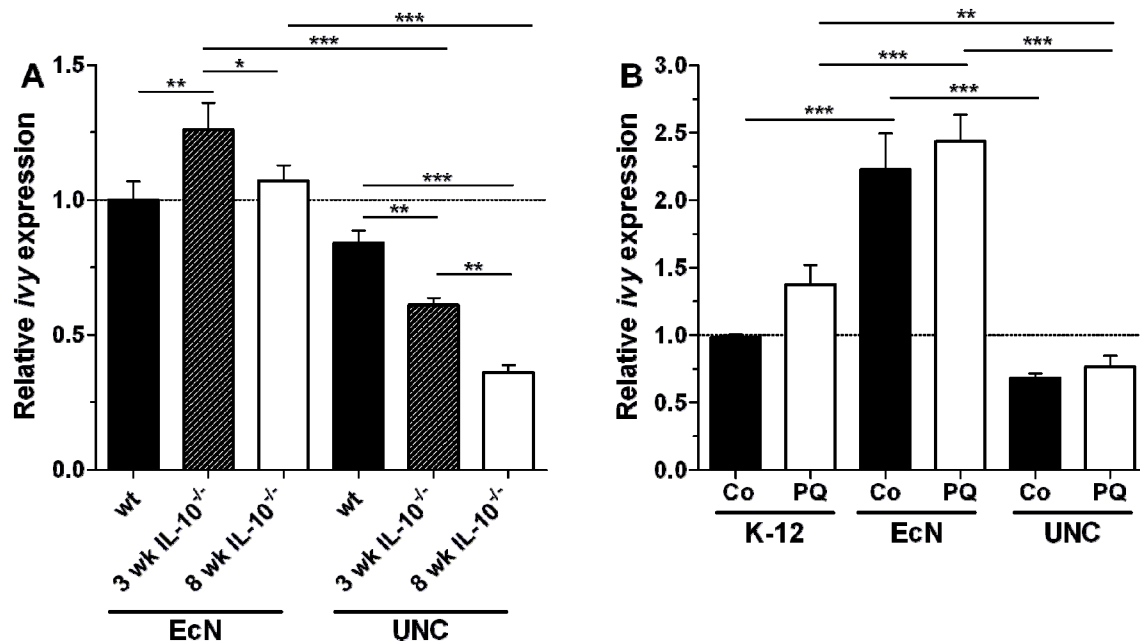

Fig. 28 ***ivy* mRNA expression *in vivo* and *in vitro* in various *E. coli* strains**
(A) Wildtype (wt) and IL-10^{-/-} mice were monoassociated with either *E. coli* Nissle (EcN) or *E. coli* UNC for 3 (only IL-10^{-/-}) or 8 wk. *ivy* gene expression was quantified by real time PCR using bacterial RNA isolated from caecal contents (n=5, pooled; qPCR measurement in triplicates). Data are expressed as means ± SD. **(B)** Cells were grown aerobically in LB-Lennox medium to the early exponential phase and then incubated for 30 min with 300 μM paraquat (PQ); control cells remained untreated. Cells were harvested and bacterial RNA was isolated. Data are expressed as means (n = 3) ± SD. *ivy* gene expression was normalised to *rrsA*. One-way ANOVA and Bonferroni's multiple comparison test were used for statistical analysis; *, $p \leq 0.05$; **, $p \leq 0.01$; ***, $p \leq 0.001$.

Several studies have demonstrated that *E. coli* Nissle induce the host factor hBD-2 (Wehkamp *et al.*, 2004a; Möndel *et al.*, 2009), which damages the bacterial outer membrane (Lehrer *et al.*, 1989) rendering Gram-negative *E. coli* more susceptible to lysozyme. Therefore it was hypothesised that the induction of *ivy* in *E. coli* Nissle is a self-protection mechanism against hBD-2 and lysozyme action. To test this hypothesis, growth experiments in presence of lysozyme and EDTA were performed. Lysozyme alone had no influence on the growth of any of the *E. coli* strains (data not shown), but in combination with EDTA it strongly inhibited the growth of *E. coli* K-12 and UNC (Fig. 29). EDTA permeabilises the bacterial outer membrane (Nossal & Heppel, 1966) and it was therefore supposed to imitate the effect of hBD-2. *E. coli* K-12 was the most sensitive strain as lysozyme-EDTA reduced its maximal OD_{600} by 42%, whereas the maximal OD_{600} of *E. coli* UNC was diminished by only 24%. In contrast, *E. coli* Nissle was resistant against the action of lysozyme-EDTA, the maximal OD_{600} of this probiotic strain was significantly increased by 5%.
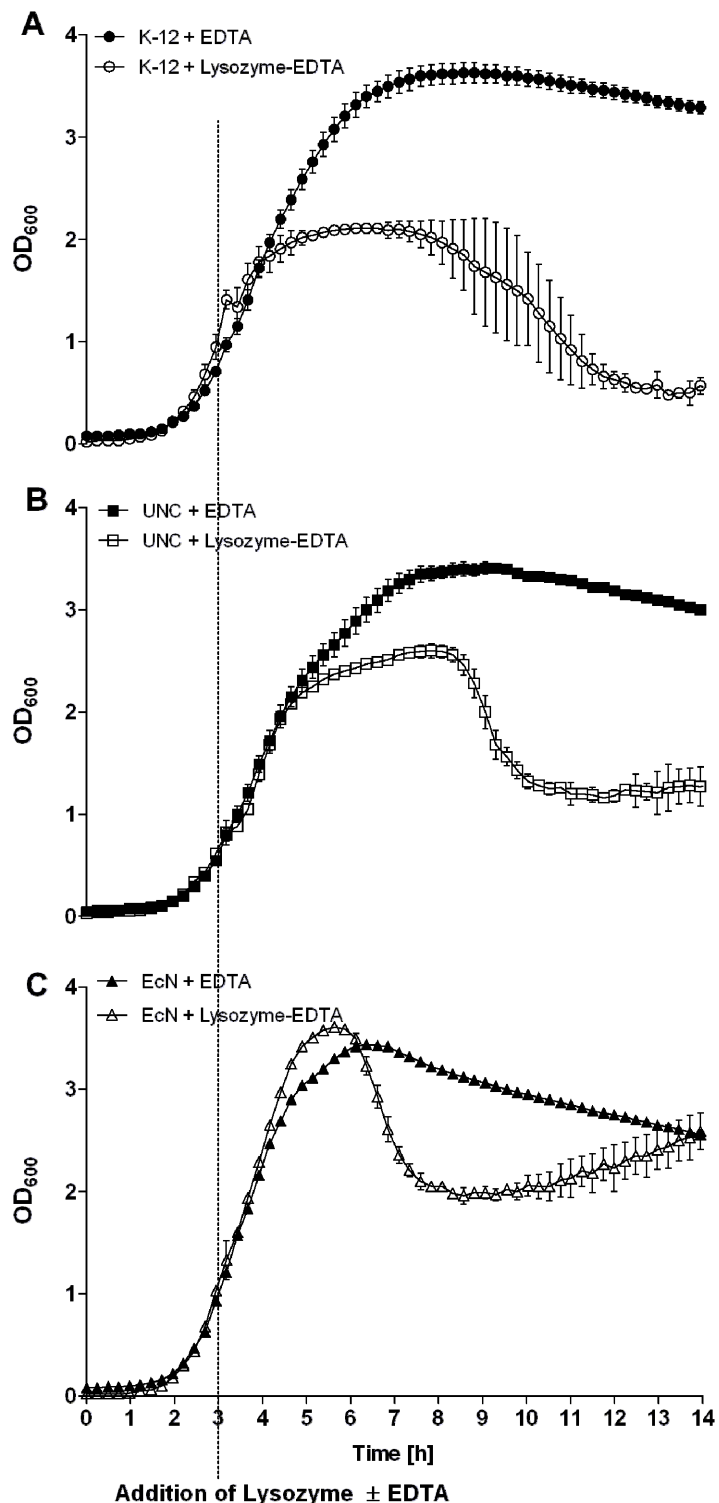
Fig. 29   Effect of lysozyme on the growth of various *E. coli* strains
E. coli K-12 **(A)**, UNC **(B)** and Nissle (EcN) **(C)** were grown aerobically in LB-Lennox medium for 3 h. The cells were subsequently treated with lysozyme (2.5 mg/ml) and 1.22 mM EDTA (open symbols). As a control, the cells were treated with EDTA alone (closed symbols). Growth was monitored by measuring the optical density at 600 nm (OD_{600}) over 14 h at 37°C. Experiments were run in triplicates. Data are expressed as means ± SD.

To investigate if differences in the genomic sequence are responsible for the observed strain-differences in *ivy* expression and lysozyme sensitivity, the *ivy* gene including its promoter region was amplified from *E. coli* K-12, Nissle, and UNC. Sequence alignment indicated 10 single point mutations in *E. coli* Nissle compared to K-12, whereas no sequence differences were observed between *E. coli* UNC and K-12 (Fig. 35, Appendix). One mutation

lies in the -10 region of the σ^{32} promoter, while another mutation in the protein-coding region alters codon 6 from TCG (Ser) to CCG (Pro). None of the point mutations, except the latter, led to changes in the protein sequence. However, the modification from Ser to Pro is a drastic one, which might influence the secondary structure of the protein and thereby affects its activity.

To test whether the observed sequence differences led to functional changes, *ivy* genomic regions were amplified from *E. coli* K-12 or Nissle and overexpressed in *E. coli* KRX cells. Since the KRX strain is an *E. coli* K-12 MG1655 derivative and therefore exhibits an endogenous *ivy* expression, the *E. coli* KRX carrying the empty pGEM-T Easy vector was used as a negative control. In presence of lysozyme and EDTA, overexpression of *ivy* originating from *E. coli* Nissle (pGEM-T*ivy*EcN) improved the growth by 19% in comparison to cells containing the empty pGEM-T vector. In contrast, overexpression of *ivy* originating from *E. coli* K-12 (pGEM-T*ivy*K12) did not result in an increased maximal OD_{600} when compared to the negative control (Fig. 30).
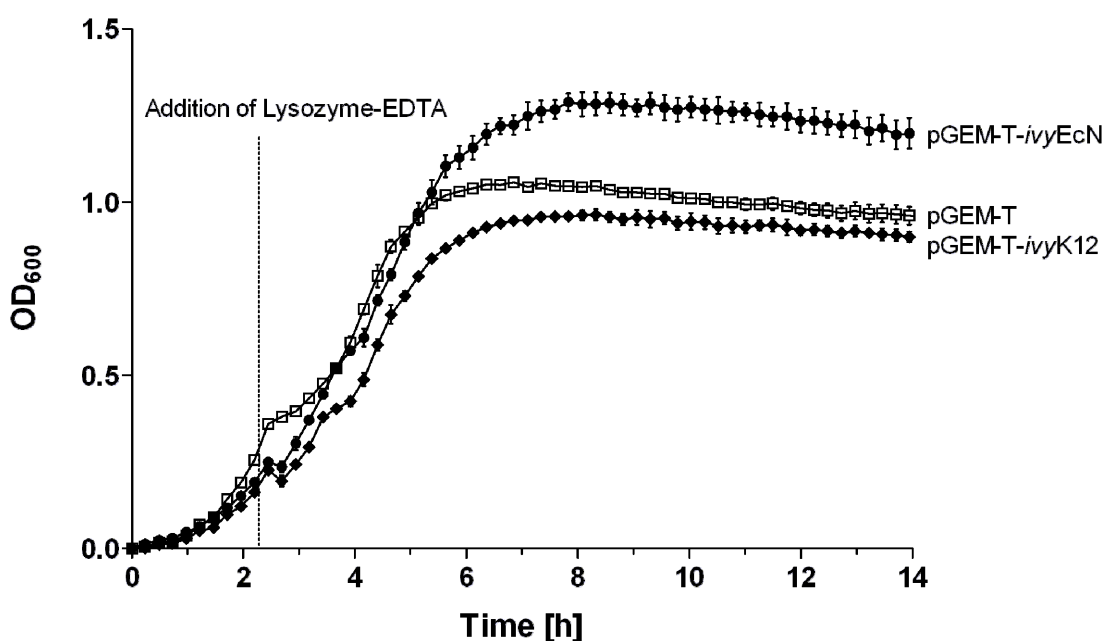
Fig. 30 Influence of *ivy* overexpression on *E. coli*'s lysozyme resistance
The genomic sequence of *ivy* was amplified from *E. coli* Nissle (EcN) or K-12, cloned into the pGEM-T Easy Vector and transformed into *E. coli* KRX, resulting in pGEM-T-*ivy*EcN and pGEM-T-*ivy*K12, respectively. As a negative control, the KRX strain was transformed with the empty pGEM-T Easy Vector. Cells were grown aerobically in LB-Lennox medium (supplemented with 0.1% rhamnose and 50 µg/ml carbenicillin) for 2.45 h at 30°C. Subsequently, lysozyme and EDTA were added to a final concentration of 2.5 mg/ml and 1.22 mM, respectively. OD_{600} was measured over 14 h at 30°C. Experiments were run in triplicates. Data are expressed as means ± SD.

To find additional support for the notion that Ivy protects *E. coli* against the action of compounds weakening the bacterial outer membrane, a very sensitive method for the determination of the antimicrobial resistance was used (Lehrer *et al.*, 1991). The radial diffusion assay revealed that lysozyme alone inhibited the growth of *E. coli* containing the empty pGEM-T vector, while cells overexpressing *ivy* were affected to a lower extent (Fig. 31). Similar results were obtained for the combination of lysozyme and hBD-2. However, in this experiment *ivy* originating from *E. coli* K-12 appears to be more protective than *ivy* from *E. coli* Nissle.

Taken together, the results from both, the growth experiments and radial diffusion assays, did not clearly identify a connection between *ivy* sequence differences and changes in Ivy protein activity. Nevertheless, it is obvious that Ivy contributes to an increased lysozyme and hBD-2 resistance in *E. coli*.
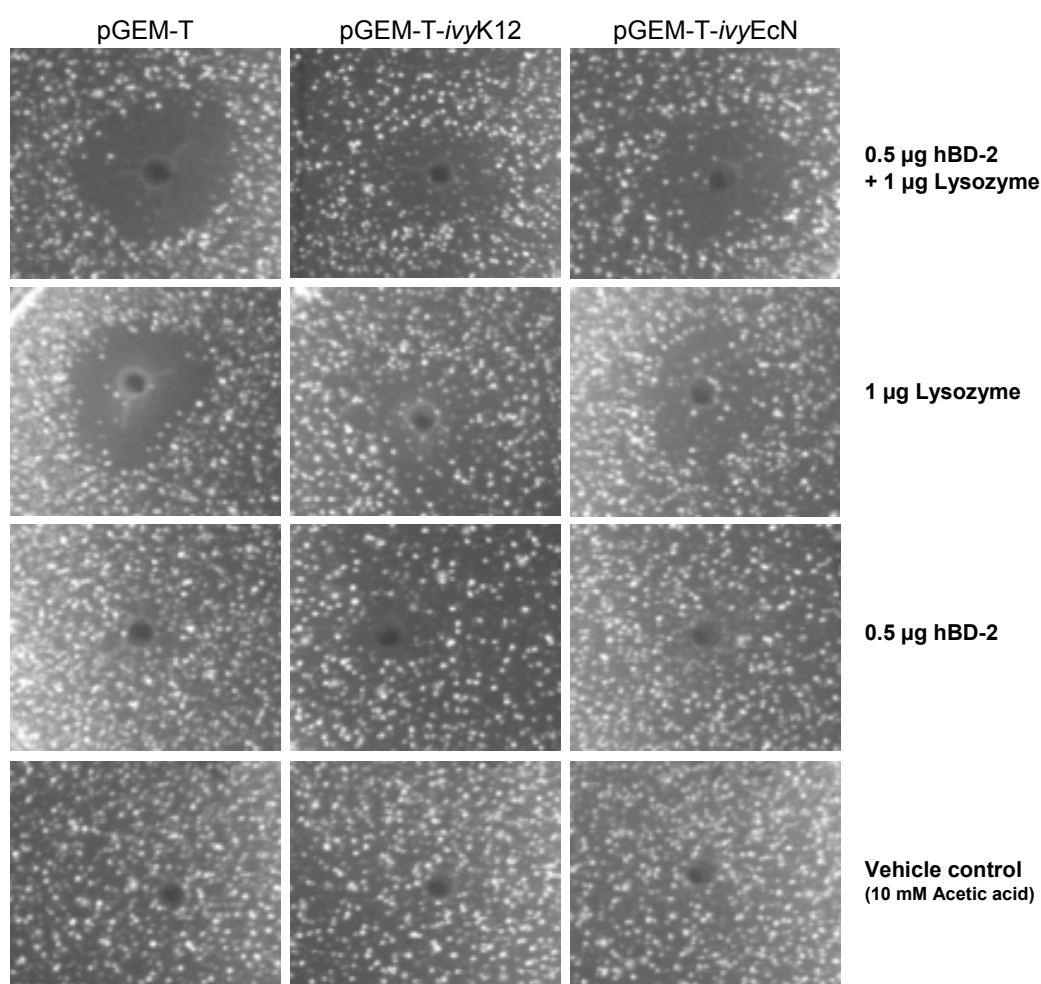
Fig. 31 Antimicrobial resistance of *E. coli* strains overexpressing *ivy*
Overnight cultures of *E. coli* KRX carrying the pGEM-T-*ivy*EcN, pGEM-T-*ivy*K12, or the empty pGEM-T Easy Vector were harvested, mixed with warm underlay agar (supplemented with 0.1% rhamnose and 50 µg/ml carbenicillin) and poured into Petri dishes. Small wells were punched and 5 µl of the test substances (1 µg lysozyme and/or 0.5 µg human β-defensin 2 [hBD-2]) were pipetted into the wells. After 3 h of incubation at 30°C, the gel was overlayed with full-nutrition agar and incubated for 3 days at 30°C. The data are representative of 3 independent experiments.

5 DISCUSSION

5.1 *E. coli*'s adaptation to intestinal inflammation

Numerous studies revealed differences in microbiota composition between IBD patients and healthy individuals. They report an overall reduction of *Firmicutes* and a concomitant increase of *Proteobacteria*, in particular *E. coli* (Swidsinski *et al.*, 2002; Gophna *et al.*, 2006; Frank *et al.*, 2011; Walker *et al.*, 2011). In CD, the *E. coli* belong mainly to the class of adherent-invasive *E. coli*, which display α-hemolysin-dependent cytolytic effects (Darfeuille-Michaud *et al.*, 1998; Darfeuille-Michaud *et al.*, 2004). The interactions between the host and the AIEC were studied in detail: Adherence to the IECs is mediated by interactions between an AIEC-specific type-1 pili and the carcinoembryogenic antigen-related adhesion molecule 6 (Barnich *et al.*, 2007), while bacterial invasion is promoted by interactions between the outer membrane protein A and the chaperone GP96 (Rolhion *et al.*, 2010). However, until today it is not clear whether the proliferation of *E. coli* is causal for IBD or whether it occurs secondary to IBD. Therefore, this PhD-thesis aimed to identify specific mechanisms, enabling *E. coli* to proliferate under the hostile conditions in the inflamed intestine. The spectrum of pathology in patients with CD and UC ranges from a chronic indolent disease state to an acute fulminant disease state. Considering these differences in disease severity two models of intestinal inflammation were used: A mild one and a severe one. To take strain differences into consideration, mice were monoassociated either with the AIEC strain UNC or the probiotic *E. coli* Nissle. Severe intestinal inflammation was induced by treating the mice with 3.5% DSS. A very mild form of an intestinal inflammation was initiated by associating germfree IL-10$^{-/-}$ mice with *E. coli* UNC. To study the response of *E. coli* to gut inflammation, caecal *E. coli* were subjected to proteome analysis

Both, the severe DSS-induced intestinal inflammation and the very mild gut inflammation in IL-10$^{-/-}$ mice, led to a downregulation of bacterial proteins belonging to the central energy metabolism, in particular to glycolysis. Central glycolytic enzymes affected by both forms of intestinal inflammation, include fructose-bisphosphate aldolase class 2 and enolase, which were downregulated in *E. coli* UNC isolated from DSS-treated mice compared to *E. coli* UNC from control mice by factors of 7 and 4, respectively. The presence of a mild intestinal inflammation could only be deduced from an increased proinflammatory cytokine expression. Nevertheless, both fructose-bisphosphate aldolase class 2 and enolase were also downregulated in *E. coli* UNC isolated from IL-10$^{-/-}$ mice after 8 wk compared to *E. coli* UNC from wildtype mice, but only by a factor of 2. Hence, it seems that the repression of bacterial glycolysis is directly correlated with the severity of intestinal inflammation. In both animal experiments, downregulation of glycolysis resulted in a reduced production of bacterial fermentation products. This provides evidence for an inflammation-driven reduction of

E. coli's metabolic activity that might be indicative for an energy deprivation in the inflamed gut. Since bacterial fermentation products can be utilised as energy source by the host, the reduction of their concentrations in caecal contents of inflamed mice could contribute to the suggested energy deficiency that has been proposed for intestinal epithelial cells in IBD patients (Roediger, 1980). In *Bacillus subtilis*, Mostertz and co-workers observed a downregulation of genes encoding enzymes of glycolysis and tricarboxylic acid cycle in response to superoxide and peroxide stress (Mostertz *et al.*, 2004). It is therefore conceivable that the observed downregulation of glycolytic proteins in response to intestinal inflammation is due to an increased ROS production in the inflamed gut.

It is generally accepted that the uncontrolled activation of the immune system in IBD results in a sustained overproduction (respiratory burst) of reactive oxygen metabolites, especially superoxide ($O_2^{\bullet-}$) and H_2O_2 (reviewed in Pavlick *et al.*, 2002). Particularly, activation of the NADPH-dependent oxidase, which is located on the cell membrane of phagocytes (macrophages, monocytes, neutrophils and eosinophils), leads to a sudden reduction of oxygen to $O_2^{\bullet-}$ and further production of H_2O_2 (reviewed in Harris *et al.*, 1992). In the Fenton reaction, these ROS can react with redox-active heme iron resulting from intestinal bleeding. This results in highly reactive hydroxyl radicals ($OH^{\bullet}$), which react in a site-specific fashion with nearly every biomolecule: They peroxidise lipids, oxidise proteins and carbohydrates and promote DNA strand breaks (reviewed in Conner *et al.*, 1996). To cope with these toxic side effects of intestinal inflammation, *E. coli* developed several defence mechanisms. Upregulation of some of these pathways was observed in response to strong DSS-induced intestinal inflammation, while induction was absent in *E. coli* UNC from mildly inflamed IL-10$^{-/-}$ mice.

The antioxidant thiol peroxidase Tpx was 3-fold upregulated in *E. coli* UNC (DSS vs. control). Tpx detoxifies peroxides in *E. coli*'s periplasmic space (Cha *et al.*, 2004) and attenuates thereby oxidative stress. Similar to the results of Zheng *et al.* (2001), caecal *E. coli* in inflamed mice adapted to oxidative stress also by upregulation of several heat shock proteins: In *E. coli* Nissle, the 60 kDa chaperonin GroL was upregulated by a factor of 4 (DSS vs. control), while in *E. coli* UNC the proteolytic chaperone protein ClpB was 3-fold upregulated (DSS vs. control). These chaperonins remove protein aggregates formed during ROS action and thereby prevent their accumulation in the cell. Furthermore, the inductor of *E. coli*'s SOS response, RecA, was upregulated in *E. coli* Nissle by a factor of 5 (DSS vs. control). In fact, RecA catalyses the repair of DNA double strand breaks by mediating a homologous recombination between the destroyed DNA region and an intact homologous region of DNA (reviewed in Courcelle & Hanawalt, 2003).

One protein upregulated in both *E. coli* strains in response to DSS-induced intestinal inflammation was the Fe-S biogenesis protein NfuA: It was induced by factors of 4 in *E. coli*

Nissle and 3 in *E. coli* UNC (DSS vs. control). Iron sulphur clusters are common co-factors in proteins of prokaryotes and eukaryotes. Besides their role as redox sensors, they participate in DNA repair/replication, gene expression and cellular metabolism (reviewed in Py & Barras, 2010). Iron sulphur clusters are in general highly sensitive to ROS, as they convert the stable $[4Fe\text{-}4S]^{2+}$ cluster to the unstable $[4Fe\text{-}4S]^{3+}$ cluster. This results in the formation of an inactive enzyme and the release of Fe^{2+}, which fuels the Fenton reaction (Jang & Imlay, 2007). Thus, under inflammatory conditions the activity of Fe-S proteins depends directly on the efficiency of Fe-S cluster biosynthesis. In *E. coli*, two major Fe-S biogenesis systems exist, the ISC (iron sulphur cluster) and the SUF (sulphur mobilisation) system (reviewed in Barras *et al.*, 2005). The core mechanism of both systems is similar: Sulphur is mobilised from L-cysteine by a cysteine desulphurase, while the iron donor is so far unknown. Scaffold proteins bind both components and assemble the cluster, which is transferred directly or via A-type carriers to the corresponding apoprotein (Py *et al.*, 2012). In addition to these two systems, other Fe-S biogenesis proteins were identified - one is the NfuA protein (Angelini *et al.*, 2008). NfuA is a [4Fe-4S] carrier protein that interacts with both, the ISC and the SUF system (Py *et al.*, 2012). Especially under specific stress conditions, such as oxidative stress and iron starvation, NfuA is important for the maturation of Fe-S proteins *in vitro* (Angelini *et al.*, 2008). In fact, besides ROS-production, iron limitation by antimicrobials, such as lactoferrin or lipocalin-2, is one host strategy to limit bacterial growth (Raffatellu *et al.*, 2009). Based on this data, it was speculated that upregulation of NfuA in both *E. coli* strains during strong DSS-induced inflammation is a general mechanism to cope with the inflammatory conditions (Fig. 32).

This hypothesis was supported by demonstrating an activation of *nfuA* promoter and an induction of *nfuA* gene expression in *E. coli* K-12, Nissle, and UNC following the destruction of Fe-S proteins by the iron chelator 2,2'-dipyridyl. In tendency, the *nfuA* mRNA level was also increased by paraquat treatment. Moreover, knock out of *nfuA* resulted in growth retardation in presence of superoxide stress and iron starvation, illustrating the important role of NfuA under these conditions. Lai and co-workers also observed an upregulation of *nfuA* (previously *yhgl*) in *Klebsiella pneumoniae* during infection of mice (Lai *et al.*, 2001). The authors of this study suggested that on entering the host, bacterial pathogens have to cope with iron deprivation and ROS production. In turn, induction of genes such as *nfuA*, helps the bacteria to deal with these stress factors. The results obtained in this PhD-study indicate that NfuA induction is a general mechanism to protect *E. coli* against the adverse effects of intestinal inflammation, which might contribute to the elevated *E. coli* numbers found in the intestines of IBD patients and in animal models of gut inflammation.
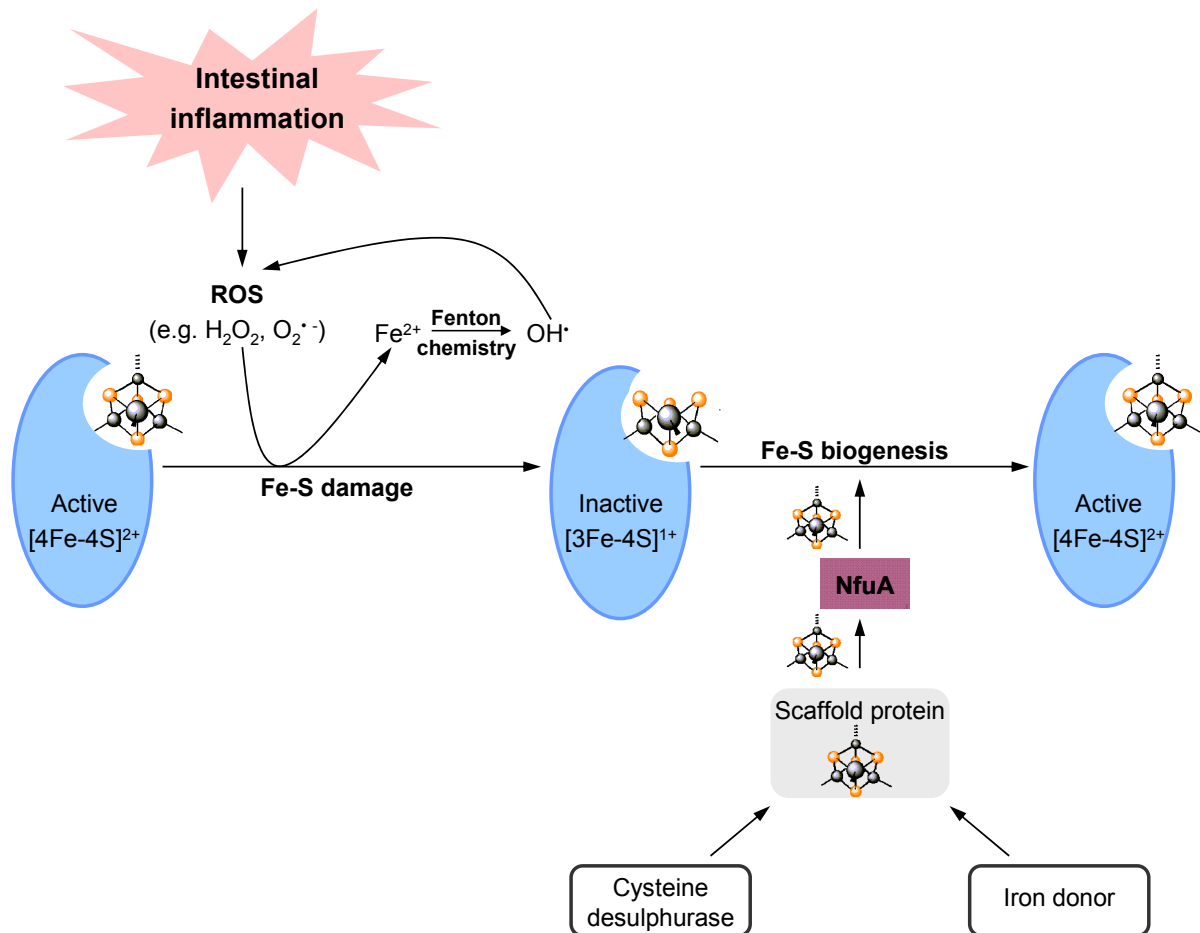
Fig. 32 Proposed role of NfuA in the state of intestinal inflammation
Intestinal inflammation leads to the production of reactive oxygen species (ROS), which cause damage to Fe-S proteins. NfuA serves as an Fe-S cluster carrier protein, as it receives an intact [4Fe-4S] cluster from the scaffold protein and transfers it to the inactive apoprotein, leading to its reactivation.

Since it was recently reported that alterations in the intestinal microbiota precede the development of a severe gut inflammation (Nagalingam *et al*., 2011), it is suggested that the intestinal microbiota detect even minor changes in the host environment. However, as mentioned above, *E. coli* UNC isolated from mildly inflamed IL-10$^{-/-}$ mice exhibited no upregulation of relevant stress response proteins. This indicates that *E. coli* did not require these proteins in the state of a weak intestinal inflammation, although *E. coli* already reacted to the inflammatory events by downregulating glycolytic proteins. Using a microarray-based approach, Patwa *et al.* (2011) recently observed an induction of the small heat shock proteins *ibpA* and *ibpB* in *E. coli* UNC isolated from inflamed IL-10$^{-/-}$ mice and predicted an important role of *ibpAB* in the oxidative stress defence induced by intestinal inflammation. In this PhD-study IbpAB were not among the differentially regulated proteins identified by 2D-DIGE. In contrast to the proteomic data, *ibpAB* gene expression was downregulated in *E. coli* from IL-10$^{-/-}$ mice, although oxidative stress generated *in vitro* by paraquat or H$_2$O$_2$ did not affect the *ibpAB* mRNA levels in *E. coli*. Contrary to their initial hypothesis, Patwa *et al.*

showed that deletion of *ibpAB* facilitate the growth of *E. coli* within the intestine. They hypothesised that IbpAB protect metabolic enzymes from oxidative damage and thereby preserve the function of proteins in several metabolic pathways that are less efficient in extracting energy from dietary substrates. Therefore it is conceivable that upregulation of *ibpAB* only takes place in response to severe intestinal inflammation. In this state, bacterial glycolysis is strongly inhibited and alternative pathways are needed for the energy generation. In the state of weak inflammation, *ibpAB* expression is not required and therefore downregulation was observed. However, Kitagawa *et al*. (2000) also demonstrated that *ibpAB*-overexpression enhances *E. coli*'s resistance towards oxidative stress, but subsequent deletion of *ibpAB* did not cause an increased sensitivity. Therefore, the role of *ibpAB* in intestinal inflammation is still obscure, although it seems that downregulation of these oxidative stress defence proteins is advantageous for the adaptation to mild inflammatory conditions. It would therefore be interesting to investigate the behaviour of *ibpAB* deletion mutants in the DSS-treated mouse, which develops a severe form of intestinal inflammation.

The discrepancy between the proteomic and the mRNA data of IbpAB/*ibpAB* clearly demonstrated how important it is to not only analyse mRNA levels, but also protein expression. Transcriptomics is a powerful tool to collect gene expression data, but it relies on the stability of mRNA, which is extremely low in prokaryotes (Redon *et al.*, 2005). Furthermore, the induction of a specific mRNA transcript does not necessarily measure its function, which is rather mediated by the encoded proteins. Proteins are more stable than mRNA and therefore proteome-based analyses can be expected to provide better and more accurate results about the bacterial adaptation to intestinal inflammation.

5.2 Probiotic and colitogenic *E. coli* differ in their protein expression

Besides the identification of bacterial proteins that enable *E. coli* to adapt to the inflammatory conditions in the intestine, the second aim of this PhD-study was to elucidate the molecular basis for strain-specific differences between probiotic and colitogenic *E. coli* strains. Principal component analysis revealed large proteomic differences between the probiotic *E. coli* Nissle and the AIEC strain UNC, which may contribute to the strain-specific characteristics. Multiplex PCR analysis for virulence genotyping indicates that *E. coli* UNC express several virulence-associated genes. These genes encode at least 3 different adhesins and 4 iron acquisition proteins. However, the number of virulence-associated genes expressed in *E. coli* UNC was reduced in comparison to *E. coli* Nissle (Steffen Wohlgemuth, personal communication). In fact, it is widely known that *E. coli* Nissle is endowed with a large number of fitness factors (Grozdanov *et al.*, 2004). These factors theoretically ensure an effective

colonisation of the host intestine (Lodinova-Zadnikova & Sonnenborn, 1997) and promote the competition with detrimental endogenous *E. coli* strains (Boudeau *et al.*, 2003). However, the subsistent expression of these factors under *in vivo* conditions has never been studied.

Bacterial proteome analysis from the DSS-treated mice identified the uncharacterised protein YggE as a so far unknown factor that enables *E. coli* Nissle to cope with the hostile conditions in the inflamed intestine. In comparison to *E. coli* UNC, YggE was highly upregulated in *E. coli* Nissle under control and inflammatory conditions, and also luciferase reporter gene assays identified a specific activation of the *yggE* promoter by H_2O_2 and 2,2'-dipyridyl only in this probiotic *E. coli* strain. YggE is a putative periplasmic protein (Hagiwara *et al.*, 2003) that is upregulated in *E. coli* exposed to UVA irradiation and increased temperatures (Ojima *et al.*, 2009). In *E. coli* expressing monoamine oxidase, overexpression of *yggE* alleviates monoamine oxidase-derived oxidative stress (Ojima *et al.*, 2009). Moreover, spontaneously derived superoxide dismutase-deficient *E. coli*, induce *yggE*. In accordance with this notion, intracellular ROS levels were lower in superoxide dismutase-deficient *E. coli* overexpressing *yggE* compared to *E. coli* that did not do so (Krishnaiah *et al.*, 2007). Therefore, *yggE* is proposed to act as an auxillary defence system against oxidative stress besides the superoxide dismutase system (Kim *et al.*, 2005b). Interestingly, in *E. coli* Nissle and *E. coli* UNC, both isolated from DSS-treated mice, the superoxide dismutase (SodB) level was reduced, but YggE expression was elevated in *E. coli* Nissle only. Caecal and colonic bacterial counts of *E. coli* UNC were reduced in the DSS-treated compared to the control mice, while the bacterial titer of *E. coli* Nissle was not affected by acute intestinal inflammation. Moreover, *in vitro E. coli* Nissle was less susceptible to paraquat treatment than the other two *E. coli* strains. Therefore it appears that *E. coli* Nissle is better equipped to cope with the oxidative stress produced during intestinal inflammation and it is conceivable that the increased YggE expression contributes to it. Unfortunately it was not possible to generate *yggE* deletion mutants in *E. coli* Nissle, so that direct experimental proof for this assumption could not be obtained. Nevertheless, higher ROS tolerance of *E. coli* Nissle enables this strain to survive the respiratory burst during intestinal inflammation, which contributes to its ability to prevent adhesion and invasion of AIEC strains (Boudeau *et al.*, 2003), an effect that is supposed to be part of its probiotic nature.

In the IL-10-deficient mouse model another potential fitness factor of *E. coli* Nissle was identified: The inhibitor of vertebrate C-type lysozyme, Ivy. It was upregulated on both, protein and mRNA level in *E. coli* Nissle isolated from IL-10^{-/-} animals in comparison to *E. coli* UNC from IL-10^{-/-} mice. *ivy* gene expression of *E. coli* Nissle was also increased *in vitro* in comparison to the lab strain *E. coli* K-12. Similar to YggE, Ivy is a periplasmic protein (Abergel *et al.*, 2007), which was discovered in 2001 as the first bacterial lysozyme inhibitor

(Monchois *et al.*, 2001). Ivy is part of the regulation of the capsular synthesis (Rcs) regulon, which is activated by β-lactam antibiotics interfering with peptidoglycan synthesis (Laubacher & Ades, 2008). The expression of lysozyme inhibitors in *E. coli* is unexpected, since Gram-negative bacteria are usually less sensitive to lysozyme. Their outer membrane forms a barrier that should limit the entry of antimicrobial molecules, such as lysozyme. The thin peptidoglycan layer lying in the periplasmic space between the inner and outer membrane should therefore be protected against the muramidase activity of lysozymes.

One well-known mode of probiotic action is the antagonistic activity against intestinal pathogens that is mediated by the production/induction of specific antimicrobials (Altenhoefer *et al.*, 2004). *E. coli* Nissle induce hBD-2 expression in IECs (Möndel *et al.*, 2009), which permeabilises cell membranes and thereby exhibits an antimicrobial effect against Gram-positive and Gram-negative bacteria (reviewed in Lehrer *et al.*, 1993). hBD-2 also destroys *E. coli* Nissle's outer membrane and renders the peptidoglycan layer more susceptible to lysozyme. Hence, upregulation of *ivy*/Ivy in *E. coli* Nissle is speculated to function as a self-protection mechanism against the combined action of hBD-2 and lysozyme. In the growth experiments, lysozyme in combination with EDTA inhibited the growth of *E. coli* K-12 and UNC, but not that of *E. coli* Nissle. Sequencing of the *ivy* gene and its promoter region identified sequence differences between *E. coli* Nissle and the other two *E. coli* strains, which may affect Ivy protein activity. Especially a mutation in codon 6 of *E. coli* Nissle's protein-coding region altered the amino acid sequence from Serine to Proline. Proline is a known α-helix breaker that affects the secondary structure of proteins and possibly influences Ivy protein activity. To test, if the higher lysozyme resistance of *E. coli* Nissle is due to an increased Ivy expression or the altered amino acid sequence, *E. coli* mutants overexpressing *ivy* from *E. coli* Nissle or *ivy* from *E. coli* K-12 were generated. Growth experiments in presence of lysozyme and EDTA revealed that Ivy from *E. coli* Nissle inactivated lysozyme to a larger extent than Ivy from *E. coli* K-12. However, this effect could not be confirmed by the radial diffusion assay using hBD-2 instead of EDTA. EDTA is a classical chelator that weakens the bacterial outer membrane by sequestering divalent cations (such as Ca^{2+} and Mg^{2+}), while hBD-2 forms channels within *E. coli*'s outer membrane (reviewed in Vaara, 1992). The contradiction between the results obtained from the growth experiments and the radial diffusion assays could therefore be explained by differences in hBD-2 and EDTA action. However, also lysozyme alone has an inhibitory effect on wildtype *E. coli* in the radial diffusion assay and the more protective effect of Ivy from *E. coli* K-12 is also visible when lysozyme is used without hBD-2. Hence, the results from both, the growth experiments and radial diffusion assays did not identify a connection between *ivy* sequence differences and changes in Ivy protein activity. Nevertheless, the results clearly demonstrate that Ivy contributes to a higher lysozyme resistance of *E. coli* Nissle.

Taken together, using a proteomic-based approach, this PhD-thesis identified YggE and Ivy as two, so far unknown, fitness factors of *E. coli* Nissle, which might contribute to an effective intestinal colonisation. This high colonisation efficiency provides the basis for *E. coli* Nissle's probiotic mode of action. Further analysis should elucidate, if the expression of these fitness factors is unique for *E. coli* Nissle or whether it is characteristic for other probiotic *E. coli* strains.

5.3 *E. coli* Nissle's probiotic effects in mice suffering from intestinal inflammation

In both animal models of intestinal inflammation the probiotic *E. coli* Nissle slightly ameliorated the symptoms of intestinal inflammation: Mice suffering from acute DSS-induced colitis lost nearly 16% of their initial body weight when they were associated with *E. coli* UNC, but only 4% when they were associated with *E. coli* Nissle ($p = 0.06$). Moreover, induction of caecal proinflammatory cytokine expression was not observed for *E. coli* Nissle-associated DSS-treated animals, while association with *E. coli* UNC led to an induction of *Tnf* and *Ifng* expression. In contrast to *E. coli* UNC, *E. coli* Nissle did not induce symptoms of intestinal inflammation in genetically susceptible IL-10$^{-/-}$ mice. In fact, neither the pathohistological score nor the expression levels of several proinflammatory cytokines were significantly increased after associating IL-10$^{-/-}$ mice with *E. coli* Nissle.

Although *E. coli* Nissle's therapeutic effects have been proven in human IBD (Kruis *et al.*, 1997; Rembacken *et al.*, 1999; Kruis *et al.*, 2004; Matthes *et al.*, 2010), studies testing its efficiency in animal models of intestinal inflammation revealed contradictory results. Similar to the data of this PhD-thesis, some studies reported that administration of *E. coli* Nissle to mice with DSS-induced colitis reduce the secretion of proinflammatory cytokines and other markers of intestinal inflammation, while the pathohistological inflammation markers are not affected (Schultz *et al.*, 2004; Kokesova *et al.*, 2006). In contrast, Kamada and co-workers demonstrated that *E. coli* Nissle prevent murine acute colitis: In conventionally raised mice treated with DSS (1.3% [wt/vol] for 7 days), *E. coli* Nissle ameliorate body weight loss, disease activity index, and macro- and microscopic tissue damage, while the expression of proinflammatory cytokines in lamina propria mononuclear cells was not affected (Kamada *et al.*, 2005). Consistent with these results, Grabig *et al.* (2006) observed in wildtype mice associated with *E. coli* Nissle an amelioration of DSS-induced colitis, while this effect was not observed in toll-like receptor knock out mice (TLR-2$^{-/-}$ and TLR-4$^{-/-}$). These data provide evidence that *E. coli* Nissle exert their probiotic effects at least in part through TLR-2 and TLR-4-dependent pathways. TLR-2 and TLR-4 are important for the respective recognition of lipoproteins and lipopolysaccharides (Grabig *et al.*, 2006). Accordingly, it was demonstrated

that *E. coli* Nissle inhibit the expansion of peripheral T cells via TLR-2 mediated signalling (summarised in Sturm *et al.*, 2005).

However, the exact molecular mechanisms leading to *E. coli* Nissle's probiotic effects are unclear. Therefore this PhD-thesis aimed to elucidate this point in more detail. The most persuading explanation for the probiotic effect of *E. coli* Nissle was given by Jan Wehkamp and his co-workers. They clearly demonstrated that viable as well as heat-inactivated *E. coli* Nissle induce the expression of the antimicrobial β-defensin 2 in cell culture in a time- and dose-dependent manner through their specific flagellin (Wehkamp *et al.*, 2004a; Schlee *et al.*, 2007). In ileal CD, the expression of hBD-2 is reduced, which may contribute to the defective intestinal barrier function in these patients (Wehkamp *et al.*, 2002; Wehkamp *et al.*, 2004b; Wehkamp *et al.*, 2005). The induction of hBD-2 may also explain various experimental and clinical findings, such as the reduction of intestinal pathogens after administration of *E. coli* Nissle (Lodinova-Zadnikova & Sonnenborn, 1997). However, in contrast to the results of Wehkamp *et al.*, another group demonstrated that only viable and not heat-killed *E. coli* Nissle are able to suppress Tnf-induced IL-8 transcription (Kamada *et al.*, 2008). They speculated that *E. coli* Nissle induce their anti-inflammatory effects without direct contact to the epithelial cells via a secreted factor.

In this PhD-thesis, indole was identified as such a secreted factor. The tryptophanase, TnaA, was upregulated in *E. coli* Nissle compared to *E. coli* UNC isolated from both, control and DSS-treated mice, and also in *E. coli* Nissle from IL-10$^{-/-}$ and wildtype mice in comparison to *E. coli* UNC. TnaA catalyses the conversion of tryptophan to indole, ammonia, and pyruvate. In a porcine model of DSS-induced colitis, tryptophan supplementation improves pathohistological markers, lowers the intestinal permeability, and decreases proinflammatory cytokine levels (Kim *et al.*, 2010). Based on the data of Kim *et al.*, tryptophan appears to exhibit beneficial effects, although it is not clear whether tryptophan or one of its bacterial metabolites is the active component. Indole, for example, was reported to reduce chemotaxis, motility, and attachment of pathogenic *E. coli* to epithelial cells (Bansal *et al.*, 2007). Owing to its ability to modulate gene expression, indole is also involved in the reinforcement of the mucosal barrier and the stimulation of mucin production. In intestinal epithelial cells, indole attenuates the Tnf-mediated activation of NF-κB and the expression of the proinflammatory chemokine IL-8, whereas it increases the expression of the anti-inflammatory cytokine IL-10 (Bansal *et al.*, 2010). Since all these listed probiotic activities are also described for *E. coli* Nissle (Boudeau *et al.*, 2003; Altenhoefer *et al.*, 2004; Sturm *et al.*, 2005; Ukena *et al.*, 2007), it is speculated that the increased TnaA expression in *E. coli* Nissle observed in the present study, contributes to *E. coli* Nissle's beneficial effects (Fig. 33).
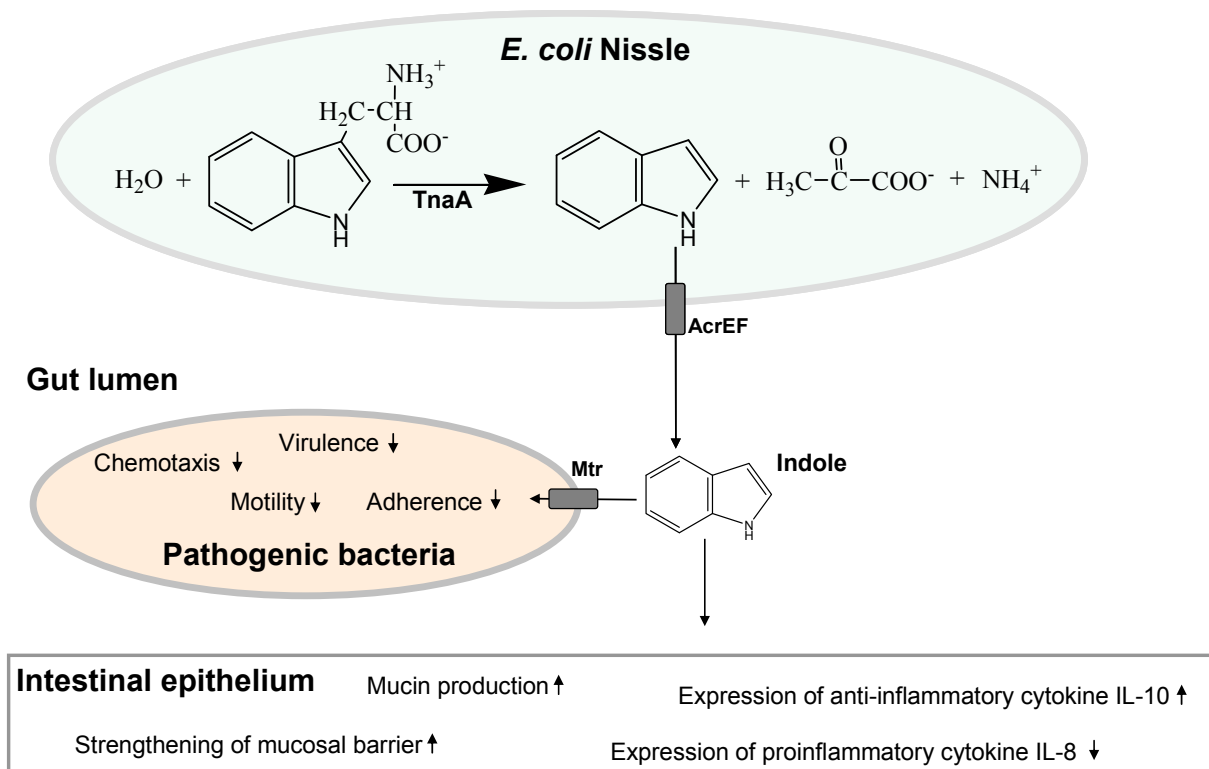
Fig. 33   Proposed mechanisms for the probiotic indole action
Indole produced in *E. coli* Nissle by TnaA is exported from the cytoplasm through the AcrEF transporter (reviewed in Lee & Lee, 2010). In the intestinal lumen, indole enters pathogenic bacteria via the Mtr transporter (reviewed in Lee & Lee, 2010) and interferes with their chemotaxis, motility, virulence, and adherence to the intestinal epithelium. In the gut epithelium, indole increases mucin production, strengthens the mucosal barrier, and increases the expression of IL-10, while the expression of IL-8 is reduced.

In fact, control mice monoassociated with *E. coli* Nissle had 36% higher caecal indole levels than control mice associated with *E. coli* UNC. Since *E. coli* Nissle exert their beneficial effect mainly in that they extend the remission phase in UC (Kruis *et al.*, 1997; Rembacken *et al.*, 1999; Kruis *et al.*, 2004), it is conceivable that the observed elevated basal TnaA level, which in turn leads to increased indole production, contributes to an extension of the remission phase. However, caecal indole concentrations were lower in the inflamed mice than in control mice. This could be explained by a loss of indole due to an increased epithelial permeability in the inflamed mice.

Secretion of a beneficial bacterial factor is also hypothesised for other probiotic bacteria. In fact, *Faecalibacterium prausnitzii* culture supernatants reduce proinflammatory IL-8 production *in vitro* and alleviate the severity of 2,4,6-trinitrobenzenesulfonic acid (TNBS)-induced colitis after oral and intraperitoneal administration (Sokol *et al.*, 2008). However, the nature of this secreted factor has yet not been identified.

To clearly identify the role of indole for *E. coli* Nissle's probiotic effects, it would be interesting to generate a *tnaA* deletion mutant of *E. coli* Nissle. Monoassociation of DSS-treated or

IL-10$^{-/-}$ animals with this mutant would demonstrate if indole production is necessary for the beneficial effects of *E. coli* Nissle.

5.4 Limitations of the experimental design

Animal models of intestinal inflammation have become indispensable for the understanding of various aspects of the pathogenesis of IBD. Although none of these models mimics exactly the human situation, each model provides different and unique insights into the specific biological mechanisms involved in the development of intestinal inflammation. In the last years, these models were excessively used to investigate the influence of the gut microbiota on the host, but until today only one publication (Patwa *et al.*, 2011) focussed on the bacterial adaptation to intestinal inflammation - therefore research in this area is still in its infancy.

In this PhD-thesis, the bacterial response to intestinal inflammation was investigated in a very simplified model using mice monoassociated with *E. coli*. These mice lack the influences of other commensal microbes on *E. coli*'s protein expression, which is necessary in order to definitely identify *E. coli*'s response to the inflammatory process. On the other hand the model is hampered by the fact that the crosstalk between different bacterial species and their overall consequences were not considered. Especially for analysing the beneficial effect of *E. coli* Nissle on disease development in the IL-10$^{-/-}$ experiment, it would be interesting to use conventional mice. Furthermore, in both animal experiments a proper control group, such as mice monoassociated with the commensal *E. coli* strain MG1655 K-12, is missing. Therefore it is difficult to conclude that *E. coli* Nissle is probiotic, whilst *E. coli* UNC is harmful. Maybe *E. coli* Nissle is only more beneficial than *E. coli* UNC, but not than *E. coli* K-12? Moreover, by isolating *E. coli* from the caecal contents, only luminal bacteria and not mucosally associated bacteria were studied. In fact, mucosa-associated bacteria would be even more suitable, since they directly interact with the host. However, these are difficult to isolate and the possible amount of the isolated cells would have been too low for proteomic analysis.

In some instances, proteins belonging to the same metabolic categories (such as carbohydrate metabolism or nucleotide synthesis) were regulated oppositely in response to DSS-induced inflammation. The explanation for this is not quite obvious. On the one hand, inflammation may lead to the release of metabolites from damaged epithelial cells, which can in part be used by *E. coli*. This, for example, requires the upregulation of salvage enzymes and the downregulation of *de novo* synthesis of enzymes within the same category. On the other hand, these discrepancies can also be explained by the limitations of the proteome analysis: In theory, 2D gel electrophoresis should result in protein spots that are represented

by only one protein, but in practice the majority of spots are represented by two or more proteins. Despite the high sensitivity of mass spectrometry, mainly high-abundant proteins are identified in these spots, leading to the exclusion of many low-abundant proteins. In some cases, the protein contributing to the differential spot expression was not clearly identified, resulting in a relatively high number of per se differentially regulated protein spots, but in a low number of identified proteins. Furthermore, one disadvantage of the 2D-DIGE technique is that only gels with the same internal standard are comparable. In fact, gels of the DSS- and IL-10$^{-/-}$ experiment were prepared at different time points and therefore they didn't include the same internal standard. Unless the protein was identified by mass spectrometry, it was almost impossible to match the gels of these two experiments and to identify proteins only on the basis of their location within the gel. For example, *E. coli* Nissle's fitness factors YggE and Ivy were identified separately, one in the DSS- and the other in the IL-10$^{-/-}$ experiment. Although, one would assume that both are also regulated in *E. coli* Nissle from the other experiment, there is no way to prove this using this proteomic approach. Nevertheless, additional *in vitro* experiments confirmed their role as important fitness factors in *E. coli* Nissle.

6 CONCLUSIONS AND PERSPECTIVES

This PhD-thesis provides insights into the cross-talk between host and intestinal bacteria during an intestinal inflammation. As observed in IL-10$^{-/-}$ mice, *E. coli* are very sensitive in detecting the health status of the host. *E. coli* perceive even minimal changes in the host environment and adapt to the changed conditions by modifying their protein expression. In the case of severe intestinal inflammation, this adaptation is characterised by a strong inhibition of *E. coli*'s central energy metabolism and an induction of several stress response proteins. Special emphasis should be placed on the upregulation of the NfuA protein, which is a general adaptation to severe inflammatory conditions. Upregulation of this protein may contribute to the high *E. coli* cell numbers found in IBD patients. Effective colonisation is also a prerequisite for *E. coli* Nissle's probiotic function and therefore it is important to know, which factors promote this colonisation efficiency under *in vivo* conditions. Two, so far unknown fitness factors (YggE and Ivy) of *E. coli* Nissle were identified that enable this probiotic strain to effectively colonise the intestine under hostile inflammatory conditions. Moreover, indole was identified as a potential new probiotic agent of *E. coli* Nissle. Since the caecal indole concentrations in healthy individuals were higher than in inflamed mice, indole is hypothesised to contribute to the main therapeutic effect of *E. coli* Nissle: Maintenance of the remission state in patients with UC.

This PhD-thesis mainly concentrated on the bacterial adaptation to intestinal inflammation and the developed hypotheses were supported initially by *in vitro* experiments and/or by literature data. Therefore, additional *in vivo* studies are needed to confirm the relevance of the identified proteins for *E. coli*'s adaptation to the intestinal inflammation. Especially the role of indole for *E. coli* Nissle's probiotic function needs to be further investigated using animal studies. In conclusion, it was demonstrated that host and intestinal bacteria interact with each other in the state of an intestinal inflammation and that the bacterial reactions have the potential to influence the host. Although this is fundamental research, these results lead to a better understanding of how host - microbe interactions, which contribute to IBD pathology. In future, they may facilitate the development of new treatment strategies against intestinal inflammatory disorders.

7 REFERENCES

[1] **Abergel C., Monchois V., Byrne D., Chenivesse S., Lembo F*., et al.* (2007).** *Structure and evolution of the Ivy protein family, unexpected lysozyme inhibitors in Gram-negative bacteria.* Proc Natl Acad Sci U S A 104(15): 6394-9.

[2] **Altenhoefer A., Oswald S., Sonnenborn U., Enders C., Schulze J*., et al.* (2004).** *The probiotic Escherichia coli strain Nissle 1917 interferes with invasion of human intestinal epithelial cells by different enteroinvasive bacterial pathogens.* FEMS Immunol Med Microbiol 40(3): 223-9.

[3] **Angelini S., Gerez C., Ollagnier-de Choudens S., Sanakis Y., Fontecave M*., et al.* (2008).** *NfuA, a new factor required for maturing Fe/S proteins in Escherichia coli under oxidative stress and iron starvation conditions.* J Biol Chem 283(20): 14084-91.

[4] **Bansal T., Alaniz R.C., Wood T.K. and Jayaraman A. (2010).** *The bacterial signal indole increases epithelial-cell tight-junction resistance and attenuates indicators of inflammation.* Proc Natl Acad Sci U S A 107(1): 228-33.

[5] **Bansal T., Englert D., Lee J., Hegde M., Wood T.K*., et al.* (2007).** *Differential effects of epinephrine, norepinephrine, and indole on Escherichia coli O157:H7 chemotaxis, colonization, and gene expression.* Infect Immun 75(9): 4597-607.

[6] **Barclay A.R., Russell R.K., Wilson M.L., Gilmour W.H., Satsangi J*., et al.* (2009).** *Systematic review: the role of breastfeeding in the development of pediatric inflammatory bowel disease.* J Pediatr 155(3): 421-6.

[7] **Barnich N., Carvalho F.A., Glasser A.L., Darcha C., Jantscheff P*., et al.* (2007).** *CEACAM6 acts as a receptor for adherent-invasive E. coli, supporting ileal mucosa colonization in Crohn disease.* J Clin Invest 117(6): 1566-74.

[8] **Barras F., Loiseau L. and Py B. (2005).** *How Escherichia coli and Saccharomyces cerevisiae build Fe/S proteins.* Adv Microb Physiol 50: 41-101.

[9] **Bartolome B., Jubete Y., Martinez E. and de la Cruz F. (1991).** *Construction and properties of a family of pACYC184-derived cloning vectors compatible with pBR322 and its derivatives.* Gene 102(1): 75-8.

[10] **Baumgart D.C. and Sandborn W.J. (2007).** *Inflammatory bowel disease: clinical aspects and established and evolving therapies.* Lancet 369(9573): 1641-57.

[11] **Baumgart M., Dogan B., Rishniw M., Weitzman G., Bosworth B*., et al.* (2007).** *Culture independent analysis of ileal mucosa reveals a selective increase in invasive Escherichia coli of novel phylogeny relative to depletion of Clostridiales in Crohn's disease involving the ileum.* Isme J 1(5): 403-18.

[12] **Berg D.J., Davidson N., Kuhn R., Muller W., Menon S*., et al.* (1996).** *Enterocolitis and colon cancer in interleukin-10-deficient mice are associated with aberrant cytokine production and CD4(+) TH1-like responses.* J Clin Invest 98(4): 1010-20.

[13] **Boudeau J., Glasser A.L., Julien S., Colombel J.F. and Darfeuille-Michaud A. (2003).** *Inhibitory effect of probiotic Escherichia coli strain Nissle 1917 on adhesion to and invasion of intestinal epithelial cells by adherent-invasive E. coli strains isolated from patients with Crohn's disease.* Aliment Pharmacol Ther 18(1): 45-56.

[14] **Boudeau J., Glasser A.L., Masseret E., Joly B. and Darfeuille-Michaud A.** (1999). *Invasive ability of an Escherichia coli strain isolated from the ileal mucosa of a patient with Crohn's disease*. Infect Immun 67(9): 4499-509.

[15] **Bradford M.M.** (1976). *A rapid and sensitive method for the quantitation of microgram quantities of protein utilizing the principle of protein-dye binding*. Anal Biochem 72: 248-54.

[16] **Bristol I.J., Farmer M.A., Cong Y., Zheng X.X., Strom T.B.*, et al.*** (2000). *Heritable susceptibility for colitis in mice induced by IL-10 deficiency*. Inflamm Bowel Dis 6(4): 290-302.

[17] **Bruewer M., Luegering A., Kucharzik T., Parkos C.A., Madara J.L.*, et al.*** (2003). *Proinflammatory cytokines disrupt epithelial barrier function by apoptosis-independent mechanisms*. J Immunol 171(11): 6164-72.

[18] **Burich A., Hershberg R., Waggie K., Zeng W., Brabb T.*, et al.*** (2001). *Helicobacter-induced inflammatory bowel disease in IL-10- and T cell-deficient mice*. Am J Physiol Gastrointest Liver Physiol 281(3): G764-78.

[19] **Canavan C., Abrams K.R. and Mayberry J.** (2006). *Meta-analysis: colorectal and small bowel cancer risk in patients with Crohn's disease*. Aliment Pharmacol Ther 23(8): 1097-104.

[20] **Cha M.K., Kim W.C., Lim C.J., Kim K. and Kim I.H.** (2004). *Escherichia coli periplasmic thiol peroxidase acts as lipid hydroperoxide peroxidase and the principal antioxidative function during anaerobic growth*. J Biol Chem 279(10): 8769-78.

[21] **Cheng H. and Leblond C.P.** (1974). *Origin, differentiation and renewal of the four main epithelial cell types in the mouse small intestine. V. Unitarian Theory of the origin of the four epithelial cell types*. Am J Anat 141(4): 537-61.

[22] **Clayburgh D.R., Shen L. and Turner J.R.** (2004). *A porous defense: the leaky epithelial barrier in intestinal disease*. Lab Invest 84(3): 282-91.

[23] **Conner E.M., Brand S.J., Davis J.M., Kang D.Y. and Grisham M.B.** (1996). *Role of reactive metabolites of oxygen and nitrogen in inflammatory bowel disease: toxins, mediators, and modulators of gene expression*. Inflamm Bowel Dis 2(2): 133-47.

[24] **Cooper H.S., Murthy S.N., Shah R.S. and Sedergran D.J.** (1993). *Clinicopathologic study of dextran sulfate sodium experimental murine colitis*. Lab Invest 69(2): 238-49.

[25] **Courcelle J. and Hanawalt P.C.** (2003). *RecA-dependent recovery of arrested DNA replication forks*. Annu Rev Genet 37: 611-46.

[26] **Darfeuille-Michaud A., Boudeau J., Bulois P., Neut C., Glasser A.L.*, et al.*** (2004). *High prevalence of adherent-invasive Escherichia coli associated with ileal mucosa in Crohn's disease*. Gastroenterology 127(2): 412-21.

[27] **Darfeuille-Michaud A., Neut C., Barnich N., Lederman E., Di Martino P.*, et al.*** (1998). *Presence of adherent Escherichia coli strains in ileal mucosa of patients with Crohn's disease*. Gastroenterology 115(6): 1405-13.

[28] **Datsenko K.A. and Wanner B.L.** (2000). *One-step inactivation of chromosomal genes in Escherichia coli K-12 using PCR products*. Proc Natl Acad Sci U S A 97(12): 6640-5.

[29]   **Di Giacinto C., Marinaro M., Sanchez M., Strober W. and Boirivant M.** (2005). *Probiotics ameliorate recurrent Th1-mediated murine colitis by inducing IL-10 and IL-10-dependent TGF-beta-bearing regulatory cells*. J Immunol 174(6): 3237-46.

[30]   **Dobson A., Cotter P.D., Ross R.P. and Hill C.** (2012). *Bacteriocin production: a probiotic trait?* Appl Environ Microbiol 78(1): 1-6.

[31]   **Dower W.J., Miller J.F. and Ragsdale C.W.** (1988). *High efficiency transformation of E. coli by high voltage electroporation*. Nucleic Acids Res 16(13): 6127-45.

[32]   **Duchmann R., Kaiser I., Hermann E., Mayet W., Ewe K.*, et al.*** (1995). *Tolerance exists towards resident intestinal flora but is broken in active inflammatory bowel disease (IBD)*. Clin Exp Immunol 102(3): 448-55.

[33]   **Falk P.G., Hooper L.V., Midtvedt T. and Gordon J.I.** (1998). *Creating and maintaining the gastrointestinal ecosystem: what we know and need to know from gnotobiology*. Microbiol Mol Biol Rev 62(4): 1157-70.

[34]   **Frank D.N., Robertson C.E., Hamm C.M., Kpadeh Z., Zhang T.*, et al.*** (2011). *Disease phenotype and genotype are associated with shifts in intestinal-associated microbiota in inflammatory bowel diseases*. Inflamm Bowel Dis 17(1): 179-84.

[35]   **Gent A.E., Hellier M.D., Grace R.H., Swarbrick E.T. and Coggon D.** (1994). *Inflammatory bowel disease and domestic hygiene in infancy*. Lancet 343(8900): 766-7.

[36]   **Gerbe F., van Es J.H., Makrini L., Brulin B., Mellitzer G.*, et al.*** (2011). *Distinct ATOH1 and Neurog3 requirements define tuft cells as a new secretory cell type in the intestinal epithelium*. J Cell Biol 192(5): 767-80.

[37]   **Gill S.R., Pop M., Deboy R.T., Eckburg P.B., Turnbaugh P.J.*, et al.*** (2006). *Metagenomic analysis of the human distal gut microbiome*. Science 312(5778): 1355-9.

[38]   **Girardin S.E., Boneca I.G., Viala J., Chamaillard M., Labigne A.*, et al.*** (2003). *Nod2 is a general sensor of peptidoglycan through muramyl dipeptide (MDP) detection*. J Biol Chem 278(11): 8869-72.

[39]   **Gomes-Santos A.C., Moreira T.G., Castro-Junior A.B., Horta B.C., Lemos L.*, et al.*** (2012). *New insights into the immunological changes in IL-10-deficient mice during the course of spontaneous inflammation in the gut mucosa*. Clin Dev Immunol 2012: 560817.

[40]   **Gophna U., Sommerfeld K., Gophna S., Doolittle W.F. and Veldhuyzen van Zanten S.J.** (2006). *Differences between tissue-associated intestinal microfloras of patients with Crohn's disease and ulcerative colitis*. J Clin Microbiol 44(11): 4136-41.

[41]   **Grabig A., Paclik D., Guzy C., Dankof A., Baumgart D.C.*, et al.*** (2006). *Escherichia coli strain Nissle 1917 ameliorates experimental colitis via toll-like receptor 2- and toll-like receptor 4-dependent pathways*. Infect Immun 74(7): 4075-82.

[42]   **Grozdanov L., Raasch C., Schulze J., Sonnenborn U., Gottschalk G.*, et al.*** (2004). *Analysis of the genome structure of the nonpathogenic probiotic Escherichia coli strain Nissle 1917*. J Bacteriol 186(16): 5432-41.

[43]   **Guarner F. and Schaafsma G.J.** (1998). *Probiotics*. Int J Food Microbiol 39(3): 237-8.

[44]   **Guslandi M.** (2011). *Rifaximin in the treatment of inflammatory bowel disease*. World J Gastroenterol 17(42): 4643-6.

[45]   **Hagiwara D., Sugiura M., Oshima T., Mori H., Aiba H.*, et al.* (2003). *Genome-wide analyses revealing a signaling network of the RcsC-YojN-RcsB phosphorelay system in Escherichia coli*. J Bacteriol 185(19): 5735-46.

[46]   **Halme L., Paavola-Sakki P., Turunen U., Lappalainen M., Farkkila M.*, et al.* (2006). *Family and twin studies in inflammatory bowel disease*. World J Gastroenterol 12(23): 3668-72.

[47]   **Hans W., Scholmerich J., Gross V. and Falk W.** (2000). *The role of the resident intestinal flora in acute and chronic dextran sulfate sodium-induced colitis in mice*. Eur J Gastroenterol Hepatol 12(3): 267-73.

[48]   **Harris M.L., Schiller H.J., Reilly P.M., Donowitz M., Grisham M.B.*, et al.* (1992). *Free radicals and other reactive oxygen metabolites in inflammatory bowel disease: cause, consequence or epiphenomenon?* Pharmacol Ther 53(3): 375-408.

[49]   **Hart A.L., Al-Hassi H.O., Rigby R.J., Bell S.J., Emmanuel A.V.*, et al.* (2005). *Characteristics of intestinal dendritic cells in inflammatory bowel diseases*. Gastroenterology 129(1): 50-65.

[50]   **Heimesaat M.M., Fischer A., Siegmund B., Kupz A., Niebergall J.*, et al.* (2007). *Shift towards pro-inflammatory intestinal bacteria aggravates acute murine colitis via Toll-like receptors 2 and 4*. PLoS One 2(7): e662.

[51]   **Henker J., Muller S., Laass M.W., Schreiner A. and Schulze J.** (2008). *Probiotic Escherichia coli Nissle 1917 (EcN) for successful remission maintenance of ulcerative colitis in children and adolescents: an open-label pilot study*. Z Gastroenterol 46(9): 874-5.

[52]   **Hoffmann J.C., Pawlowski N.N., Kuhl A.A., Hohne W. and Zeitz M.** (2002). *Animal models of inflammatory bowel disease: an overview*. Pathobiology 70(3): 121-30.

[53]   **Hooper L.V., Xu J., Falk P.G., Midtvedt T. and Gordon J.I.** (1999). *A molecular sensor that allows a gut commensal to control its nutrient foundation in a competitive ecosystem*. Proc Natl Acad Sci U S A 96(17): 9833-8.

[54]   **Hou J.K., Abraham B. and El-Serag H.** (2011). *Dietary intake and risk of developing inflammatory bowel disease: a systematic review of the literature*. Am J Gastroenterol 106(4): 563-73.

[55]   **Hou J.K., El-Serag H. and Thirumurthi S.** (2009). *Distribution and manifestations of inflammatory bowel disease in Asians, Hispanics, and African Americans: a systematic review*. Am J Gastroenterol 104(8): 2100-9.

[56]   **Hudcovic T., Stepankova R., Cebra J. and Tlaskalova-Hogenova H.** (2001). *The role of microflora in the development of intestinal inflammation: acute and chronic colitis induced by dextran sulfate in germ-free and conventionally reared immunocompetent and immunodeficient mice*. Folia Microbiol (Praha) 46(6): 565-72.

[57]   **Hugot J.P., Chamaillard M., Zouali H., Lesage S., Cezard J.P.*, et al.* (2001). *Association of NOD2 leucine-rich repeat variants with susceptibility to Crohn's disease*. Nature 411(6837): 599-603.

[58]   **Inohara N., Ogura Y., Fontalba A., Gutierrez O., Pons F.*, et al.* (2003).** *Host recognition of bacterial muramyl dipeptide mediated through NOD2. Implications for Crohn's disease*. J Biol Chem 278(8): 5509-12.

[59]   **Jang S. and Imlay J.A. (2007).** *Micromolar intracellular hydrogen peroxide disrupts metabolism by damaging iron-sulfur enzymes*. J Biol Chem 282(2): 929-37.

[60]   **Jess T., Rungoe C. and Peyrin-Biroulet L. (2012a).** *Risk of colorectal cancer in patients with ulcerative colitis: a meta-analysis of population-based cohort studies*. Clin Gastroenterol Hepatol 10(6): 639-45.

[61]   **Jess T., Simonsen J., Jorgensen K.T., Pedersen B.V., Nielsen N.M.*, et al.* (2012b).** *Decreasing risk of colorectal cancer in patients with inflammatory bowel disease over 30 years*. Gastroenterology 143(2): 375-81 e1; quiz e13-4.

[62]   **Joossens M., Huys G., Cnockaert M., De Preter V., Verbeke K.*, et al.* (2011).** *Dysbiosis of the faecal microbiota in patients with Crohn's disease and their unaffected relatives*. Gut 60(5): 631-7.

[63]   **Joossens M., Simoens M., Vermeire S., Bossuyt X., Geboes K.*, et al.* (2007).** *Contribution of genetic and environmental factors in the pathogenesis of Crohn's disease in a large family with multiple cases*. Inflamm Bowel Dis 13(5): 580-4.

[64]   **Kamada N., Inoue N., Hisamatsu T., Okamoto S., Matsuoka K.*, et al.* (2005).** *Nonpathogenic Escherichia coli strain Nissle1917 prevents murine acute and chronic colitis*. Inflamm Bowel Dis 11(5): 455-63.

[65]   **Kamada N., Maeda K., Inoue N., Hisamatsu T., Okamoto S.*, et al.* (2008).** *Nonpathogenic Escherichia coli strain Nissle 1917 inhibits signal transduction in intestinal epithelial cells*. Infect Immun 76(1): 214-20.

[66]   **Kaplan G.G., Hubbard J., Korzenik J., Sands B.E., Panaccione R.*, et al.* (2010).** *The inflammatory bowel diseases and ambient air pollution: a novel association*. Am J Gastroenterol 105(11): 2412-9.

[67]   **Kaser A. and Blumberg R.S. (2011).** *Autophagy, microbial sensing, endoplasmic reticulum stress, and epithelial function in inflammatory bowel disease*. Gastroenterology 140(6): 1738-47.

[68]   **Kaser A., Zeissig S. and Blumberg R.S. (2010).** *Inflammatory bowel disease*. Annu Rev Immunol 28: 573-621.

[69]   **Kim C.J., Kovacs-Nolan J.A., Yang C., Archbold T., Fan M.Z.*, et al.* (2010).** *l-Tryptophan exhibits therapeutic function in a porcine model of dextran sodium sulfate (DSS)-induced colitis*. J Nutr Biochem.

[70]   **Kim S.C., Tonkonogy S.L., Albright C.A., Tsang J., Balish E.J.*, et al.* (2005a).** *Variable phenotypes of enterocolitis in interleukin 10-deficient mice monoassociated with two different commensal bacteria*. Gastroenterology 128(4): 891-906.

[71]   **Kim S.Y., Nishioka M., Hayashi S., Honda H., Kobayashi T.*, et al.* (2005b).** *The gene yggE functions in restoring physiological defects of Escherichia coli cultivated under oxidative stress conditions*. Appl Environ Microbiol 71(5): 2762-5.

[72]   **Kitagawa M., Matsumura Y. and Tsuchido T.** (2000). *Small heat shock proteins, IbpA and IbpB, are involved in resistances to heat and superoxide stresses in Escherichia coli*. FEMS Microbiol Lett 184(2): 165-71.

[73]   **Kitajima S., Morimoto M., Sagara E., Shimizu C. and Ikeda Y.** (2001). *Dextran sodium sulfate-induced colitis in germ-free IQI/Jic mice*. Exp Anim 50(5): 387-95.

[74]   **Kobayashi K.S., Chamaillard M., Ogura Y., Henegariu O., Inohara N.*, et al.* ** (2005). *Nod2-dependent regulation of innate and adaptive immunity in the intestinal tract*. Science 307(5710): 731-4.

[75]   **Kokesova A., Frolova L., Kverka M., Sokol D., Rossmann P.*, et al.* ** (2006). *Oral administration of probiotic bacteria (E. coli Nissle, E. coli O83, Lactobacillus casei) influences the severity of dextran sodium sulfate-induced colitis in BALB/c mice*. Folia Microbiol (Praha) 51(5): 478-84.

[76]   **Kotlowski R., Bernstein C.N., Sepehri S. and Krause D.O.** (2007). *High prevalence of Escherichia coli belonging to the B2+D phylogenetic group in inflammatory bowel disease*. Gut 56(5): 669-75.

[77]   **Krishnaiah D., Bono A., Sarbatly R., Nishioka M., Kim S.Y.*, et al.* ** (2007). *Physiological responses of Escherichia coli cells cultivated under a sublethal oxidative stress condition*. Malaysian Journal of Microbiology Vol 3(1) 2007: 14-18.

[78]   **Kruidenier L., Kuiper I., Lamers C.B. and Verspaget H.W.** (2003). *Intestinal oxidative damage in inflammatory bowel disease: semi-quantification, localization, and association with mucosal antioxidants*. J Pathol 201(1): 28-36.

[79]   **Kruis W., Fric P., Pokrotnieks J., Lukas M., Fixa B.*, et al.* ** (2004). *Maintaining remission of ulcerative colitis with the probiotic Escherichia coli Nissle 1917 is as effective as with standard mesalazine*. Gut 53(11): 1617-23.

[80]   **Kruis W., Schutz E., Fric P., Fixa B., Judmaier G.*, et al.* ** (1997). *Double-blind comparison of an oral Escherichia coli preparation and mesalazine in maintaining remission of ulcerative colitis*. Aliment Pharmacol Ther 11(5): 853-8.

[81]   **Kühn R., Lohler J., Rennick D., Rajewsky K. and Muller W.** (1993). *Interleukin-10-deficient mice develop chronic enterocolitis*. Cell 75(2): 263-74.

[82]   **Lai Y.C., Peng H.L. and Chang H.Y.** (2001). *Identification of genes induced in vivo during Klebsiella pneumoniae CG43 infection*. Infect Immun 69(11): 7140-5.

[83]   **Lakatos P.L., Fischer S., Lakatos L., Gal I. and Papp J.** (2006). *Current concept on the pathogenesis of inflammatory bowel disease-crosstalk between genetic and microbial factors: pathogenic bacteria and altered bacterial sensing or changes in mucosal integrity take "toll" ?* World J Gastroenterol 12(12): 1829-41.

[84]   **Laubacher M.E. and Ades S.E.** (2008). *The Rcs phosphorelay is a cell envelope stress response activated by peptidoglycan stress and contributes to intrinsic antibiotic resistance*. J Bacteriol 190(6): 2065-74.

[85]   **Laukoetter M.G., Nava P. and Nusrat A.** (2008). *Role of the intestinal barrier in inflammatory bowel disease*. World J Gastroenterol 14(3): 401-7.

[86]   **Le Borgne S., Palmeros B., Bolivar F. and Gosset G.** (2001). *Improvement of the pBRINT-Ts plasmid family to obtain marker-free chromosomal insertion of cloned DNA in E. coli.* Biotechniques 30(2): 252-4, 256.

[87]   **Lee J.H. and Lee J.** (2010). *Indole as an intercellular signal in microbial communities.* FEMS Microbiol Rev 34(4): 426-44.

[88]   **Lehrer R.I., Barton A., Daher K.A., Harwig S.S., Ganz T.*, et al.** (1989). *Interaction of human defensins with Escherichia coli. Mechanism of bactericidal activity.* J Clin Invest 84(2): 553-61.

[89]   **Lehrer R.I., Lichtenstein A.K. and Ganz T.** (1993). *Defensins: antimicrobial and cytotoxic peptides of mammalian cells.* Annu Rev Immunol 11: 105-28.

[90]   **Lehrer R.I., Rosenman M., Harwig S.S., Jackson R. and Eisenhauer P.** (1991). *Ultrasensitive assays for endogenous antimicrobial polypeptides.* J Immunol Methods 137(2): 167-73.

[91]   **Lin Y.P., Thibodeaux C.H., Pena J.A., Ferry G.D. and Versalovic J.** (2008). *Probiotic Lactobacillus reuteri suppress proinflammatory cytokines via c-Jun.* Inflamm Bowel Dis 14(8): 1068-83.

[92]   **Lodinova-Zadnikova R. and Sonnenborn U.** (1997). *Effect of preventive administration of a nonpathogenic Escherichia coli strain on the colonization of the intestine with microbial pathogens in newborn infants.* Biol Neonate 71(4): 224-32.

[93]   **Loetscher Y., Wieser A., Lengefeld J., Kaiser P., Schubert S.*, et al.** (2012). *Salmonella transiently reside in luminal neutrophils in the inflamed gut.* PLoS One 7(4): e34812.

[94]   **Loftus E.V., Jr.** (2004). *Clinical epidemiology of inflammatory bowel disease: Incidence, prevalence, and environmental influences.* Gastroenterology 126(6): 1504-17.

[95]   **Louis E., Libioulle C., Reenaers C., Belaiche J. and Georges M.** (2009). *Genetics of ulcerative colitis: the come-back of interleukin 10.* Gut 58(9): 1173-6.

[96]   **Macpherson A., Khoo U.Y., Forgacs I., Philpott-Howard J. and Bjarnason I.** (1996). *Mucosal antibodies in inflammatory bowel disease are directed against intestinal bacteria.* Gut 38(3): 365-75.

[97]   **Macpherson A.J. and Harris N.L.** (2004). *Interactions between commensal intestinal bacteria and the immune system.* Nat Rev Immunol 4(6): 478-85.

[98]   **Mahler M., Bristol I.J., Leiter E.H., Workman A.E., Birkenmeier E.H.*, et al.** (1998). *Differential susceptibility of inbred mouse strains to dextran sulfate sodium-induced colitis.* Am J Physiol 274(3 Pt 1): G544-51.

[99]   **Marshall O.J.** (2004). *PerlPrimer: cross-platform, graphical primer design for standard, bisulphite and real-time PCR.* Bioinformatics 20(15): 2471-2.

[100] **Matthes H., Krummenerl T., Giensch M., Wolff C. and Schulze J.** (2010). *Clinical trial: probiotic treatment of acute distal ulcerative colitis with rectally administered Escherichia coli Nissle 1917 (EcN).* BMC Complement Altern Med 10: 13.

[101] **Mattivi F., Vrhovsek U. and Versini G.** (1999). *Determination of indole-3-acetic acid, tryptophan and other indoles in must and wine by high-performance liquid chromatography with fluorescence detection*. J Chromatogr A 855(1): 227-35.

[102] **May G.R., Sutherland L.R. and Meddings J.B.** (1993). *Is small intestinal permeability really increased in relatives of patients with Crohn's disease?* Gastroenterology 104(6): 1627-32.

[103] **Melgar S., Karlsson L., Rehnstrom E., Karlsson A., Utkovic H*., et al.*** (2008). *Validation of murine dextran sulfate sodium-induced colitis using four therapeutic agents for human inflammatory bowel disease*. Int Immunopharmacol 8(6): 836-44.

[104] **Molodecky N.A., Soon I.S., Rabi D.M., Ghali W.A., Ferris M*., et al.*** (2012). *Increasing incidence and prevalence of the inflammatory bowel diseases with time, based on systematic review*. Gastroenterology 142(1): 46-54 e42; quiz e30.

[105] **Monchois V., Abergel C., Sturgis J., Jeudy S. and Claverie J.M.** (2001). *Escherichia coli ykfE ORFan gene encodes a potent inhibitor of C-type lysozyme*. J Biol Chem 276(21): 18437-41.

[106] **Möndel M., Schroeder B.O., Zimmermann K., Huber H., Nuding S*., et al.*** (2009). *Probiotic E. coli treatment mediates antimicrobial human beta-defensin synthesis and fecal excretion in humans*. Mucosal Immunol 2(2): 166-72.

[107] **Moreau M.C., Ducluzeau R., Guy-Grand D. and Muller M.C.** (1978). *Increase in the population of duodenal immunoglobulin A plasmocytes in axenic mice associated with different living or dead bacterial strains of intestinal origin*. Infect Immun 21(2): 532-9.

[108] **Mostertz J., Scharf C., Hecker M. and Homuth G.** (2004). *Transcriptome and proteome analysis of Bacillus subtilis gene expression in response to superoxide and peroxide stress*. Microbiology 150(Pt 2): 497-512.

[109] **Nagalingam N.A., Kao J.Y. and Young V.B.** (2011). *Microbial ecology of the murine gut associated with the development of dextran sodium sulfate-induced colitis*. Inflamm Bowel Dis 17(4): 917-26.

[110] **Nossal N.G. and Heppel L.A.** (1966). *The release of enzymes by osmotic shock from Escherichia coli in exponential phase*. J Biol Chem 241(13): 3055-62.

[111] **Ogura Y., Bonen D.K., Inohara N., Nicolae D.L., Chen F.F*., et al.*** (2001a). *A frameshift mutation in NOD2 associated with susceptibility to Crohn's disease*. Nature 411(6837): 603-6.

[112] **Ogura Y., Inohara N., Benito A., Chen F.F., Yamaoka S*., et al.*** (2001b). *Nod2, a Nod1/Apaf-1 family member that is restricted to monocytes and activates NF-kappaB*. J Biol Chem 276(7): 4812-8.

[113] **Ojima Y., Kawase D., Nishioka M. and Taya M.** (2009). *Functionally undefined gene, yggE, alleviates oxidative stress generated by monoamine oxidase in recombinant Escherichia coli*. Biotechnol Lett 31(1): 139-45.

[114] **Patwa L.G., Fan T.J., Tchaptchet S., Liu Y., Lussier Y.A*., et al.*** (2011). *Chronic intestinal inflammation induces stress-response genes in commensal Escherichia coli*. Gastroenterology 141(5): 1842-51 e1-10.

[115] **Pavlick K.P., Laroux F.S., Fuseler J., Wolf R.E., Gray L.*, et al.* (2002).** *Role of reactive metabolites of oxygen and nitrogen in inflammatory bowel disease*. Free Radic Biol Med 33(3): 311-22.

[116] **Peeters M., Geypens B., Claus D., Nevens H., Ghoos Y.*, et al.* (1997).** *Clustering of increased small intestinal permeability in families with Crohn's disease*. Gastroenterology 113(3): 802-7.

[117] **Peeters M., Ghoos Y., Maes B., Hiele M., Geboes K.*, et al.* (1994).** *Increased permeability of macroscopically normal small bowel in Crohn's disease*. Dig Dis Sci 39(10): 2170-6.

[118] **Py B. and Barras F. (2010).** *Building Fe-S proteins: bacterial strategies*. Nat Rev Microbiol 8(6): 436-46.

[119] **Py B., Gerez C., Angelini S., Planel R., Vinella D.*, et al.* (2012).** *Molecular organization, biochemical function, cellular role and evolution of NfuA, an atypical Fe-S carrier*. Mol Microbiol 86(1): 155-71.

[120] **Rabilloud T., Strub J.M., Luche S., van Dorsselaer A. and Lunardi J. (2001).** *A comparison between Sypro Ruby and ruthenium II tris (bathophenanthroline disulfonate) as fluorescent stains for protein detection in gels*. Proteomics 1(5): 699-704.

[121] **Raffatellu M., George M.D., Akiyama Y., Hornsby M.J., Nuccio S.P.*, et al.* (2009).** *Lipocalin-2 resistance confers an advantage to Salmonella enterica serotype Typhimurium for growth and survival in the inflamed intestine*. Cell Host Microbe 5(5): 476-86.

[122] **Ransford R.A. and Langman M.J. (2002).** *Sulphasalazine and mesalazine: serious adverse reactions re-evaluated on the basis of suspected adverse reaction reports to the Committee on Safety of Medicines*. Gut 51(4): 536-9.

[123] **Redon E., Loubiere P. and Cocaign-Bousquet M. (2005).** *Role of mRNA stability during genome-wide adaptation of Lactococcus lactis to carbon starvation*. J Biol Chem 280(43): 36380-5.

[124] **Rembacken B.J., Snelling A.M., Hawkey P.M., Chalmers D.M. and Axon A.T. (1999).** *Non-pathogenic Escherichia coli versus mesalazine for the treatment of ulcerative colitis: a randomised trial*. Lancet 354(9179): 635-9.

[125] **Resta-Lenert S. and Barrett K.E. (2003).** *Live probiotics protect intestinal epithelial cells from the effects of infection with enteroinvasive Escherichia coli (EIEC)*. Gut 52(7): 988-97.

[126] **Roediger W.E. (1980).** *The colonic epithelium in ulcerative colitis: an energy-deficiency disease?* Lancet 2(8197): 712-5.

[127] **Rogler G. (2011).** *Interaction between susceptibility and environment: examples from the digestive tract*. Dig Dis 29(2): 136-43.

[128] **Rolhion N., Barnich N., Bringer M.A., Glasser A.L., Ranc J.*, et al.* (2010).** *Abnormally expressed ER stress response chaperone Gp96 in CD favours adherent-invasive Escherichia coli invasion*. Gut 59(10): 1355-62.

[129] **Rothe M., Alpert C., Engst W., Musiol S., Loh G.*, et al.* (2012).** *Impact of nutritional factors on the proteome of intestinal Escherichia coli: induction of OxyR-dependent proteins AhpF and Dps by a lactose-rich diet*. Appl Environ Microbiol 78(10): 3580-91.

[130] **Rothe M., Alpert C., Loh G. and Blaut M.** (2013). *Novel Insights into E. coli's Hexuronate Metabolism: KduI Facilitates the Conversion of Galacturonate and Glucuronate under Osmotic Stress Conditions*. PLoS One 8(2): e56906.

[131] **Round J.L. and Mazmanian S.K.** (2009). *The gut microbiota shapes intestinal immune responses during health and disease*. Nat Rev Immunol 9(5): 313-23.

[132] **Sanchez-Munoz F., Dominguez-Lopez A. and Yamamoto-Furusho J.K.** (2008). *Role of cytokines in inflammatory bowel disease*. World J Gastroenterol 14(27): 4280-8.

[133] **Sartor R.B.** (2006). *Mechanisms of disease: pathogenesis of Crohn's disease and ulcerative colitis*. Nat Clin Pract Gastroenterol Hepatol 3(7): 390-407.

[134] **Sasaki M., Sitaraman S.V., Babbin B.A., Gerner-Smidt P., Ribot E.M*., et al.* (2007). *Invasive Escherichia coli are a feature of Crohn's disease*. Lab Invest 87(10): 1042-54.

[135] **Schlee M., Wehkamp J., Altenhoefer A., Oelschlaeger T.A., Stange E.F*., et al.* (2007). *Induction of human beta-defensin 2 by the probiotic Escherichia coli Nissle 1917 is mediated through flagellin*. Infect Immun 75(5): 2399-407.

[136] **Schultz M., Strauch U.G., Linde H.J., Watzl S., Obermeier F*., et al.* (2004). *Preventive effects of Escherichia coli strain Nissle 1917 on acute and chronic intestinal inflammation in two different murine models of colitis*. Clin Diagn Lab Immunol 11(2): 372-8.

[137] **Sekirov I., Russell S.L., Antunes L.C. and Finlay B.B.** (2010). *Gut microbiota in health and disease*. Physiol Rev 90(3): 859-904.

[138] **Sellon R.K., Tonkonogy S., Schultz M., Dieleman L.A., Grenther W*., et al.* (1998). *Resident enteric bacteria are necessary for development of spontaneous colitis and immune system activation in interleukin-10-deficient mice*. Infect Immun 66(11): 5224-31.

[139] **Seok J., Warren H.S., Cuenca A.G., Mindrinos M.N., Baker H.V*., et al.* (2013). *Genomic responses in mouse models poorly mimic human inflammatory diseases*. Proc Natl Acad Sci U S A.

[140] **Sokol H., Pigneur B., Watterlot L., Lakhdari O., Bermudez-Humaran L.G*., et al.* (2008). *Faecalibacterium prausnitzii is an anti-inflammatory commensal bacterium identified by gut microbiota analysis of Crohn disease patients*. Proc Natl Acad Sci U S A 105(43): 16731-6.

[141] **Sokol H., Seksik P., Furet J.P., Firmesse O., Nion-Larmurier I*., et al.* (2009). *Low counts of Faecalibacterium prausnitzii in colitis microbiota*. Inflamm Bowel Dis 15(8): 1183-9.

[142] **Sturm A., Rilling K., Baumgart D.C., Gargas K., Abou-Ghazale T*., et al.* (2005). *Escherichia coli Nissle 1917 distinctively modulates T-cell cycling and expansion via toll-like receptor 2 signaling*. Infect Immun 73(3): 1452-65.

[143] **Swidsinski A., Ladhoff A., Pernthaler A., Swidsinski S., Loening-Baucke V*., et al.* (2002). *Mucosal flora in inflammatory bowel disease*. Gastroenterology 122(1): 44-54.

[144] **Takagi M., Nishioka M., Kakihara H., Kitabayashi M., Inoue H*., et al.* (1997). *Characterization of DNA polymerase from Pyrococcus sp. strain KOD1 and its application to PCR*. Appl Environ Microbiol 63(11): 4504-10.

[145] **Taurog J.D., Richardson J.A., Croft J.T., Simmons W.A., Zhou M.*, et al.* (1994). *The germfree state prevents development of gut and joint inflammatory disease in HLA-B27 transgenic rats*. J Exp Med 180(6): 2359-64.

[146] **Thompson A.I. and Lees C.W.** (2010). *Genetics of ulcerative colitis*. Inflamm Bowel Dis 17(3): 831-48.

[147] **Turnbaugh P.J., Hamady M., Yatsunenko T., Cantarel B.L., Duncan A.*, et al.* (2009). *A core gut microbiome in obese and lean twins*. Nature 457(7228): 480-4.

[148] **Tuvlin J.A., Raza S.S., Bracamonte S., Julian C., Hanauer S.B.*, et al.* (2007). *Smoking and inflammatory bowel disease: trends in familial and sporadic cohorts*. Inflamm Bowel Dis 13(5): 573-9.

[149] **Ukena S.N., Singh A., Dringenberg U., Engelhardt R., Seidler U.*, et al.* (2007). *Probiotic Escherichia coli Nissle 1917 inhibits leaky gut by enhancing mucosal integrity*. PLoS ONE 2(12): e1308.

[150] **Vaara M.** (1992). *Agents that increase the permeability of the outer membrane*. Microbiol Rev 56(3): 395-411.

[151] **Vandesompele J., De Preter K., Pattyn F., Poppe B., Van Roy N.*, et al.* (2002). *Accurate normalization of real-time quantitative RT-PCR data by geometric averaging of multiple internal control genes*. Genome Biol 3(7): RESEARCH0034.

[152] **Veltkamp C., Anstaett M., Wahl K., Moller S., Gangl S.*, et al.* (2011). *Apoptosis of regulatory T lymphocytes is increased in chronic inflammatory bowel disease and reversed by anti-TNFalpha treatment*. Gut 60(10): 1345-53.

[153] **Vignali D.A., Collison L.W. and Workman C.J.** (2008). *How regulatory T cells work*. Nat Rev Immunol 8(7): 523-32.

[154] **Vogel-Scheel J., Alpert C., Engst W., Loh G. and Blaut M.** (2010). *Requirement of purine and pyrimidine synthesis for colonization of the mouse intestine by Escherichia coli*. Appl Environ Microbiol 76(15): 5181-7.

[155] **Walker A.W., Sanderson J.D., Churcher C., Parkes G.C., Hudspith B.N.*, et al.* (2011). *High-throughput clone library analysis of the mucosa-associated microbiota reveals dysbiosis and differences between inflamed and non-inflamed regions of the intestine in inflammatory bowel disease*. BMC Microbiol 11: 7.

[156] **Wehkamp J., Fellermann K., Herrlinger K.R., Baxmann S., Schmidt K.*, et al.* (2002). *Human beta-defensin 2 but not beta-defensin 1 is expressed preferentially in colonic mucosa of inflammatory bowel disease*. Eur J Gastroenterol Hepatol 14(7): 745-52.

[157] **Wehkamp J., Harder J., Wehkamp K., Wehkamp-von Meissner B., Schlee M.*, et al.* (2004a). *NF-kappaB- and AP-1-mediated induction of human beta defensin-2 in intestinal epithelial cells by Escherichia coli Nissle 1917: a novel effect of a probiotic bacterium*. Infect Immun 72(10): 5750-8.

[158] **Wehkamp J., Harder J., Weichenthal M., Mueller O., Herrlinger K.R.*, et al.* (2003). *Inducible and constitutive beta-defensins are differentially expressed in Crohn's disease and ulcerative colitis*. Inflamm Bowel Dis 9(4): 215-23.

[159] **Wehkamp J., Harder J., Weichenthal M., Schwab M., Schaffeler E.*, et al.* (2004b). *NOD2 (CARD15) mutations in Crohn's disease are associated with diminished mucosal alpha-defensin expression*. Gut 53(11): 1658-64.

[160] **Wehkamp J., Salzman N.H., Porter E., Nuding S., Weichenthal M.*, et al.* (2005). *Reduced Paneth cell alpha-defensins in ileal Crohn's disease*. Proc Natl Acad Sci U S A 102(50): 18129-34.

[161] **Wehkamp J. and Stange E.F.** (2010). *Paneth's disease*. J Crohns Colitis 4(5): 523-31.

[162] **Wei B., Huang T., Dalwadi H., Sutton C.L., Bruckner D.*, et al.* (2002). *Pseudomonas fluorescens encodes the Crohn's disease-associated I2 sequence and T-cell superantigen*. Infect Immun 70(12): 6567-75.

[163] **White S.H., Wimley W.C. and Selsted M.E.** (1995). *Structure, function, and membrane integration of defensins*. Curr Opin Struct Biol 5(4): 521-7.

[164] **Willing B., Halfvarson J., Dicksved J., Rosenquist M., Jarnerot G.*, et al.* (2009). *Twin studies reveal specific imbalances in the mucosa-associated microbiota of patients with ileal Crohn's disease*. Inflamm Bowel Dis 15(5): 653-60.

[165] **Winter S.E., Winter M.G., Xavier M.N., Thiennimitr P., Poon V.*, et al.* (2013). *Host-derived nitrate boosts growth of E. coli in the inflamed gut*. Science 339(6120): 708-11.

[166] **Wohlgemuth S., Haller D., Blaut M. and Loh G.** (2009). *Reduced microbial diversity and high numbers of one single Escherichia coli strain in the intestine of colitic mice*. Environ Microbiol 11(6): 1562-71.

[167] **Wohlgemuth S., Loh G. and Blaut M.** (2010). *Recent developments and perspectives in the investigation of probiotic effects*. Int J Med Microbiol 300(1): 3-10.

[168] **Yan Y., Kolachala V., Dalmasso G., Nguyen H., Laroui H.*, et al.* (2009). *Temporal and spatial analysis of clinical and molecular parameters in dextran sodium sulfate induced colitis*. PLoS One 4(6): e6073.

[169] **Zheng M., Wang X., Templeton L.J., Smulski D.R., LaRossa R.A.*, et al.* (2001). *DNA microarray-mediated transcriptional profiling of the Escherichia coli response to hydrogen peroxide*. J Bacteriol 183(15): 4562-70.

VII. APPENDIX

Table 10 Influence of strong intestinal inflammation on bacterial protein expression
Germ-free mice (129/SvEv) were monoassociated with *E. coli* Nissle or UNC. Mice of the DSS group received 3.5% DSS in sterile drinking water for 7 days, control mice received sterile drinking water without DSS. Bacterial proteins were isolated from caecal contents and proteome analysis was performed by 2D-DIGE.

Swiss-Prot accession no.	Gene	Protein description[a]	Fold change[a] (DSS vs. control)
Proteins differentially expressed in *E. coli* Nissle			
P0A9B2	gapA	Glyceraldehyde-3-phosphate dehydrogenase A	-7.06
P40120	mdoD	Glucans biosynthesis protein D	-6.46
P75733	ybfM	Uncharacterised protein YbfM	-5.31
P0AEE5	mglB	D-galactose-binding periplasmic protein	-5.1; -8.23
P77376	ydgJ	Uncharacterised oxidoreductase YdgJ	-5.08
P0ABB0	atpA	ATP synthase subunit alpha	-4.73; -6.49; -5.42; -4.51
P0A8F0	upp	Uracil phosphoribosyltransferase	-4;69
P0ACE0	hybC	Hydrogenase-2 large chain	-4.67
P0AGD3	sodB	Superoxide dismutase [Fe]	-4.52
P0A8N5	lysU	Lysyl-tRNA synthetase, heat inducible	-4.06
P02925	rbsB	D-ribose-binding periplasmic protein	-4.04; -5.67; -7.11
P0A858	tpiA	Triosephosphate isomerase	-4.03
P27302	tktA	Transketolase 1	-3.97
P0A7R1	rplI	50S ribosomal protein L9	-3.88
P06720	melA	Alpha-galactosidase	-3.82
P00509	aspC	Aspartate aminotransferase	-3.71; -8.82
P0AG55	rplF	50S ribosomal protein L6	-3.69; -3.68
P22259	pckA	Phosphoenolpyruvate carboxykinase [ATP]	-3.46
P0AE08	ahpC	Alkyl hydroperoxide reductase subunit C	-3.41
P0CE47	tufA	Elongation factor Tu 1	-3.24; -3.52; -4.55
P27248	gcvT	Aminomethyltransferase	-3.22
P0ABP8	deoD	Purine nucleoside phosphorylase deoD-type	-3.16
P09373	pflB	Formate acetyltransferase 1	-3.15
P0A7D7	purC	Phosphoribosylaminoimidazole-succinocarboxamide synthase	-3.01
P28248	dcd	Deoxycytidine triphosphate deaminase	3.00
P19926	agp	Glucose-1-phosphatase	3.14
P0A8E7	yajQ	UPF0234 protein YajQ	3.15
P76177	ydgH	Protein YdgH	3.24
P63020	nfuA	Fe-S biogenesis protein NfuA	3.75
P02413	rplO	50S ribosomal protein L15	4.00
P0A6F5	groL	60 kDa chaperonin	4.13
P0A7G6	recA	Protein RecA	4.46
P0A6Q3	fabA	3-hydroxydecanoyl-[acyl-carrier-protein] dehydratase	5.58

Swiss-Prot accession no.	Gene	Protein description[a]	Fold change[a] (DSS vs. control)
P0A9C5	*glnA*	Glutamine synthetase	5.58; 6.16
P02358	*rpsF*	30S ribosomal protein S6	9.51
Proteins differentially expressed in *E. coli* UNC			
P0A9B2	*gapA*	Glyceraldehyde-3-phosphate dehydrogenase A	-8.41
P62623	*ispH*	4-hydroxy-3-methylbut-2-enyl diphosphate reductase	-7.47
P0AB71	*fbaA*	Fructose-bisphosphate aldolase class 2	-6.92
P0A858	*tpiA*	Triosephosphate isomerase	-6.10
P0AEZ3	*minD*	Septum site-determining protein mind	-5.56; -6.97
P07862	*ddlB*	D-alanine--D-alanine ligase B	-5.48
P0A7J7	*rplK*	50S ribosomal protein L11	-5.16
P0A8F0	*upp*	Uracil phosphoribosyltransferase	-5.09
P09148	*galT*	Galactose-1-phosphate uridylyltransferase	-5.05
P0A9L3	*fklB*	FKBP-type 22 kDa peptidyl-prolyl cis-trans isomerase	-4.96
P0A6F5	*groL*	60 kDa chaperonin	-4.49
P0AGD3	*sodB*	Superoxide dismutase [Fe]	-4.41; -5.43
P0AAT9	*ybeL*	Uncharacterised protein YbeL	-4.20
P0ABA6	*atpG*	ATP synthase gamma chain	-4.17; -4.63
P0ABB0	*atpA*	ATP synthase subunit alpha	-4.16
P76541	*eutL*	Ethanolamine utilization protein EutL	-4.11
P08331	*cpdB*	2',3'-cyclic-nucleotide 2'-phosphodiesterase/3'-nucleotidase	-4.09; -8.58
P40120	*mdoD*	Glucan biosynthesis protein D	-4.02
P0AEE5	*mglB*	D-galactose-binding periplasmic protein	-3.86; -6.68
P0A6T3	*galK*	Galactokinase	-3.81
P67910	*hldD*	ADP-L-glycero-D-manno-heptose-6-epimerase	-3.68
P0ACE0	*hybC*	Hydrogenase-2 large chain	-3.58
P04982	*rbsD*	D-ribose pyranase	-3.55
P0AG18	*purE*	Phosphoribosylaminoimidazole carboxylase catalytic subunit	-3.51
P0A799	*pgk*	Phosphoglycerate kinase	-3.46; -3.61
P0A9J6	*rbsK*	Ribokinase	-3.46
P0A8N5	*lysU*	Lysyl-tRNA synthetase, heat inducible	-3.44
P0A6P9	*eno*	Enolase	-3.38; -4.5
P0CE47	*tufA*	Elongation factor Tu 1	-3.30; -3.75; -4.06; -4.83; -26.15
P11875	*argS*	Arginyl-tRNA synthetase	-3.26
P27248	*gcvT*	Aminomethyltransferase	-3.23
P02358	*rpsF*	30S ribosomal protein S6	-3.15
P0AE08	*ahpC*	Alkyl hydroperoxide reductase subunit C	-3.10
P02925	*rbsB*	D-ribose-binding periplasmic protein	-3.03; -4.43; -5.17; -7.13; -7.39; -8.84

Swiss-Prot accession no.	Gene	Protein description[a]	Fold change[a] (DSS vs. control)
P0A7D7	*purC*	Phosphoribosylaminoimidazole-succinocarboxamide synthase	-3.03
P0A864	*tpx*	Thiol peroxidase	3.00
P35340	*ahpF*	Alkyl hydroperoxide reductase subunit F	3.03
P09373	*pflB*	Formate acetyltransferase 1	3.03; 3.11; 3.18; 4.2
P0A7E5	*pyrG*	CTP synthase	3.05
P63020	*nfuA*	Fe-S biogenesis protein NfuA	3.13
P27302	*tktA*	Transketolase 1	3.13; 3.58; 3.82
P0AC38	*aspA*	Aspartate ammonia-lyase	3.17; 4.85
P63284	*clpB*	Chaperone protein ClpB	3.31
P0A853	*tnaA*	Tryptophanase	3.36; 5.93
P00722	*lacZ*	Beta-galactosidase	3.75; 4.77
P0AC41	*sdhA*	Succinate dehydrogenase flavoprotein subunit	4.0
P77804	*ydgA*	Protein YdgA	4.09
P42632	*tdcE*	Keto-acid formate acetyltransferase	4.49
P0A6Q3	*fabA*	3-hydroxydecanoyl-[acyl-carrier-protein] dehydratase	6.18
P0AFF6	*nusA*	Transcription elongation protein nusA	6.38
P0A9C5	*glnA*	Glutamine synthetase	6.87

[a] Proteins with differential expression factors ≥ 3, ≤ -3 ($p \leq 0.05$) in caecal samples (DSS vs. control group)

Table 11 Proteomic differences between *E. coli* UNC and Nissle from control and DSS mice
Germ-free mice (129/SvEv) were monoassociated with *E. coli* Nissle (EcN) or UNC. Mice of the DSS group received 3.5% DSS in sterile drinking water for 7 days, control mice received sterile drinking water without DSS. Bacterial proteins were isolated from caecal contents and proteome analysis was performed by 2D-DIGE.

Swiss-Prot accession no.	Gene	Protein description[a]	Fold change[a] (UNC vs. EcN)
Proteins differentially expressed in the control group			
P06720	*melA*	Alpha-galactosidase	-11.19
P19926	*agp*	Glucose-1-phosphatase	-11.17
P00805	*ansB*	L-asparaginase 2	-10.64; -13.96; -29.66
P0AES2	*gudD*	Glucarate dehydratase	-9.62
P21420	*nmpC*	Putative outer membrane porin protein NmpC	-8.29
P0A855	*tolB*	Protein TolB	-7.67
P0A853	*tnaA*	Tryptophanase	-7.03
P0AEK4	*fabI*	Enoyl-[acyl-carrier-protein] reductase [NADH]	-6.76
P0A915	*ompW*	Outer membrane protein W	-6.49
P10121	*ftsY*	Cell division protein FtsY	-6.11
P23256	*malY*	Protein MalY	-5.75
P17169	*glmS*	Glucosamine--fructose-6-phosphate aminotransferase [isomerizing]	-5.69
P26646	*yhdH*	Putative quinone oxidoreductase YhdH	-5.53
P0A825	*glyA*	Serine hydroxymethyltransferase	-5.31
P16456	*selD*	Selenide, water dikinase	-5.29
P61889	*mdh*	Malate dehydrogenase	-5.11; -6.73
P23893	*hemL*	Glutamate-1-semialdehyde 2,1-aminomutase	-5.09
P0AAT9	*ybeL*	Uncharacterised protein YbeL	-5.06
P75733	*ybfM*	Uncharacterised protein YbfM	-5.04
P0ABH0	*ftsA*	Cell division protein FtsA	-4.98
P0AFF6	*nusA*	Transcription elongation protein NusA	-4.72
P12758	*udp*	Uridine phosphorylase	-4.63
P0ADS6	*yggE*	Uncharacterised protein YggE	-4.40
P0A850	*tig*	Trigger factor	-4.20; -10.58
Q8FAD9	*arcA*	Arginine deiminase	-4.19; -4.92; -10.75
P15639	*purH*	Bifunctional purine biosynthesis protein PurH	-4.18
P27248	*gcvT*	Aminomethyltransferase	-4.13; -7.19; -12.15
P77376	*ydgJ*	Uncharacterised oxidoreductase YdgJ	-3.87
P0A6Y8	*dnaK*	Chaperone protein DnaK	-3.83
P0AG55	*rplF*	50S ribosomal protein L6	-3.70
P00722	*lacZ*	Beta-galactosidase	-3.67; -9.27
P0A786	*pyrB*	Aspartate carbamoyltransferase catalytic chain	-3.66
P0ABT2	*dps*	DNA protection during starvation protein	-3.64
P0AC81	*gloA*	Lactoylglutathione lyase	-3.46

Swiss-Prot accession no.	Gene	Protein description[a]	Fold change[a] (UNC vs. EcN)
P35340	ahpF	Alkyl hydroperoxide reductase subunit F	-3.30; -3.48
P0AET8	hdhA	7-alpha-hydroxysteroid dehydrogenase	-3.25
P0A862	tpx	Thiol peroxidase	-3.19
P37773	mpl	UDP-N-acetylmuramate:L-alanyl-gamma-D-glutamyl-meso-diaminopimelate ligase	-3.16
P0AGF6	tdcB	Threonine dehydratase catabolic	-3.08
P0CE47	tufA	Elongation factor Tu 1	3.07; 4.21
P0A8G6	wrbA	Flavoprotein WrbA	3.20, 4.84
P08200	icd	Isocitrate dehydrogenase [NADP]	3.22
P0AEE5	mglB	D-galactose-binding periplasmic protein	3.25; 4.25
P63224	gmhA	Phosphoheptose isomerase	3.27
P02358	rpsF	30S ribosomal protein S6	3.32
P00509	aspC	Aspartate aminotransferase	3.34; 3.76
P0A794	pdxJ	Pyridoxine 5'-phosphate synthase	3.37
P02925	rbsB	D-ribose-binding periplasmic protein	3.40; 3.55; 3.93; 4.24; 4.89
P0A7G6	recA	Protein RecA	3.60
P0A9L3	fklB	FKBP-type 22 kDa peptidyl-prolyl cis-trans isomerase	3.67
P27302	tktA	Transketolase 1	4.13
P07862	ddlB	D-alanine--D-alanine ligase B	4.14
P62623	ispH	4-hydroxy-3-methylbut-2-enyl diphosphate reductase	4.31
P0ABA6	atpG	ATP synthase gamma chain	4.32
P0A817	metK	S-adenosylmethionine synthase	4.34
P0A6F5	groL	60 kDa chaperonin	4.42
P0A858	tpiA	Triosephosphate isomerase	4.54
P0A7L0	rplA	50S ribosomal protein L1	4.57
P04982	rbsD	D-ribose pyranase	4.69
P09127	hemX	Putative uroporphyrinogen-III C methyltransferase	5. 45
P09148	galT	Galactose-1-phosphate uridylyltransferase	5.30
P67910	hldD	ADP-L-glycero-D-manno-heptose-6-epimerase	5.84
P0AEZ3	minD	Septum site-determining protein MinD	6.32
P0A9C3	galM	Aldose 1-epimerase	7.04
P0ACF8	hns	DNA-binding protein H-NS	14.52

Proteins differentially expressed in the DSS group

P02358	rpsF	30S ribosomal protein S6	-16.72
P23256	malY	Protein MalY	-9.52
P00805	ansB	L-asparaginase 2	-9.19; -10.76; -22.90
P0A9A9	fur	Ferric uptake regulation protein	-8.93; -20.62
P0AAT9	ybeL	Uncharacterised protein YbeL	-8.54
P0ABT2	dps	DNA protection during starvation protein	-8.16

Swiss-Prot accession no.	Gene	Protein description[a]	Fold change[a] (UNC vs. EcN)
P0ADS6	yggE	Uncharacterised protein YggE	-8.13
P06720	melA	Alpha-galactosidase	-7.24
P19926	agp	Glucose-1-phosphatase	-6.69
P0AES2	gudD	Glucarate dehydratase	-6.47; -12.5
P21420	nmpC	Putative outer membrane porin protein NmpC	-6.20
P12758	udp	Uridine phosphorylase	-6.05
P0A915	ompW	Outer membrane protein W	-5.99
P26646	yhdH	Putative quinone oxidoreductase YhdH	-5.93
P16456	selD	Selenide, water dikinase	-5.83
P0AEK4	fabI	Enoyl-[acyl-carrier-protein] reductase [NADH]	-5.54
P18843	nadE	NH(3)-dependent NAD(+) synthetase	-4.75
Q8FAD9	arcA	Arginine deiminase	-4.61; -6.77; -8.72; -15.2
P0A786	pyrB	Aspartate carbamoyltransferase catalytic chain	-4.60
P0AET8	hdhA	7-alpha-hydroxysteroid dehydrogenase	-4.58
P69441	adk	Adenylate kinase	-4.41
P0A9C5	glnA	Glutamine synthetase	-4.40
P11875	argS	Arginyl-tRNA synthetase	-4.34
P0A853	tnaA	Tryptophanase	-4.16
P61889	mdh	Malate dehydrogenase	-4.14; -8.13
P76576	yfgM	UPF0070 protein YfgM	-4.10
P0A9J6	rbsK	Ribokinase	-4.09
P08331	cpdB	2',3'-cyclic-nucleotide 2'-phosphodiesterase/3'-nucleotidase	-3.48
P37903	uspF	Universal stress protein F	-3.47
P0AC81	gloA	Lactoylglutathione lyase	-3.41
P0A855	tolB	Protein TolB	-3.28; -3.32
P0A9Q7	adhE	Aldehyde-alcohol dehydrogenase	-3.12
P0A6K6	deoB	Phosphopentomutase	3.04
P14407	fumB	Fumarate hydratase class I, anaerobic	3.14; 3.70
P77318	ydeN	Uncharacterised sulfatase YdeN	3.38
P0A8N5	lysU	Lysyl-tRNA synthetase, heat inducible	3.40
P0CE47	tufA	Elongation factor Tu 1	3.41
P0A6A3	ackA	Acetate kinase	3.52
P00509	aspC	Aspartate aminotransferase	3.82; 4.26; 6.01; 6.16
P27302	tktA	Transketolase 1	3.86; 8.04
P0A858	tpiA	Triosephosphate isomerase	3.88
P02925	rbsB	D-ribose-binding periplasmic protein	3.98; 4.81; 37.35
P0A794	pdxJ	Pyridoxine 5'-phosphate synthase	4.39
P0A8G6	wrbA	Flavoprotein WrbA	5.27
P0A817	metK	S-adenosylmethionine synthase	5.53; 7.47
P10121	ftsY	Cell division protein FtsY	5.87

Swiss-Prot accession no.	Gene	Protein description[a]	Fold change[a] (UNC vs. EcN)
P00722	*lacZ*	Beta-galactosidase	6.06; 6.29; 7.88; 32.21; 49.06
P63224	*gmhA*	Phosphoheptose isomerase	6.40
P02931	*ompF*	Outer membrane protein F	6.50; 18.71
P09148	*galT*	Galactose-1-phosphate uridylyltransferase	6.52
P0A6Y8	*dnaK*	Chaperone protein DnaK	7.56
P0A7L0	*rplA*	50S ribosomal protein L1	9.00
P0ACF8	*hns*	DNA-binding protein H-NS	34.21

[a] Proteins with differential expression factors ≥ 3, ≤ -3 ($p \leq 0.05$) in caecal samples (UNC vs. EcN)

Table 12 Influence of mild intestinal inflammation on bacterial protein expression in *E. coli* UNC
Wildtype (wt) and IL-10^{-/-} mice were monoassociated with *E. coli* UNC for 3 (only IL-10^{-/-}) or 8 wk. After isolation of the caecal bacterial proteins, proteome analysis was performed using 2D-DIGE.

Swiss-Prot accession no.	Gene	Protein description	Fold change[a] 3 wk IL-10^{-/-} vs. wt	Fold change[a] 8 wk IL-10^{-/-} vs. wt
P06996	*ompC*	Outer membrane protein C	-3.28	
P62707	*gpmA*	2,3-bisphosphoglycerate-dependent phosphoglycerate mutase	-1.85; -2.25	
P0A8E7	*yajQ*	UPF0234 protein YajQ	-1.85	
P0AGD3	*sodB*	Superoxide dismutase [Fe]	-1.65; -2.04	-1.80; -1.71
P0A7V0	*rpsB*	30S ribosomal protein S2	-1.77	
P0A9B2	*gapA*	Glyceraldehyde-3-phosphate dehydrogenase A	-1.75	
P15639	*purH*	Bifunctional purine biosynthesis protein PurH	-1.71	
P0A7L0	*rplA*	50S ribosomal protein L1	-1.72	-1.70
P0A6P9	*eno*	Enolase	-2.05; -2.52	-1.69
P0A9C3	*galM*	Aldose 1-epimerase	-1.68	
P0A817	*metK*	S-adenosylmethionine synthase	-1.68	
P0A8G3	*uxaC*	Uronate isomerase		-1.67
P08200	*icd*	Isocitrate dehydrogenase [NADP]	-1.65	
P67826	*cutC*	Copper homeostasis protein CutC	-1.51	-1.63
P0AB71	*fbaA*	Fructose-bisphosphate aldolase class 2	-1.53	-1.60
P0A825	*glyA*	Serine hydroxymethyltransferase	-1.58	
P0AD61	*pykF*	Pyruvate kinase I	-2.02	-1.57
P00722	*lacZ*	Beta-galactosidase	-1.53	
P0A8Y5	*yidA*	Sugar phosphatase YidA		2.94; 1.56
P26646	*yhdH*	Putative quinone oxidoreductase YhdH	-2.43	2.21
P0AB77	*kbl*	2-amino-3-ketobutyrate coenzyme A ligase		2.07
P23843	*oppA*	Periplasmic oligopeptide-binding protein	1.66	1.97
P0A763	*ndk*	Nucleoside diphosphate kinase	1.67	
P64557	*ygfM*	Uncharacterised protein ygfM		1.62
P0CE47	*tufA*	Elongation factor Tu 1		1.56
P0A7D4	*purA*	Adenylosuccinate synthetase	1.52	
P0A910	*ompA*	Outer membrane protein A	3.81	

[a] Proteins with differential expression factors ≥ 1.5, ≤ -1.5 ($p \leq 0.01$) in cecal samples (n = 4/5)

	Control	Paraquat	2,2'-Dipyridyl
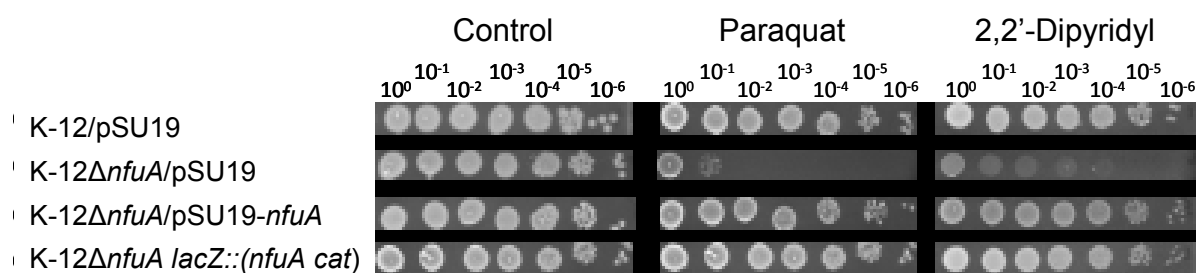
Fig. 34   Complementation of *nfuA* deletion

The deletion was complemented either with the plasmid pSU19 carrying a copy of the *nfuA* gene or by insertion of *nfuA* into the chromosomal *lacZ* gene. Exponentially growing cells were harvested by centrifugation, resuspended to equal optical densities and decimally diluted. Five µl of each suspension were spotted onto LB-Lennox agar containing 20 µg/ml chloramphenicol (control), or on plates containing additionally either 300 µM paraquat or 375 µM 2,2'-dipyridyl. Photographs were taken after overnight incubation at 37°C. Each block depicts four dilution series from the same plate.

Fig. 35 Sequence alignment of *ivy*: *E. coli* Nissle (EcN) vs. *E. coli* K-12
The genomic sequence of *ivy* promoter and gene region was compared using the Vector NTI Suite 9 (Align X) software. The black arrow indicates the starting point of the promoter region. The blue line marks the start codon ATG. The black letters indicate the sequence differences. The data are representative of 3 independent experiments.

VIII. LIST OF ORIGINAL COMMUNICATIONS

Full length articles

Schumann S, Alpert C, Engst W, Loh G, Blaut M (2012) *Dextran sodium sulfate-induced inflammation alters the expression of proteins by intestinal Escherichia coli strains in a gnotobiotic mouse model.* Appl Environ Microbiol 78(5): 1513-22

Schumann S, Alpert C, Engst W, Klopfleisch R, Loh G, Bleich A, Blaut M (2013) *Initially mild gut inflammation modulates the proteome of intestinal E. coli*. Submitted in Environ Microbiol (under revision)

Scientific events

Schumann S, Alpert C, Engst W, Klopfleisch R, Loh G, Bleich A, Blaut M (2012) *Influence of inflammatory bowel disease on bacterial protein expression*. NuGOweek 2012 "Nutrition, lifestyle and genes in the changing environment", 28.-31. August 2012, Helsinki, Finland (Poster presentation)

Schumann S, **Alpert C**, Engst W, Loh G, Blaut M (2011) *Protection mechanisms in Escherichia coli during gut inflammation*. 4th Seeon Conference "Microbiota, Probiotica and Host", 15.-17- April 2011, Monastery Seeon, Germany (Oral presentation)

Schumann S, Alpert C, Engst W, Loh G, Blaut M (2010) *Influence of inflammatory bowel disease on bacterial protein expression*. 1st annual conference of the German Society of Mucosal Immunology and Microbiome (DGMIM), 15.-16. October 2010, Stuttgart, Germany (Oral presentation, Awarded PhD work)

Schumann S, Alpert C, Engst W, Loh G, Blaut M (2010) *Influence of inflammatory bowel disease on bacterial protein expression*. 2nd Workshop on Symbiotic Interactions, 7.-8. October 2010, Würzburg, Germany (Poster presentation)

Schumann S, Alpert C, Engst W, Loh G, Blaut M (2010) *Influence of inflammatory bowel disease on bacterial protein expression*. 3rd Seeon Conference "Microbiota, Probiotica and Host", 18.-20. June 2010, Monastery Seeon, Germany (Poster presentation)

IX. ACKNOWLEDGEMENT

X. DECLARATION OF ACADEMIC HONESTY

I hereby confirm that my thesis entitled "Influence of intestinal inflammation on bacterial protein expression in monoassociated mice" is my own original work and has not previously, in part or in its entirety, been submitted at any university for a degree. Information derived from published work of others has been stated in the text and a list of references is given in the bibliography.

Potsdam, March 2013

Sara Schumann